Intrinsic and Extrinsic Influences on Neuromuscular Synaptic Degeneration in *Wld*^{S} Mutant Mice

Li Fan

Submitted for the degree of PhD in Neuroscience
at the University of Edinburgh

2007

Declaration

I hereby declare that the work described within, and composition of, this thesis is my own and has not been submitted for any other degree.

Li Fan

Abstract

Background and Aims

It is now well established that mutant *Wld*^{S} mice show slow Wallerian degeneration after nerve injury: The aim of the present thesis was to extend knowledge and understanding of the protective effect of the *Wld*^{S} gene, and its protein product on neuromuscular synapses. I used homozygous and heterozygous *Wld*^{S} mice in studies that addressed three hypotheses:

1. Neuromuscular synaptic protection is more sensitive to *Wld*^{S} gene dose than axon protection.

2. Age-dependent loss of neuromuscular synaptic protection is related to changes in Wld^S protein expression levels.

3. Synaptic degeneration in *Wld*^{S} mice can be further altered by other extrinsic factors including nerve stump length and blocking neurotransmitter release.

Methods and Results

To test the first hypothesis, rates of synaptic degeneration were measured in young (2 months old) heterozygous *Wld*^{S} mice crossbred with mice expressing Yellow Fluorescent Protein (*thy1. 2-YFP16* strain) in motor neurones. The results suggest that synaptic degeneration in *Wld*^{S} mice is more sensitive to *Wld*^{S} gene-dose dependence than axon degeneration

The second hypothesis was addressed by comparing synaptic degeneration in young (2 months old) heterozygous and homozygous *Wld*^{s} mice with, older (>6 months) homozygous *Wld*^{s} mice. The old mice were also crossbred with *thy.1-YFP16* mice but some data were also obtained using fluorescence immunocychemistry for neurofilament and synaptic vesicle proteins. Confocal microscopy and PDD's were used to obtain and analyse the data as before. The rate and pattern of synaptic degeneration in old homozygous *Wld*^{s} mice were similar to those in young heterozygous *Wld*^{s} mice and wild-type mice. Immunofluorescence measurements showed significant difference between Wld^s protein levels in young homozygotes and old homozygous *Wld*^{s} mice. Therefore, the loss of synaptic protection in old *Wld*^{s} mice may also be explained by its sensitive gene-dose dependence.

The third hypothesis was addressed first by comparing synaptic degeneration protected by the length of nerve stump; specifically by comparing sciatic nerve section and tibial nerve section. Second, the role of synaptic transmission was examined by injecting botulinum toxin into the hind foot, sufficient to cause local paralysis. Surprisingly, the result following sciatic/tibial cut did not show apparent protection by increasing nerve stump length. The result from injection of botulinum toxin into young *Wld*^{s} mice suggested that blocking transmitter release can delay synaptic degeneration. However, in old *Wld*^{s} mice its effect disappeared. Therefore neither the paralysis nor the length of nerve stump is sufficient to prevent or delay

synaptic degeneration.

PDD

Testing these hypotheses was facilitated by a novel geometric method was facilitated by novel devised for representing different stages in the breakdown or retraction of motor nerve endings. These representations (Polyhedral Degeneration Diagrams, PDD) demonstrated clear differences in the rate and pattern of synaptic degeneration following nerve injury in the different experimental groups of mice examined.

Conclusions

Overall, the data I obtained provide evidence in support of a compartmental neurodegeneration model which proposes that the survival or death of cell bodies, motor axons and terminals of motor neurons are controlled by independent regulatory mechanisms. The data further suggest that motor nerve terminals are an especially vulnerable neurodegenerative compartment. Geometric PDD analysis of synaptic degeneration may also find general utility and applicability to studies of development or pathological models of neurodegenerative disease.

Acknowledgement

The entire endeavour of my doctoral studies would not have been possible without the collective efforts from those who have worked alongside me at different stages.

Firstly, I am extremely grateful to Professor Richard R. Ribchester, my principal supervisor, who invested his intelligence, guidance, patience, encouragement and time in his supervision. His careful re-reading of each draft chapter has been indispensable for the production of this thesis. His thoughtful questioning has allowed me to reach and then to go beyond some of my own limitations.

I would like to thank Derek Thomson, not only for his expert technical assistance, but also for helping me improve my English since the first year; all past and present members of the Ribchester Lab: Drs. Tom Gillingwater, Jane Haley, and Tom Wishart, for their encouragement and kind help, and Adrian Thomson for being the confocal microscope technical assistant in many of my studies. Moreover I should also like to thank my second supervisor, Dr. Paul Skehel for his steadfast guidance in the third year, and all of the postgraduate and postdoctoral workers in the Department of Neuroscience for providing a friendly environment for debate, and for their kindness, generosity, warmth, and support throughout my PhD studies.

I would like to thank my parents, for their constant support, understanding and love throughout my studies. Many thanks to my friends, Xu-cheng Yang for his generous help, and sharing his strength and positivity, especially in difficult time; Dr. Li-hui Wang for her kind technical assistance and concern; Dr. Hong-yu Deng for her thoughtful and valuable suggestions in my thesis; and Dr. Marcella Fok for her attentive help with my English writing.

Table of Contents

Abbreviation

α-BTX	Alpha-bungarotoxin
Ach	Acetylcholine
AchR	Acetylcholine receptors
ALS	Amyotrophic lateral sclerosis
ATP	Adenosine Triphosphate
BSA	Bovine Serum Albumin
BTX	Bungarotoxin
BoTox	Botulinum toxin
CAP	Compound action potential
CFP	Cyan fluorescent protein
CGC	Cerebellar granule cells
CK	Creatine kinase
CNS	Central Nervous System
CNTF	Ciliary Neurotrophic Factor
EM	Electron Microscopy
EPP	End-Plate Potential
FALS	Familial amyotrophic lateral sclerosis
FDB	Flexor Digitorum Brevis
FF	Fast fatiguable
FITC	Fluorescein Isothiocyanate
FR	Fast resistant
INOS	Inducible Nitric Oxide Synthase
MAG	Myelin-Associated Glycoprotein
MEPP	Minature End-Plate Potential
NAD	Nicotinamide Adenine Dinucleotide
NF	Neurofilament
NGF	Nerve Growth Factor
NMJ	Neuromuscular Junction
Nmnat	Nicotinamide Mononucleotide Adenylyl transferase
PBS	Phosphate Buffered Saline
PDD	Polyhedral Degeneration Diagram
PNS	Peripheral Nervous System
SALS	Sporadic amyotrophic lateral sclerosis
SD	Standard Deviation
SEM	Standard Error of the Mean
SNAP-25	synaptosome-associated protein of 25000 daltons
SOD	Superoxide dismutase
SV	Synaptic Vesicles

TRITC	Tetramethylrhodamine Isothiocyanate
Ube4b	Ubiquitination Factor E4b

1. Introduction

The vertebrate nervous system is an extraordinarily complex communication system that sends and receives information simultaneously in parallel pathways. The nervous system has two distinct parts: the central nervous system and the peripheral nervous system (the nerves outside the brain and spinal cord). Afferent and efferent axons in the peripheral nervous system are gathered into nerve trunks, forming defined peripheral nerves.

1.1 Neurons

The neurons that project axon into peripheral nerves are either sensory or motor. Both sensory and motor neurons consist of a large cell body (or soma) with branching dendrites (signal receivers) and a projection called an axon, which conducts the nerve signal (Fig 1.1). At the other end of the axon, the axon terminals transmit an electro-chemical signal across a synapse (the gap between the axon terminal and the receiving cell).

The cell body is the bulbous end of a neuron, containing the nucleus. The cell nucleus is a key feature of the cell body. It is the source of most of the RNA that is produced in neurons and most proteins are produced from mRNAs that do not travel far from the nucleus. Other RNA comes from cytoplasm, such as tRNA.

An axon is a long, slender projection of a nerve cell that conducts electrical impulses away from the neuron's cell body.Axons are in effect the primary

transmission lines of the nervous system, and are bundled together to form nerves. Individual axons are microscopic in diameter - typically about one micrometre across (1μm) - but may extend to macroscopic (>1mm) lengths. The longest axons in the human body, for example, are those of the sciatic nerve, which run from the base of the spine to the big toe of each foot. These single-cell fibers of the sciatic nerve may extend a meter or even longer.

In vertebrates, the axons of many neurons are sheathed in myelin, which is formed by either of two types of glial cells: Schwann cells ensheathing peripheral neurons and oligodendrocytes insulating neurons of the central nervous system. Along myelinated nerve fibers, gaps in the sheath known as nodes of Ranvier occur at evenly-spaced intervals, enabling a particularly rapid mode of electrical impulse propagation called saltation.

This myelin sheath resembles insulation, such as that around an electrical wire. Nerve impulses travel much faster in nerves with a myelin sheath than in those without one. Velocity of impulse is a factor of axon diameter, myelin thickness and internodal length. If the myelin sheath of a nerve is damaged, nerve conduction is dramatically reduced (Tsao et al., 1994; Court et al., 2004).

Dendrites are the branched projections of a neuron that act to conduct the electrical stimulation received from other neural cells to the cell body of the neuron from which the dendrites project. Electrical stimulation is transmitted by upstream

neurons onto dendrites, via synapses which are located at various points throughout the dendritic arbor. Dendrites play a critical role in integrating these synaptic inputs and in determining the extent to which subsequent action potentials are produced by the neuron.

Synapses

The "Neuron doctrine" was first proposed by Santiago Ramon Y Cajal and his colleagues in late of 19th century. He proposed that the connections between the neurons are made at a specialized site. These sites were subsequently named "synapses" by Charles Sherrington (Sherrington, 1897; 1906). Synapses are symmetric and asymmetrical communication junctions formed between two neurons. The term 'synapse' has since been extended to include communication between a neuron and non-neuronal target cell; for instance, at the neuromuscular junction (NMJ), between a motor neuron and a muscle cell.

Synapses play a critical role in neural function by transmitting signals from one neuron to another or muscle fibres at NMJs. There are in fact two ways of synaptic transmission occurs between neurons: electrical and chemical. At electrical synapses, the ion channels bridge the pre and post-synaptic membrane and information may be carried symmetrically between the two connected cells directly. The other, more common form of synapses makes use of chemical intermediaries. At chemical synapses, the two neurons are separated by a 30nm gap, the synaptic cleft. Signals

are transmitted asymmetrically, when the presynaptic neuron releases a chemical neurotransmitter by exocytosis from synaptic vesicles into the synaptic cleft. These molecules are detected by the postsynaptic neuron through activation of specific molecular receptors exactly opposite the release site of the presynaptic terminals. At NMJ the receptors are acetylcholine receptors.

1.2 Neuromuscular Junctions

The vertebrate neuromuscular junction (NMJ) is arguably the best system for studying the formation, maturation, elimination and regeneration of synaptic connections. The NMJ is constructed from three main cellular components—nerve terminal, muscle fibre, and terminal (presynaptic) Schwann cell (Sanes and Lichtman., 1999). With the advent of electron microscopy, a clear picture of NMJ strucuture became available, showing the synaptic cleft that separates the motor nerve terminal and skeletal muscle fibre, numerous synaptic vesicles and mitochodria in the presynaptic terminal, the electron dense postsynaptic membranes thrown into numerous postsynaptic folds and a layer of extracellular matrix lining the synaptic cleft (Figure 1.2). Many studies have been carried out on at the NMJs since these observation were made.

Figure 1.2

Diagram showing the cellular organization of the NMJ

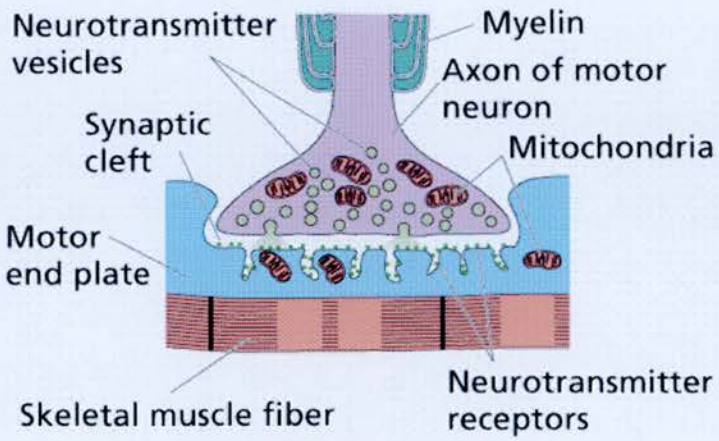

(Image from Purves et al., Life: the Science of Biology, 4th Edition, by Sinauer Associates and WH Freeman)

Dale et al (1939) were first to describe chemical neurotransmitter release in the synapses of the vertebrate NMJs. After that, a series of experiments on electrophysiology of chemical synaptic transmission at NMJs were carried out by Fatt and Katz (Fatt and Katz, 1951; Fatt and Katz, 1952). They suggested that the change in permeability of the nerve terminal membrane to Ca^{2+} ions triggers synaptic transmission, exocytosis of synaptic vesicles, releasing quantal packets of acetylcholine. Subsequent analysis established that neurotransmitter is released in packets of 5000-molecule "quanta" and that this occurs randomly and spontaneously at resting synapses. Excitation of the nerve terminal, for example by a depolarizing action potential, leads to influx of Ca^{2+} ions, leading to synchronous synaptic release

of many tens or hundreds of synaptic vesicles (Fatt and Katz, 1952; del Castillo and Katz, 1954; Katz and Miledi, 1969; Wood and Slater, 1997). Within the presynaptic nerve terminal, synaptic vesicles containing neurotransmitter acetylcholine are clustered near to the presynaptic membrane (Palade and Palay, 1954; Robertson, 1956; Whittaker et al., 1964). Synaptic vesicles often aggregate around the 'active zones' and neurotransmitters are secreted by exocytosis of synaptic vesicles at these sites which produces postsynaptic activation. Using electron microscope tomography in the frog's NMJ, Harlow et al (2001) suggested that active zone material facilitates vesicle docking and localizes calcium channels to release sites.

Many proteins play crucial roles in regulating and driving the synaptic vesicle cycle, namely docking, fusion, endocytosis, and recycling (Betz and Angleson 1998). P-type calcium channels are distributed throughout the presynaptic membrane and are important for vesicle exocytosis as they allow Ca^{2+} to enter. Voltage-gated potassium and calcium channels are also found to localize within active zones of presynaptic membrane to help increase the release of neurotransmitter (Uchitel et al., 1992, Robitaille et al., 1993.; Day et al., 1997). One study suggests that the presynaptic membrane protein plays an important role in vesicle docking at the presynaptic membrane (Pevsner et al., 1994). Integrins also help facilitate neurotransmitter secretion. They attach the nerve terminal, which assist neurotransmitter release sites anchored firmly on the postsynaptic receptors (Chen

and Grinnell, 1995).

The membrane opposite presynaptic nerve terminals is corrugated into junctional folds. At the rat neuromuscular junction, the postsynaptic folds appear to enhance the safety factor for neuromuscular transmission (Wood and Slater, 1997). Moreover, the presynaptic active zones (transmitter release sites) in the presynaptic terminal position are positioned directly opposite the opening of junctional folds in the postysynaptic membrane (Patton et al., 2001). The majority of nicotinic acetylcholine receptors (AChRs) are located at peaks of the junctional folds of the postsynaptic membrane (Salpeter and Loring, 1985). Voltage-gated sodium channels are located in the troughs of the folds (Flucher and Daniels, 1989). The muscle action potential is triggered by the local endplate potential produced by activating the AChRs, which then leads to voltage-dependent activation of these sodium channels.

Many cytoskeletal elements are thought to play an important role in generating and maintaining the postsynaptic folds (Sanes and Lichtman, 1999). For example, at the top of junctional folds, α-dystrobrevin-1, a member of the dystrophin family of proteins (Bewick et al ., 1992; Peters et al., 1998), rapsyn (Wang et al., 1999), and utrophin (Gramolini et al., 2000) are associated with the AChRs. Other proteins such as α-dystrobrevin-2 (Peters et al., 1998) ankyrin (Zhou et al., 1998) and β-spectrin (Wood and Slater., 1998) are found in the depths of the junctional folds.

Terminal Schwann cells are a non-myelinating population around the nerve terminals. They cover the terminal and isolate it from the surrounding environment. These Schwann cells are distinct from those that form myelin sheaths (Waxman, 1997) around the axon. Although, non-myelinating Schwann cells and myelin-forming Schwann cells come from the same progenitor, they express different genes during development. For instance, myelin basic protein Po and myelin associated glycoprotein (MAG) are expressed higher in the axonal Schwann cells than S-100 and N-CAM, in contrast to S-100 and N-CAM which are expressed higher in the terminal Schwann cells than protein Po and MAG (Mirsky and Jessen, 1996). Myelin-forming Schwann cells help increase conduction velocity, along the axon, moreover the cells may supply trophic factors that support the axons. On the other hand, terminal Schwann cells play an active role in the formation, maintenance and repair of developing NMJs (Meier and Wallace, 1998). For example, at developing neuromuscular junctions, Schwann cells appear to support motor neurons through the release of neurotrophic factors, such as, CNTF, GDNF, BDNF, and NT-3. Furthermore, during denervation, terminal Schwann cells guide sprouting or regenerating axons back to the original place of innervation (Reynolds and Woolf, 1992; Son and Thompson 1995).

Schwann cells express muscarinic and purinergic receptors, which are related to the release of acetylcholine and ATP (Robitaille, 1995; Robitaille et al., 1997). Synaptic activity leads to a rise in intracellular calcium, (Jahromi et al., 1992), which

in turn may alter in gene expression. For example, the gene for glial fibrillary acidic protein, which plays a role in the formation of the terminal schwann cell sprout, is stimulated by a blockage in synaptic activity (Love and Thompson, 1998).

1.3 Synaptic plasticity, development, degeneration

The nervous system has been described as a dynamic and flexible network that responds to change in the surrounding environment. Information in this entire dynamic neuronal system is mediated by neural activity, and this activity brings about changes in the patterning and strengths of neuronal connections. Activity-dependent plasticity of synaptic connection is important both in the CNS and the PNS, for example, at the synapses in the visual cortex as well as at neuromuscular synapses during development (Thompson et al., 1977; Ridge and Betz, 1984; Walsh and Lichtman, 2003; Kasthuri and Lichtman, 2003; Buffelli et al., 2003). However, arguably the most dramatic changes in motor nerve terminal form and function occur after an axon is injured, separating the synaptic terminals from their motor neuron cell bodies, an event that may also occur in neurodegenerative diseases, such as motor neuron diseases (MND; Schaefer et al., 2005; Fischer et al., 2004; Pun et al., 2006).

Withdrawal of motor terminals (synapse elimination) is a type of synaptic rearrangement and plasticity which has been most heavily researched. Early studies showed that in the neonatal mammals, each immature muscle fibre is supplied by

two or more motor axons which converge on to a single end-plate, which thus receives multiple "polyneuronal" synaptic inputs. At two weeks after birth all muscle fibres are innervated by only a single motor axon (Redfen, 1970; Brown et al., 1976). Similar changes in the innervation pattern are also found following axonal regeneration in the adult muscle after nerve injury (McArdle, 1975; Ribchester, 1988; Costanzo et al., 1999).

Synapse elimination has also been studied in regions of the CNS; for example, the cerebellum (Lohof et al., 1996) the autonomic ganglia (Lichtman, 1977) and the visual system (Hubel et al., 1977).

1.4 Wallerian degeneration

In 1850, Augustus Waller first described the orthograde degeneration of axons after nerve injury, and what we now called this process "Wallerian degeneration". Waller cut the glosspharyngeal and hypoglossal nerves of the frogs, then observed the distal nerves that were separated from their cell axons becoming discontinuous, and fragmented after parting from the cell bodies. He also suggested that "trophic influence" plays a role in maintaining the distal extremities of a neuron, for example, that distal axons degenerate after injury because the trophic substances can not be supplied.

Due to the limitation of the staining techniques available in that period, Waller's

findings were not accepted until in the late 19th century (1878). Ranvier, among others, extended studies of Wallerian degeneration in axons. He observed the fragmentation of the axon following nerve section and the later invasion of phagocytotic leucocytes later. He first described Schwann cell division during this process which was later confirmed by the findings of Büngner (1891). He was also the first person to observe structures he named as "bands of Büngner". Band of Büngner, also called the Schwann cell column, are formed by Schwann cells, which lose contact with axons, proliferate, then form a cell strand within the basal lamina tube. In 1928, these studies were confirmed by Ramon y Cajal who used silver staining techniques to demonstrate the degeneration of the distal nerve stump after axotomy.

1.4.1 Wallerian degeneration in the Axon

After a nerve has been transected, the lesioned axon begins to fragment; the myelin sheath retracts from the nodes of Ranvier to form the large spaces called 'digestive chambers' or ellipsoids', and the nerves are separated in these compartments (Allt, 1976). The axon fragments then proceed to a complete degradation. While the distal stump continues to degrade, the debris of the axons is cleaned by the phagocytosing Schwann cells and invading macrophages. At the same time, Schwann cells transiently proliferate. Abercrombie and Johnson (1946) demonstrated that in the rabbit sciatic nerve, the number of Schwann cells increased

13-fold by 25 days post lesion. The proliferating Schwann cells form a cell strand called Schwann cell column or band of Büngner (Büngner, 1891) within the basal lamina tube. The regenerating axons from the proximal stump of the lesion are guided by these bands back to the distal nerve segment. During this process, many different growth and adhesive factors such as NGF (Heumann et al., 1987), N-CAM(Nieke and Schachner, 1985) and cytokines (including members of the interleukin (IL-x) family (for review see Fu and Gordon, 1997), all of which are secreted from the Schwann cells, appear to play important roles in assisting axonal regeneration.

During axonal fragmentation and degradation, Wallerian degeneration is naturally accompanied by failure of conduction of action potentials in the nerve (Mastalgia et al., 1976; Nicholls et al., 1992). The lag period after axotomy in the axons varies in the different species. In mice, for example, the sciatic nerve fails to conduct action potentials for 1 — 2 days following axotomy. This is in contrast to the effect of axotomy in frogs, where the action potential can still be recorded up to 7 days post sciatic nerve axotomy (Levenson and Rosenbluth, 1990; Chaudry, Glass and Griffin, 1992). Remarkably, in the giant squid, crayfish and fish, the isolated axons are preserved even for months (Sheller and Bittner, 1992; Tanner et al., 1995; Raabe et al., 1996).

The fragmentation of endoplasmic reticulum and distintegration of

neurofilaments and microtubules in the 24-72 hours following nerve axotomy are the early axonal changes observed by electron microscopy (Vial, 1958; Honjin et al., 1959; Ballin and Thomas, 1969; Donat and Wisniewski, 1973; Schlaeper and Hasler, 1979a). A subsequent marker of degeneration is the swelling and dissolution of axonal mitochondria. There is evidence that axonal degradation during Wallerian degeneration is a calcium-mediated event when the intracellular calcium concentration rises above a threshold concentration of 0.2mM, neurofilament degradation occurs (Glass et al., 1994). Evidence in support of this hypothesis is neurofilament can be maintained intact when incubated in calcium-free media (Schlaepfer and Hasler, 1979b).

The velocity of Wallerian degeneration is dependent on temperature, the age of the animal, and the myelination and caliber of the nerve. Low temperatures slow the rate of Wallerian degeneration in mammalian, invertebrate and lower vertebrate axons (Usherwood et al., 1968; Wang, 1985; Bittner, 1988; Sea et al., 1995; Tsao et al., 1999). The rate of Wallerian degeneration in the optic nerve of cats is slower in the older animals, (Cook et al., 1974). In a study with teased fibres of transected phrenic nerves, the amount of Wallerian degeneration was shown to be least in the thickest fibre at 24 hours (Lubinska, 1977). Thus, unmyelinated axons degenerate first, then the smallest myelinated nerve fibres, and the largest myelinated fibres are the last to degenerate (Weddel and Glees, 1941; Friede and Martinez, 1970). Recent research suggests that mice which lack inducible nitric oxide (iNOS) also show slow

Wallerian degeneration in myelinated axons (Levy et al., 2001), suggesting a role for oxidative enzymes in this process.

In contrast to the rapid degeneration of the distal portion of an axotomised neuron, the proximal portion does not degenerate, at least in adults. There are however some distinct markers of change, in the cell body and its nucleus, the cell body swells, the Nissl substance becomes dispersed, and the nucleus translocates, the nucleus moves from the center of the cell soma to an eccentric location. In some proximal axons motor neuron cell bodies degenerate after avulsion of the spinal roots, a procedure which leaves a very short proximal nerve stump (see Adalbert et al., 2006).

1.4.2 Wallerian degeneration in synaptic terminals

The progression of Wallerian degeneration at the NMJ has been well-documented, in frogs, rats and mice, by such people as Birks, Katz and Miledi (1960), Miledi & Slater (1968 and 1970), Manolov (1974) and Winlow and Usherwood (1975). The degeneration of nerve terminals post axotomy occurs before the degeneration of the axons. In some animals, like rat and frog, initial degenerative changes in the nerve terminals occur within 3-8hours; (Manolov, 1974; Miledi and Slater, 1970). These changes include the swelling and destruction of mitochondria; reduction in the number, and clustering of synaptic vesicles, and subsequently invasion of terminal Schwann cells into the synaptic cleft. More degenerative

changes occur with passing time, like nerve terminals becoming completely fragmented and the terminal Schwann cell engulfing the synaptic terminal.

The numbers and localization of the synaptic vesicle population in motor nerve terminals changes following axotomy, as described by Manolov (1974) and Winlow and Usherwood (1975). From 6hrs to 20 hours the numbers of synaptic vesicles decrease dramatically (Manolov, 1974). Manolov and Winlow and Usherwood described a small reduction in synaptic vesicle numbers occuring 3 hours after nerve section. However, at 20 hours post-axotomy, the majority of nerve terminal profiles had no vesicles left. Manolov found greatly increased neurofilaments, following the reduction in number of synaptic vesicles and degeneration of mitochondria in many nerve terminals which survive for more than 20 hours post axotomy.

Mitochondria are used as an important marker for synaptic terminal degeneration. Miledi and Slater (1970) studied the changes in normal NMJs and axotomised NMJs. In normal nerve endings, diameter of mitochondria is 0.1 -0.2 μm, whereas in endplates undergoing degeneration, mitochondria become swollen and have large circular profiles with diameters as large as 0.7μm. The cristae in the mitochondria often appear "disorganized and broken up into small vesicular fragments" (Miledi and Slater, 1970). In Manolov's (1974) experiments, the same phenomenon was reported as the occurrence of 'dense bodies'.

1.5 Synapse Elimination at the Neruomuscular junction

In rodents, neuromuscular synaptogenesis occurs after myoblast fusion during development, when each motor neuron establishes synapses on different muscle fibres randomly (Bennett and Pettigrew, 1974, Jennings, 1994). By the end of this period each skeletal muscle fibre is supplied by more than one motor axon. Synapse elimination then begins to refine these connections during the first two postnatal weeks (Redfen, 1970; Brown et al., 1976; Betz et al., 1979). Studies have shown that synapse elimination also occurs in other species' nervous systems, such as humans and kittens (Huttenlocher 1982 et al., Bagust et al., 1973).

In 1976, Brown and colleagues studied the elimination of polyneuronal innervation in the soleus muscle of new-born rats. It was found that during the poly-innervation to mono-innervation transition period, there was no significant reduction in the number of motor neurons innervating the soleus muscle. Therefore they concluded that the disappearance of supernumerary inputs reflects a decrease in the number of synapses made by each motor neuron (Brown et al., 1976). The ultrastructure of nerve terminals on neonatal muscle fibres was studied using electron microscopy. This provided evidence that synapse elimination involved retraction of motor nerve terminals from the endplates rather than the Wallerian degeneration process that occurs after nerve injury. No signs of degenerative

processes were found in any nerve terminal during synapse elimination, either in rats, or in rabbits' experiments (Korneliussen et al., 1976; Bixby, 1981). Moreover Bixby described how the nerve terminals and axons are retracted from the endplates to form retraction bulbs.

However, one study suggested that the supernumerary terminals are removed by degenerative mechanisms. Rosenthal and Taraskevich (1977) described that signs of abnormal ultrastructure were observed in neonate end-plates during the period of synapse elimination. Some terminals had a high condensation of synaptic vesicles as well as Schwann cell encroachment into the synaptic cleft, and it was evident that the large areas of postsynaptic membrane opposed only with Schwann cell. All of these characteristics are similar to Wallerian degeneration of motor nerve terminals in the denervated adult mice. However, there have been no published reports to confirm their findings, so they may be incorrect, more research is needed before ruling out this mechanism entirely.

The majority of evidence from other studies support that the supernumerary inputs are removed by withdrawal process rather than degeneration. Although previously focused on reinnervated NMJs, in recent years, Lichtman and his colleagues have studied the mechanism of synaptic elimination at the developing neuromuscular junction using a time–lapse imaging technique. In 2001, they used transgenic mice that express fluorescent proteins in subsets of axons. The results

suggested that branch elimination within a same motor unit appears to be distributed randomly and asynchronously, and that the local competitive environment plays a critical role in deciding branch loss and maintaintenance (Keller-Peck et al., 2001). Subsequently, Lichtman and his colleagues used two transgenic mouse lines designated YFPH and CFP which expressed yellow and cyan fluorescent proteins in different motor axons and developed the time-lapse imaging technique further. They suggested that competition between two axons from two different motor neurons innervating the same synaptic area leads to one axon's retraction accompanied by another axon's expansion (Walsh et al., 2003). In the same year, they used the same technique to further investigate the nature of the neuronal competitors. Their findings suggest that motor neurons form a hierarchy indicated by the endplates they acquire and exclude from other motor units (Kasthuri et al., 2003).

1.6 The *Wld*^{s} phenotype

The *Wld*^{s} mice mouse phenotype was first discovered by H Lunn, M.C. Brown, and V.H. Perry, by accident while investigating the role of recruited myelomonocytic cells in Wallerian degeneration of peripheral nerve (Lunn et al., 1989). Mice were originally supplied by Harlan-Olac to Oxford and many other universities and research institutes in the UK and abroad as C57/Bl6 mice. However, these mice bear the spontaneous mutation that slows axonal degeneration, which neither C57/Bl6J nor C57/Bl6 mice (nor any other mouse line studies to date) show. The initial studies

of the mutant mice referred to them as "Ola" mice. The formal "*Wld*^{S}" was adopted after the chromosomal location of the mutant gene was established (Lyon et a., 1993). Evidently, at some point in the lineage of the Harlan-Olac C57/Bl6 mice there was a spontaneous mutation that was conserved. The mutant mice breed easily and don't show any discernible, neurological phenotype compared with wild type mice. The most distinguishing characteristic of these mice is that Wallerian degeneration is significantly delayed after axotomy or nerve injury. The distal axotomised section and their nerve terminals are preserved completely for as long as 3 weeks in some cases. Of note, the isolated distal axons are still be able to conduct action potentials, and the motor neuromuscular nerve terminals continue to release neurotransmitter and recycle synaptic vesicle for at least 3 days, and in some cases, up to 2 weeks after axotomy (Tsao et al., 1994; Ribchester et al., 1995). Wallerian degeneration is delayed in both sensory and motor axons in these mutant mice after peripheral nerve injury. Moreover the mutation also delays axonal and synaptic degeneration in the central nervous system (Perry et al., 1990a; Ludwin and Bisby, 1992; Gillingwater et al., 2006a).

1.7 The *Wld*^{S} genotype

Perry et al (1990b) showed that the mutant gene in *Wld*^{S} is autosomal dominant. The mutant gene in *Wld*^{S} mice was then mapped to the distal end of chromosome 4 (Lyon et al., 1993), and was subsequently identified within the candidate region to be

an 85-kb tandem triplication; this is a mutant unique to the *Wld*^{S} mice (Coleman et al., 1998). From recent studies exons of three genes were found within the triplicated 85 kb domain (Conforti et al., 2000). Expression of two genes spanning the proximal and distal boundaries of the repeat unit can be found in the nervous system namely the N-terminal 70 amino acids of ubiquitin fusion degradation protein 2 (Ufd2) and the C-terminal 302 amino acids of D4Colele were identified. In the *Wld*^{S} mutant, these two transcripts form an open reading frame for a 43 kDa chimeric protein. However, the third exon in the repeat unit, Rbp7 (a novel member of the cellular retinoid –binding protein family), does not express in the nervous system (Conforti et al., 2000; Figure 1.3). Naturally, attention was focused on the chimeric gene as the best candidate for conferring the slow Wallerian phenotype. Ufd2 has now been demonstrated to be homologous to the human ubiqutination factor E4b (Ube4b) (Mack et al., 2001). Similarly, the novel sequence D4Colele is now shown to incorporate a complete sequence that encodes Nicotinamide mononucleotide adenylyl transferase-1 (Nmnat-1). This enzyme is a nuclear protein and is responsible for NAD synthesis (Emanueli et al., 2001). In addition, the chimeric gene (N70Ube4b/Nmant) includes an N-terminal sequence coding for an additional 18 amino acids in *Wld*^{S} mice. The gene sequence for this peptide is not normally found in wild-type Nmnat. Mack et al (2001) made several lines of transgenic mice expressing N70Ube4b/Nmnat. The amount and rate of Wallerian degeneration after axotomy was shown to be gene dose—dependence (Figure 1.4). For instance, the

data demonstrated that axonal preservation in the heterozygous transgenic mouse line $4836^{Tg/+}$ was similar to that in the mutant *Wld*^{s} mice after the same duration of axotomy, In contrast, heterozygous Tg 4830 mice exhibited only half the axonal preservation compared to *Wld*^{s} homozygotes.

It is important to point out at this stage that homozygous *Wld*^{s} mice therefore express four copies of the chimeric *Wld*^{s} gene, in addition to normal expression levels of Nmnat and Ube4b that make up the mutant gene. Heterozygous *Wld*^{s} mice have only two copies of the chimeric gene. Evidence suggests that Wld^{s} protein in expressed in proportion to the number of copies of the *Wld*^{s} gene (Mack et al., 2001; see figure 1.3). Thus comparing phenotypes in homozygous and heterozygous *Wld*^{s} mice gives a simple and effective way of testing for the effect of the *Wld*^{s} "gene-dose".

A recent genome-wide analysis protein expression profile of *Wld*^{s} mutant in both the mouse cerebellum and human cell cultures revealed that the Nmnat-1/Ube4b chimeric protein regulates a wide range of proteins both positively and negatively. Two prominent candidates were examined in further detail: pituitary tumor transforming gene-1(pttg-1) and erythroid differentiation regulator-1 (edr1/-EST). mRNA expression of pttg-1 was dramatically reduced by 10 fold, whilst edr1/-EST mRNA expression was increased by 5 fold. Interestingly, Nmnat-1 and Ube-4b have different roles in regulating the expression of pttg-1 and edr1/-EST

(Gillingwater et al 2006b). These data strongly suggest that the *Wld*^{S} gene product has a gobal control over a large pool of genes in mediating a neuroprotective effect in *Wld*^{S} mutant mice, with a similar pattern also observed in human cell lines.

1.8 Mechanism of Neurodegeneration in *Wld*^{S} mice

Work on finding the cellular mechanism of the slow Wallerian degeneration in the *Wld*^{S} mice has long preceded the understanding of its molecular nature. In 1989, Lunn et al. first postulated that the failure to recruit systemic macrophages to the distal stump cells in C57BL/6/Ola mice (the line subsequently renamed C57Bl6/*Wld*^{S} mice) accounts for the slow rate of degeneration. However, in subsequent experiments, they refuted this hypothesis by performing transplant experiments (Perry et al., 1990c) which suggested that slow degeneration was caused by an intrinsic property of the peripheral nerve. This finding was confirmed by Glass et al (1993), who found that axonal degeneration in *Wld*^{S} mice was host-dependent after axotomy. In their experiments, *Wld*^{S} axons which regenerated through grafts of peripheral nerve sheaths which containing wild-type Schwann cells degenerated slowly after the regenerated axons were removed, whereas, wild-type axons containing *Wld*^{S} Schwann cells still degenerated rapidly after removal. Moreover, *Wld*^{S} axons still degenerated slowly after nerve injury when the perineurial sheath was injected with the lysophosphatidyl choline to produce a demyelinating lesion (Hall, 1993). Thus, Schwann cells don't appear to show any critical effect on the

slow degeneration of axons in *Wld*^{S} mice. This conclusion is supported by studies of the *Wld*^{S} phenotype in vitro. However, Deckwerth & Johnson (1994) showed that when NGF was deprived, in cultures of *Wld*^{S} neurons, the axons persisted, but the cell bodies underwent apoptosis.

Recent researches have been focused on the molecular mechanism of axon protection by the *Wld*^{S} gene. In particular, efforts have been made to reveal the function of the N70Ube4b and NMNAT genes involved in protection of axons and nerve terminals in the axotomised *Wld*^{S} mice. Hershko, Liechnover and colleagues in 1980 first described the role of ubiquitin (a small, 76 amino acid polypeptide) as a macromolecular tag, which marks proteins destined for degradation to 26s proteosomes (Glickman and Ciechnover, 2002). In 1984 Thomas and Wyman first suggested that the ubiqutination pathway might be involved in the regulation of synaptic connectivity. They described that abnormal synaptic connection between the giant and the tergotrochanter motor neurons resulted from the disruption of the ubiquitin gene in Drosophila. Therefore, one hypothesis is that the partial incorporation of E4 ubiqutination factor Ube4b in the *Wld*^{S} may block degeneration by interfering with protein ubiqutination (Gillingwater and Ribchester, 2001; Mack et al., 2001; Coleman and Perry, 2002).

Nicotinamide mononucleotide adenylyl-transferased (Nmnat) is a whole sequence in the *Wld* gene. This enzyme plays various roles in cells. It is involved in

the NAD biosynthesis, electron-transport in the respiratory chain within mitochondria, and regulates DNA repair and transcription. Therefore, Nmnat could play a critical role in neuroprotective effects observed in the *Wld*^{s} mice. Araki et al (2004) reported that increased nuclear NAD biosynthesis by SIRT1 activation could prevent axonal degeneration. The SIRT1 is located in the nucleus and involved in the regulation of transcription factors such as P53 and chromatin remodeling factors. Thus Araki et al concluded that axonal protection in *Wld*^{s} was mediated by increased Nmnat activity. However, their study was partially refuted by Wang et al (2005), and Conforti et al (2007) who showed that transgenic mice overexpressing Nmnat alone did not show significant protection as in the *Wld*^{s} mice. However, other studies suggested that overexpression of Nmnat in Drosophila does protect axons and synapses from degeneration (Hoopfer et al., 2006; MacDonald et al., 2006). Taken together, all these studies suggest that the role of Nmnat has yet to be fully resolved.

Slow Wallerian degeneration is not the only effect of the *Wld*^{s} mutant gene. Although *Wld*^{s} mice show no obvious difference from the wild-type in appearance and behaviour, other phenotypic features can also be found in the operated and unoperated *Wld*^{s} mice. In unoperated *Wld*^{s} mice, the soleus muscles have more fibres, fewer resident macrophages and lower levels of acetylcholine sensitivity than in wild-type mice. Moreover, the level of serum creatine kinase is lower in C57BL/Ola mice compared to wild type (Brown et al., 1991). As most creatine kinase (CK) is expressed in muscles, a rise in the amount of CK released into the blood indicates

that muscle damage has started to occur. In operated *Wld*^{S} mice, increases of both acetylcholine and CK occurred more slowly compared to wild-type mice. This slowly-occurring increase of supersensitivity to ACh is perhaps not surprising since this could be partially induced by a release of products from nerve degeneration in *Wld*^{S} mice (Brown et al., 1991). Schwann cells show different characteristics in wild type and mutant *Wld*^{S} mice in response to axotomy. In vivo, the resident Schwann cells play an important role in the maintenance of cell types producing maintenance factors which are absorbed by the axon. In peripheral nerves, ciliary neurotrophic factor (CNTF) is expressed in a subset of Schwann cells, when Wallerian degeneration occurs, synthesis of CNTF is decreased. Subang et al (1997) showed that both mRNA and protein levels of CNTF decreased quickly and synchronously and quickly in the axotomised wild type mice. Nevertheless, in *Wld*^{S} mice following axotomy, CNTF remains normal both as mRNA and protein level for up to 4 days. During Wallerian degeneration, the levels of the CNTF protein decrease at a slower pace than the levels of CNTF mRNA in *Wld*^{S} mice. This suggests that the stability of CNTF protein in the axotomised *Wld*^{S} mice, may contribute to the protection of axons. However, it is also plausible that the delayed response of Schwann cells to nerve injury in *Wld*^{S} is due to the absence of signal from degenerating axons in *Wld*^{S} mice (since the axons don't degenerate).

Chemotactic factors produced by the injured nerve, or the loss of inhibitory factor produced by the intact axon could influence macrophage recruitment after

axotomy (Perry et al., 1990c). In particular, one of the chemotactic factors, monocyte chemoattractant protein-1 (JE) fails to be produced in the axotomised *Wld*^{s} mice (Carroll and Frohnert, 1998). Another chemoattractant, granulocyte macrophage colony stimulating factor (GM-CSF), is deficient in *Wld*^{s} mice following axotomy. Furthermore, it is likely that distal axons produce an inhibitory factor to prevent macrophage recruitment in axotomised *Wld*^{s} (Perry et al., 1987; 1990c, Brown et al 1991; 1991a), this does not occur in the axotomised wild-type mice (Ludwin and Bisby, 1992, Gillingwater and Ribchester, 2001).

1.9 Synapse Degeneration in Young *Wld*^{s} Mice

Motor nerve terminals in young *Wld*^{s} mice appear undergo a different process from the classic Wallerian degeneration. *Wld*^{s} NMJs still retain the ability to release neurotransmitter and recycle synaptic vesicle membrane for at least 3 days, and in some cases for 2 weeks, following nerve axotomy (Ribchester et al., 1995).

At wild–type denervated NMJs, synaptic terminals degenerate synchronously. However, the morphology of terminal degeneration in axotomised *Wld*^{s} mice is distinct. Using vital dye labeling immunocyto-chemistry and electrophysiology, a piecemeal form or withdrawal of axotomised *Wld*^{s} nerve terminals and retraction of axons have been suggested by several studies indicated by the progressive, asynchronous loss of synaptic contract at individual endplate (Mattison et al., 1996; Parson et al., 1998; Ribchester et al., 1999). These studies suggest that axotomised

nerve terminals are gradually removed from the endplates, until they retract back to the distal end of the axon. The ends of the axons appear to the swollen "retraction bulbs", which are detached from the endplates (Mattison, 1999). Physiological experiments also demonstrated changes in the synaptic terminals, such as a reduced quantal content and the occasional appearance of 'giant' miniature endplate potentials (MEPPs). Likewise, in ultrastructure, the axotomised synaptic endplates in *Wld*^{S} neurons are different from wild type mice. None of the classical signs of degeneration such as mitochondrial swelling and disruption can be found during degeneration, but some large vesicles as large as 130nm appear in the pre-synaptic membrane. This perhaps suggests that the synaptic vesicle retrieval mechanism has been impaired during nerve terminal withdrawal in the *Wld*^{S} mice (Ribchester et al., 1995, Gillingwater et al., 2001). These authors also draw attention to the remarkable resemblance between motor nerve terminal "degeneration" as it appears in *Wld*^{S} mice and the natural process of synapse elimination, which underlies the remodeling of neuromuscular connections during normal postnatal development. Both procedures appear to be qualitatively distinct from Wallerian degeneration of synaptic terminals in wild-type mice.

1.10 Synapse degeneration in the Older (> 7months) *Wld*^{S} mice

In 1992, Perry et al first elucidated that the rate of degeneration slowed by the

Wld^S gene increased with the age of the animals. In the four weeks old *Wld*^{S} mouse nerve stimulation produced compound action potentials (CAP) that could be evoked in the distal nerve stump after section for up to 3 weeks. In 1-year-old mice however, the authors didn't find any action potentials 5 days after nerve section, this was similar to the wild type mice, where all axons were completely degenerated by 5 days after axotomy. In the young *Wld*^{S} mice, functional neuromuscular transmission is presented in all muscle fibres up to 3 days after nerve section, while, in *Wld*^{S} mice more than 8 weeks old, the neuromuscular transmission is lost after around 2 days.

On the other hand, data published by Gillingwater et al (2002) suggest that, rather than axonal degeneration, the degeneration of synaptic terminals in the *Wld*^{S} mice is age dependent. When *Wld*^{S} mice are over 4 months old, the morphology of nerve terminal degeneration reverts to that in wild type mice (Gillingwater et al., 2002). In contrast to these studies, Crawford et al (1995) proposed that both axonal loss and synapse loss were independent of age.

Ultrastructural analysis of the response to axotomy in motor nerve terminals of 4-month-old *Wld*^{S} mice showed swollen and distorted mitochondria, but intact synaptic vesicles. In ultrastructural analysis of synaptic boutons originating from the same motor nerve axon, some boutons contained abnormal mitochondria, but other boutons did not. In 7 months old *Wld*^{S} mice, at 2 days post axotomy, more classical degenerative characteristics were found, such as disrupted mitochondria, reduced

synaptic vesicle densities, membrane disruption, and terminal Schwann cell phagocytosis. From morphological analysis of preparations observed by immunocytochemical staining very few partially-occupied endplates were seen, which reflects that endplates degeneration is a rapid process in old *Wld*^{s} mice. Most endplates were either fully occupied or vacant, In 4 months old *Wld*^{s} mice about 35% endplates were occupied following 3 days axotomy, but in 7 months old mice, fewer than 5% occupied endplates remained by 3 days. Thus, it was proposed that the synapses were removed synchronously in the older *Wld*^{s} mice. Arguably, this could simply mean that synaptic degeneration is more rapid in wild type mice, such that few partially-occupied endplates are observed at any given time point. However, at present this interpretation can not be distinguished from a qualitatively different mechanism.

1.11 Compartmental Neurodegeneration

Under normal circumstances, death of the cell body is followed by rapid degeneration of other neuronal compartments: dendrites, axons and synaptic terminals. With the discovery of phenotype in *Wld*^{s} mutant mice, a dissociation between normal cell body apoptosis and Wallerian degeneration was revealed (Lunn et al., 1989; Mack et al., 2001). Wallerian degeneration is absent or delayed after axotomy in these mice. Further studies of *Wld*^{s} mice suggested that soma, axons and synapse represent independent neurodegeneration compartments (Gillingwater and

Ribchester, 2001; 2002, and Figure 1.4).

All evidence obtained to date suggests that the *Wld*^{s} gene protects the axons and synapses but not cell bodies (Gillingwater and Ribchester, 2001; 2003, Wang et al., 2006). For instance, conversely Wld^{s} expression does not protect cell bodies from apoptosis (Adalbert et al., 2006), it has been found that when genes such as Bcl-2 are overexpressed, apoptosis is inhibited, but Wallerian degeneration is not. Bcl-2 is one of three main regulators of apoptosis in neurons (Gillingwater and Ribchester, 2001). However, Burne et al (1996) and Sagot et al (1995) showed that in retinal ganglion cells and facial and phrenic motorneurons respectively overexpression of the human Bcl-2 protein protected cell bodies, but there was no effect on the rate of axonal degeneration. Thus, Bcl-2 selectively protects cell bodies while *Wld*^{s} selectively protect axons.

Might nerve terminals be a distinct neurodegenerative compartment? Motor nerve terminals are among the first junction to describe the degeneration after nerve injury (Miledi and Slater, 1968; 1970). They are weakly protected in *Wld*^{s} mice that is, they degenerate more slowly than in wild-type mice and more rapidly than axons in *Wld*^{s} mice. However, as yet no genes have been identified that selectively protect motor nerve terminals to the same extent as *Wld*^{s} protects axons. Cregan et al (1999), Lebanc et al (1999), and Kuida (2000), suggested that Caspases 3, 6, and 9 regulate apoptotic cell death in neuron. Mattson et al (1998) found no caspase activation in

axons, and instead reported that caspases were activated in cortical synaptosome. But it remains to be seen whether mutation in these signaling pathway leads to synaptic protection. Thus the independence of synaptic terminal degeneration from axonal degeneration remains to be firmly established.

It has been suggested that the withdrawal of nerve terminals in *Wld*^{s} mice is similar to the pattern of synapse elimination that occurs at NMJs during postnatal development and reinnervation in mice (Sanes and Lichtman, 1999; Gillingwater et al., 2001; 2002; 2003). Synaptic elimination occurs at a normal rate in neonatal *Wld*^{s} mice (Parson et al., 1997). Gillingwater et al (2002) also found that age is a significant factor, influencing the rate and pattern of synaptic degeneration in *Wld*^{s} mice after axotomy (Figure 1.5). Another variable is the length of severed axons. An open question also remains as to the role of neuromuscular activity in the maintenance of axotomised nerve stumps. It is perhaps reasonable to expect this, because activity influences other aspects of neuromuscular synaptic plasticity, including synapse elimination, sprouting and nerve regeneration (see for example, Richester & Taxt 1984, Ribchester, 1988, Barry & Ribchester, 1995, Costanzo et al., 2000).

1.12 Neurodegenerative disease

Many recent studies have shown that synaptic degeneration is among the first step in the development of several types of neurodegenerative diseases. For example,

Alzheimer's disease is now thought to be primarily a disease of synapses (Mattson et al., 1999; Selkoe, 2002). In Parkinson's disease, and some variants of Alzheimer's disease dementia with Lewy bodies, α-synuclein is known to play an important role in neurodegeneration (George, 2001; Lotharius and Brundin, 2002; Kotzbauer et al, 2001; Iwai, 2000). Transgenic overexpression of the human presynaptic protein α-synuclein in mice resulted in a retraction of nerve terminals from dendritic spines in the brain (Van der putten et al., 2000). Gillingwater et al (2006a) have shown that in the young *Wld*^{s} mice morphological degeneration of nerve terminals following axotomy in the CNS is distinct from that in the PNS. Although they were still delayed by the *Wld*^{s} gene following axotomy, the pattern of synaptic degeneration reverted back to that in the PNS of wild type mice. The axons nonetheless remained well-protected by the *Wld*^{s} gene. These new findings in the CNS of *Wld*^{s} mice could provide new directions for investigating Parkinson's, and Alzheimer's diseases, in which synaptic dysfunction and degeneration are also thought to precede neuronal cell death (Selkoe, 2002, Isacson et al., 2003).

Motor neuron diseases (MND) are a kind of progressive neurological disorder. Motor neurons, the cells that control speaking, walking, breathing and swallowing, are destroyed. They are a group of chronic progressive diseases (Gros-Louis et al., 2006), for which there is no effective treatment or cure. Amyotrophic lateral sclerosis (ALS) is an adult-onset form of motor neuron disease, also called Lou Gehrig's disease. It was first described by the French neurologist Jean-Martin

Charcot in 1869. The main hallmark of ALS is the progressive degeneration of neurons in the spinal cord and motor cortex, especially motor nerves that form corticospinal tracts.

ALS is classified into two forms, such as 90% of cases are sporadic ALS (SALS), and as they are not associated with a family history, and 10% are familial ALS (FALS), which are inherited. Among familial cases, nearly 20% are caused by dominantly inherited mutations in the protein Cu/Zn superoxide dismutase (SOD1) (Bruijn et al., 2004). Sporadic and familial forms display a similar clinical pathology, hence suggesting a common pathogenesis (Bruijin et al., 2004; Gonzalez de Aguilar et al., 2007). However, the exact cause in most cases is still unknown.

Since the 20% of familial ALS cases are caused by an inherited mutation in the protein Cu/Zn superoxide dismutase (SOD1) (Rosen et al 1993), animal models of ALS, such as SOD1 mice, provide a unique opportunity to study the mechanism of familial and sporadic ALS diseases, by virtue the conspicuous pathological and clinical similarity between them. To date there have been many findings based on experiments on SOD1 mice, from neuronal to nonneuronal cells, from pathology to ultrastructure. Pramatarova et al (2001) and Boillee et al (2006) have shown that changing SOD1 expression only in motor neurons does not trigger ALS disease or alter the lifespan of animals. Ultrastructure, studies have shown, for example, accumulation of manganese superoxide dismutase 2 in the mitochondrial matrix,

which exacerbates disease in transgenic SOD1 mice. (Andreassen et al., 2000). Accumulation and abnormal assembly of neurofilaments are found in familial ALS (Hirane, 1984). Furthermore, life span is increased in the $SOD1^{G37}$ line by increasing expression of NF-H in the neuron cell body. Dynein, a microtubule cytoplasmic motor protein involved in processes of vesicular transport, cell division, and retrograde transport in the axon (Levy and Holzbaur, 2006) has also been studied. Overexpression of an ALS-linked mutant dynactin, which activates dynein is sufficient to induce motor neuron degeneration (Gonzalez de Aguilar et al., 2007). When microglia activation is blocked by minocycline, an antibiotic, ALS disease is slowed in the ALS mice. (Yrjanheikki et al., 1999; Kriz et al., 2002; Zhu et al., 2002) Moreover some growth factors and neurotrophic factors might play a role in ALS, for example, vascular endothelial growth factor (VEGF) decreases the age at onset of disease and life span, when its own levels were reduced in $SOD1^{G93A}$ transgenic mice (Bruijin et al., 2004). Gene mutation, CNTF, a neurotrophic factor, have also been found in ALS patients (Giess, 2002). From biochemical analysis, several hypotheses have been proposed such as, aberrant chemistry of the active copper and zinc sites of the misfolded enzyme causing ALS (Beckman et al., 1993).

Although there have been many discoveries made from studies of SOD1 mice, none of these has yet been translated into effective treatment for ALS. Given that ALS is thought to be a complicated and "systemic disease" (Gonzalez de Aguilar et al., 2007), finding effective treatments for ALS remains a challenge in the future, but

one in which the SOD1 mouse model is still likely to play a significant role.

Nevertheless, studying motor neuron degeneration at the NMJs of SOD1 mice may yield some new insights that aid our understanding of ALS disease in SOD1 mice. Schaefer et al (2005) demonstrated in the $SOD1^{G93A1}$ mouse model that degenerative and regenerative changes both occur in different branches of the same motor neuron pool. Hence, protecting compensatory growth could be a new target in disease treatment. Moreover, Pun et al (2006) suggest that different types of motor neurons show distinct responses in the disease. For instance, fast fatiguable axons (FF) degenerate more rapidly than axons of fast-fatigue (FR) resistant and slow (S) motor neuron. These findings indicate that a fuller understanding of the mechanism of disease in SOD1 mice may well be accomplished in due course.

Discovery of *Wld*^{s} mice presents potential benefit for treatment of ALS mice, since the *Wld*^{s} gene protects against both axonal and synaptic degeneration. Studies have shown that when *pmn* mice are crossed with *Wld*^{s} mutant mice, the synapse loss and neuronal death are reduced (Ferri et al., 2003). Thus it was anticipated that crossing SOD1 mice with *Wld*^{s} might be have a similar result, since progressive synaptic loss had been found in the early stages of ALS disease in the SOD1 transgenic mouse (Maselli et al., 1993; Frey et al., 2000; Gillingwater et al., 2003) Unfortunately, this result was not obtained. Only modestly prolonged survival and delayed denervation could be found at the neuromuscular junction in $SOD1^{G93A,}$

when crossed with *Wld*^{S} mice (Fischer, 2005). Evidently, the *Wld*^{S} gene can not delay regression of axons and synapses in SOD1 mice.

In conclusion, although axotomy-induced retraction of motor nerve terminals in the *Wld*^{S} mutant has provided new possibilities for using neuromuscular preparations to investigate synaptic form and function in the early stages of neurodegeneration, the utilization of the *Wld*^{S} phenotype to protect against disease has yet to reach fruition. This is in part for the reason that our understanding of the causes and limitations of the *Wld*^{S} phenotype is yet incomplete. .

1.13 Aims of the present study

This thesis is primarily concerned with those features that significantly alter the strength, pattern and rate of degeneration of neuromuscular synapses in *Wld*^{S} mice. I have used conventional fluorescence microscopy, confocal microscopy and immunochemical staining techniques to find out more about the gene-dose and age-dependent effects of the gene on the degeneration of axons and synapses in the *Wld*^{S} mice, in an endeavour to discover the possible relationships between theses features.

My aim in this thesis is to advance our knowledge of nerve degeneration mechanisms and its inhibition by the *Wld*^{S} gene, focusing in particular on synapse degeneration. I developed a new analytical method, representing synaptic

degeneration under different conditions in the form of "Polyhedral Degeneration Diagrams" (PDD). Analysis of synaptic degeneration using PDD facilitates the interpretation of different patterns of degeneration of axons and nerve terminals, extending our knowledge of the neural degeneration patterns and how it is regulated, for example by the *Wld*^{s} gene dose. The specific objectives of this thesis are three -fold:

1. To extend knowledge and understanding of the degeneration of axons and synapses in normal and in homozygous and heterozygous *Wld*^{s} mice following axotomy. Qualitative and quantitative immuncytochemical staining and confocal microscopy and conventional fluorescent microscopy were carried out on nerve terminal preparations of young C57/Bl6 mice, young (1-2month) homozygous *Wld*^{s} mice, and young heterozygous *Wld*^{s} mice. The main purpose of these experiments was to obtain evidence that would further evaluate the hypothesis that neuromuscular synaptic protection is more sensitive than axon protection to the *Wld*^{s} gene dose. PDD were used to analyse the patterns of synaptic degeneration among these types of mice. Wld^{18} antibody was used to stain the Wld^{s} protein in cerebella granule cells, and fluorescence intensity from labelled secondary antibodies was determined, as a measure of Wld^{s} protein

2. To extend previous studies of nerve terminal degeneration and its age-dependence in *Wld*^{s} mice. Data and PDD analysis from old (>7months)

axotomised *Wld*^{s} NMJs at different time points were compared with those in young homozygous and heterozygous *Wld*^{s} mice. Furthermore, I measured protein expression in cerebullar granule cells in these mice to examine whether age-dependent loss of synaptic protection is related to changes in levels of *Wld*^{s} protein expression.

3. To test the hypothesis that synaptic degeneration in *Wld*^{s} mice can be altered by factors such as nerve stump length and blocking neurotransmitter release. In the first experiment, degeneration of nerve terminals at *Wld*^{s} mouse NMJs following tibial nerve section was compared with that following sciatic nerve section. I compared the effect of injection of botulinum toxin (BoTox) in young and old mice.

The results presented in the following chapters support a compartmental model of neurodegeneration, in which *Wld*^{s} synapses are much more sensitive than axons to the gene dose of *Wld*^{s}. The findings also suggest that loss of synaptic protection in more mature *Wld*^{s} mice could be explained by an age dependent decrease in Wld^{s} protein expression. Neither nerve stump length nor activity appeared to mitigate the rate of synaptic degeneration to any great extent.

Preliminary reports of my research were presented at international meetings of the Federation of European Neuroscience Societies (Fens, 2004) and the Society for Neuroscience (SFN, 2005). See Appendix II for Abstracts.

Figure 1.1

Schematic diagram of compartmental model of neurodegeneration showing distinct degeneration in cell body, axons and synapses of neurons (blue=cell body; purple = axon; yellow = synaptic terminals). From *Gillingwater et al* 2003

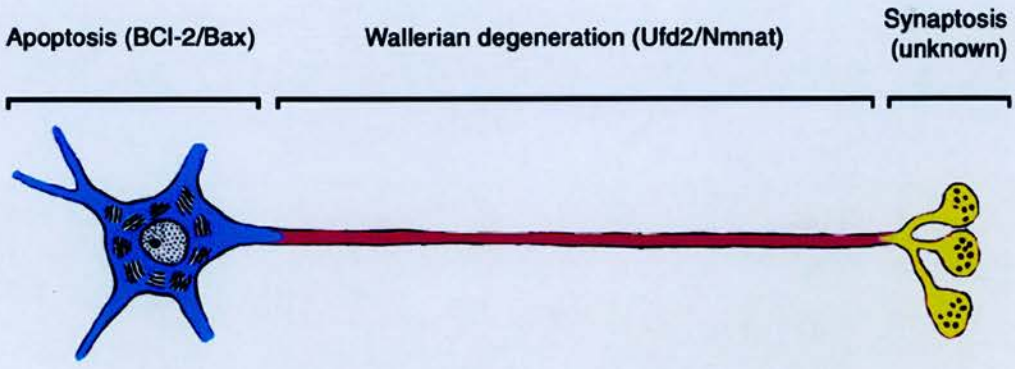

Based on Gillingwater & Ribchester 2003 J Neurocytol. 32:863-81

Figure 1.3

85-kb *Wld*^{S} triplication repeat unit with exons (Nmnat, Rbp7, Ube4b) In *Wld*^{S}, three adjacent repeat units are shown to explain (*a*) how *Ube4b* and *Nmnat* are brought together to form a chimeric gene, (*b*) how *Rbp7* is present at three points in the *Wld*^{S} gene. From *Conforti et al (2000)*

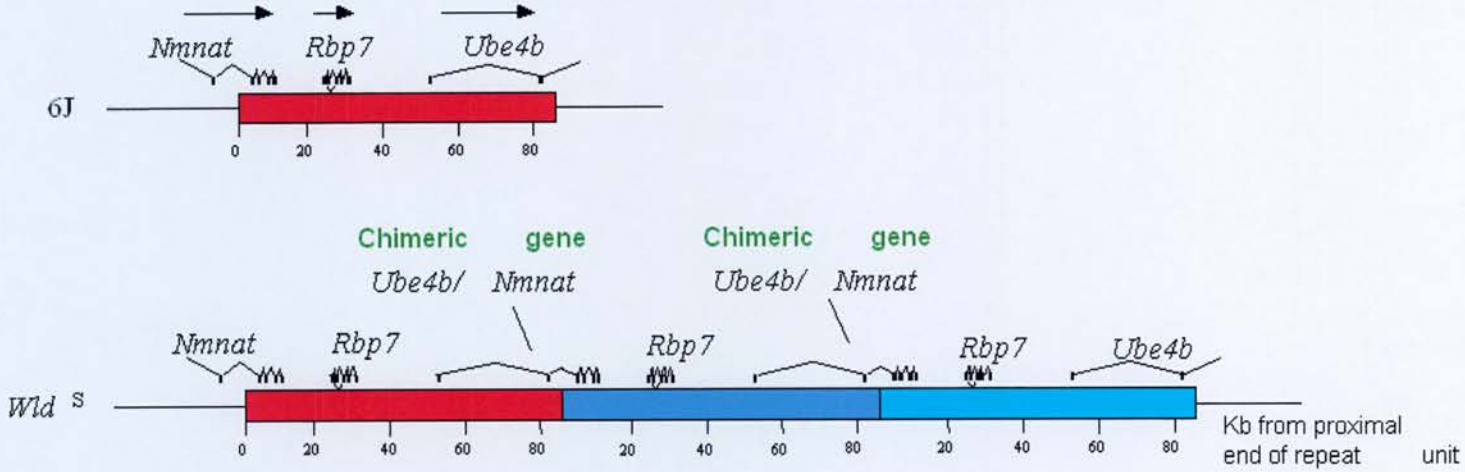

Conforti et al. (2000) Proc. Natl. Acad. Sci. 97: 11377-82

Figure 1.4

Axon protection by the *Wld*^{s} gene is gene-dose dependent. Axon preservation is associated with the expression level of Wld^{s} protein. Black circles, white circles and crosses represent 3, 5 and 14 days post axotomy respectively. From *Mack et al 2001*

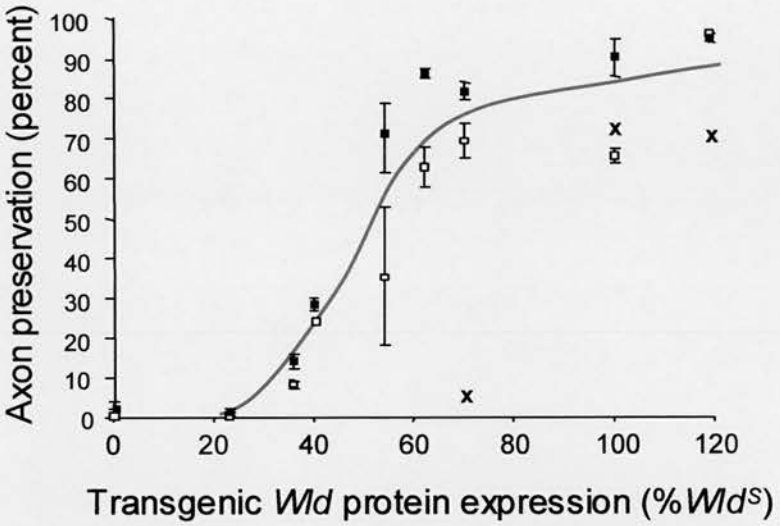

From ***Mack et al. 2001 Nat Neurosci.1199-206.***

Figure 1.5

Schematic diagram showing different models of synaptic degeneration from developmental synapse elimination (left) to Wallerian degeneration (right). In the middle two are the responses to axotomy in young *Wld*^{s} mice (middle left) and mature *Wld*^{s} mice (middle right). Synapse degeneration in young *Wld*^{s} mice resembles wild type mice. In mature mice the synapse degeneration resembles wild type mice, although axons are protected well by the *Wld*^{s} gene.

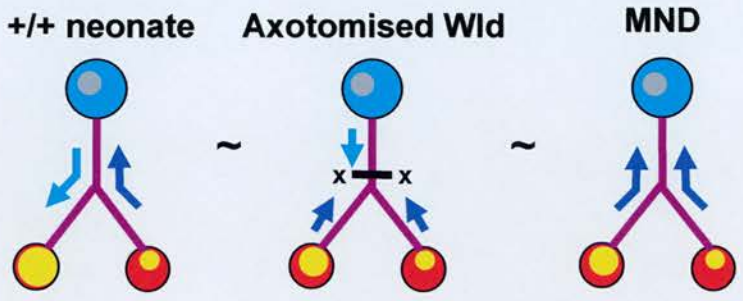

Based on Gillingwater & Ribchester 2003 J Neurocytol. 32:863-81

2. Methods

2.1 General

The protocols discussed in this section are common to all chapters. Methods specific to individual chapters are briefly described in the relevant chapters.

2.1.1 Animals and Animal Care

Male and female young and old YFP16/*Wld*^{S} mice (5-10 weeks old defined as 'young', 7 months old defined as 'old'), young heterozygous YFP16/*Wld*^{S} mice (*Wld*^{S} crossbred with Balb/c mice), young YFP16/Bl6 mice (2 months old) and young CFP/*Wld*^{S} mice were used for experiments. Animals were housed in cages of 5 or less with free access to food and water. Environmental conditions were those of a standard animal house.

YFP/CFP transgenic mice: Two kinds of YFP mice were used: YFP16 transgenic mice which express the yellow-green fluorescent protein (YFP) in all axons, and YFP-H transgenic mice which are expressed in very few axons (< 10%). CFP: CFP transgenic mice which express cyan fluorescent proteins in their axons, nerve terminals, and dendrites (Feng et al., 2000). There is no expression of fluorescent protein in either myelinating or terminal Schwann cells in these mouse lines. These lines were initially obtained from Jackson labs and crossed with *Wld*^{S} mice in Edinburgh.

2.1.2 Aseptic Procedures

All surgical procedures were undertaken under aseptic conditions and were fully licensed by the Home Office (PIL: 60/9199; PPP 60/3277). Sterile instruments, and cloths were used during surgical procedures.

2.1.3 Surgical Procedures

All surgical procedures were carried out under licence in accordance with the Animal (Scientific Procedures) Act of 1986.

Anaesthesia

The animal was placed in a sealed Perspex chamber into which Halothane (Rhone-Poulenc Rorer, Ltd. France) at 1-5% in N_2O/O_2 (1:1) was delivered, using a Fluovac System (International Market Supply, UK). Once the animal was unconscious, a toe-pinch reflex test was used to assess depth of anesthesia. It was then transferred to the operation table where anaesthesia was continued via a face mask. The level of halothane was reduced at this point to 1-3% in N_2O/O_2 (1:1). The flow rate was adjusted during the whole procedure to maintain deep anaesthesia.

2.1.4 Nerve Cut

The operative areas of the animal were shaved before incisions were made. Either the sciatic or the tibial nerve was exposed by using sharp scissors, and a 1-2 mm section of nerve was removed. The wounds were closed and sutured using 6/0

silk suture (Ethicon). Lumbrical muscles were examined 6 hours – 9 hours later. The distance between the lesion sites in the sciatic and tibial nerve was almost 2cm (Figure 2.1). These lesion sites are the same as those used to test for nerve – stump length effects in a previous study (Ribchester et al, 1995).

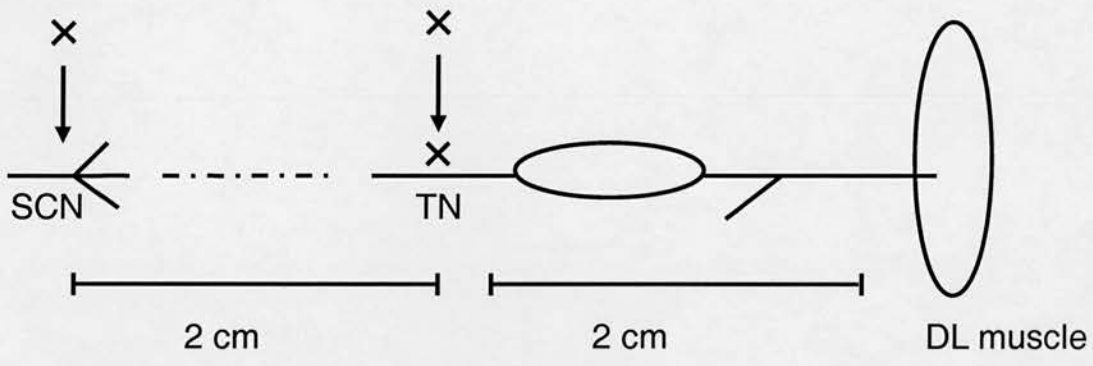

Figure 2.1 Diagram of transaction sites between tibial nerve and sciatic nerve

2.1.5 Animal Sacrifice

All animals were killed by cervical dislocation, in accordance with schedule 1 of the licensing regulations provided by the Home Office.

2.2 Isolation of Muscles

After sacrificing the mice, hind limbs were removed and the four deep lumbrical muscles in both hind feet were dissected, in mammalian physiological

saline concentrations in millimolar: NaCl 120; KCl 5; $CaCl_2$ 2; NaH_2PO_4 0.4 $NaHCO_3$ 23.8; D-glucose 5.6). Dissected muscles were pinned out in Sylgard-coated Petri dishes, using 0.2mm diameter minutien pins.

2.3 Neuromuscular Junction (NMJ) Staining (Immunocytochemistry)

Lumbrical muscles pinned out in Sylgard coated Petri dishes were fixed in 4 % paraformaldehyde (Sigma) for 30-45 mins before labeling acetycholine receptors with TRITC-α-BTX (Molecular Probes) in 0.2M PBS. The preparation was placed on a rocking platform to agitate the buffering solution for 30 mins in the dark. After discarding the α-BTX solution, the muscles were washed in PBS (0.01 M phosphate and 0.9% NaCl, PH7.5). Muscles were then incubated in primary monoclonal antibodies against 165 kDa neurofilament proteins (2H3), and the synaptic vesicle protein (SV2), both primary antibodies obtained from (Development Studies Hybridoms Bank, Iowa).

The primary antibodies were then labeled with FITC-conjugated rabbit (Dako A/S company, Denmark) anti-mouse secondary antibody. Finally the muscles were mounted on glass slides for imaging.

2.4 Visualisation of NMJs Staining Using Confocal Microscopy

Since the main technique used in the present thesis work was fluorescence confocal microscopy, a brief review is provided here to describe this method.

2.4.1 What is fluorescence?

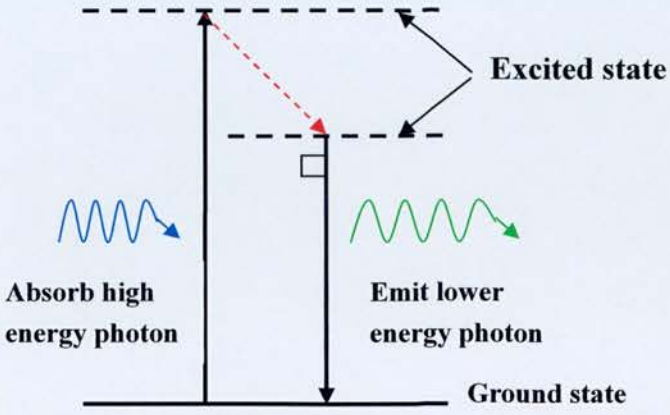

Figure 2.2

The phenomenon that molecules absorb light of energy (475nm blue, for example) and emit light of lower energy (515nm green, for example), is commonly called fluorescence. The emitted light typically has a larger wavelength (Stoke's shift), since emitted photons have less energy than that used to propel them into the excited state. The fluorescence process is sketched in Fig.2.2 Incident blue-light photons excite an electron from a ground state to one of the available excited energy

levels of the molecule. The excited electron may partially lose its energy by heat (infrared light), and then makes a transition back to the ground state, emitting green light. Fluorescein acts this way and is a commonly used fluorophore for staining a sample for fluorescence microscopy.

YFP has an excitation maximum of 520nm and an emission maximum of 532nm; CFP has an excitation maximum of 430nm and an emission maximum Of 476nm, and TRITC has excitation/emission maximum of 550nm and 573nm respectively.

2.4.2 Fluorescence Microscopy

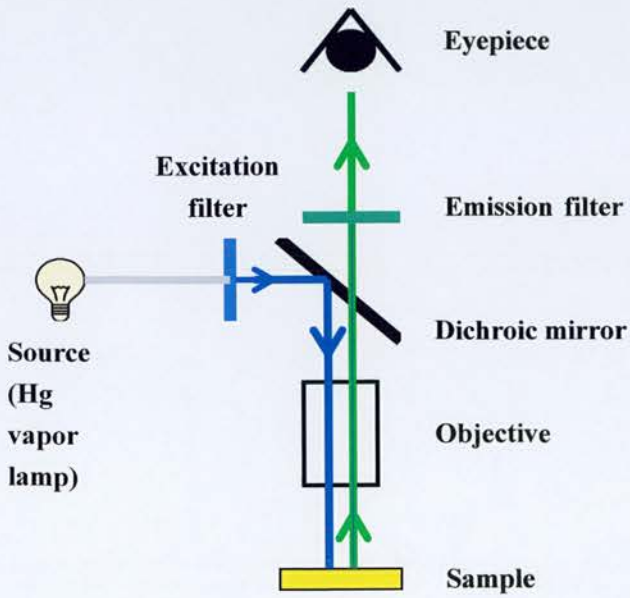

Figure 2.3

In a typical flurorescence microscope, as shown in Fig 2.3, Light from a mercury vapor lamp (blue, for example) is filtered to yield an appropriate wavelength. This light enters the microscope and hits a **dichroic mirror**. This reflects light at the excitation wavelength onto the specimen. The excitation (blue, for example) excites fluorescence (green) within molecules in the specimen. The emitted green light is collected by the objective lens and passes through the dichroic mirror, and an emission filter which blocks stray excitation wavelengths forming an image through the eyepiece. For YFP fluorescence, a conventional FITC filter cube is adequate and was used in this study. A standard TRITC filter cube was used to view labeled Ach receptors (via TRITC-α-BTX binding). For CFP fluorescence a customized filter block, comparing a 435nm excitation filter, 475nm dichroic mirror and 515nm emission filter was used.

In conventional fluorescence microscopy, the entire view of the sample is completely illuminated, making the whole region fluoresce at the same time. The objective collects fluorescence light from whole region, and then forms an image through the eyepiece. Out-of-focus regions above and below the focal plane contribute to a background haze in the resulting image.

2.4.3 Confocal Microscopy

In order to create less haze and better contrast images from the sample, confocal fluorescence microscopy was developed as an enhancement to conventional

fluorescence microscopy.

The first confocal microscope was invented by Marvin Minsky in the mid-1950s (Minsky, 1988). However, his invention remained unnoticed for a long time, mainly due to the lack of good imaging technology at that time. With the invention of the laser and digital image processing ,confocal microscopes became practical during the late 1970s and the 1980s (Amos and White., 2003). A nice summary about the history and principle of confocal fluorescence microscopy was given by J. W. Lichtman in 1994 (Lichtman, 1994).

The main improvement in a confocal microscope is obtained by placing a pinhole aperture in front of a detector. The pinhole is placed at the exact position of the image of focal point of the objective lens on the sample. Thus, the pinhole is conjugate to the focal point of the lens; hence the name "confocal pinhole". Fluorescent light from the focal point on the sample will pass through the pinhole and thereby reaches the detector. In contrast, most of the light from location above and below in the focal point are deflected outside the pinhole and are blocked by the screen. So the detected light is mainly from the focal point region, resulting in a sharp image of that region.

In a confocal microscope, only one point of the sample is observed at any given instant. Complete data from a specimen are obtained by laterally scanning a focused laser beam across the specimen. This point of illumination is brought to focus in the

specimen by the objective lens, and scanned using some form of scanning device under computer control. The sequences of points of light from the specimen are detected by a photomultiplier tube **(PMT)** though the pinhole, and the output from the PMT is built into a complete master-screen image displayed on a computer monitor (Figure 2.4).

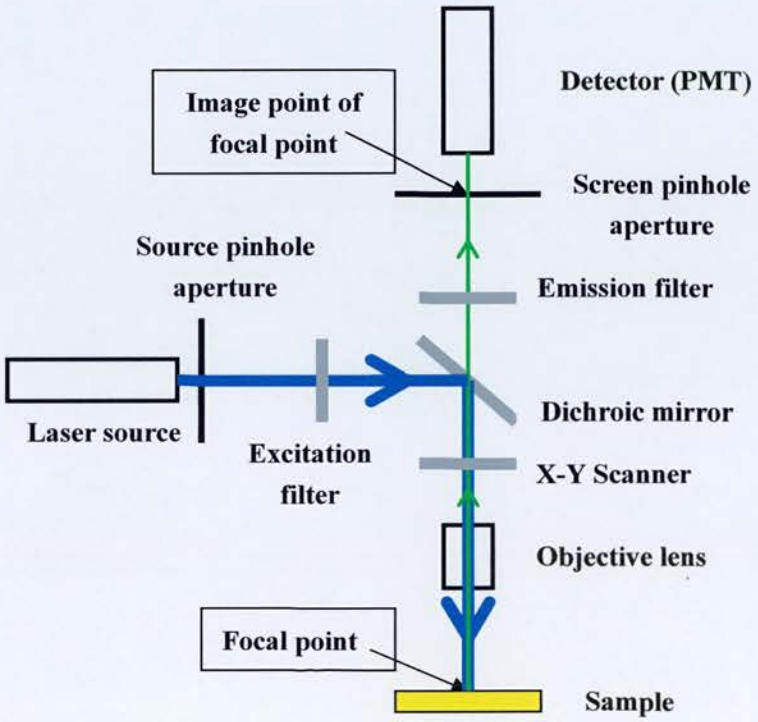

Figure 2.4

The confocal microscopy offers several advantages over conventional optical microscopy, including shallow depth of field, elimination of out-of-focus glare, and the ability to collect serial optical sections from thick specimens. In the biomedical

sciences, a major application of confocal microscopy involves imaging either fixed or living cells and tissues that have usually been labeled with one or more fluorescent probes. These advantages were used to good effect in my studies.

2.5 Confocal Images of NMJs

My samples were viewed in a Bio-Rad-Radiance 2000 confocal laser scanning unit, configured on an upright Nikon Eclipse E600FN microscope. Multi-line Argon (457nm, 477, 488 and 514nm), Green HeNe (543nm) and Red Diode lasers (637nm) were used as laser light sources. The external detector unit with built-in photomultiplier was connected to the microscope via a fiber optic-cable. The microscope was connected to a Dell PC with systems Control Boards and Lasersharp Application Software, including Image Acquisition, Scan Settings, Rea-time image calculation, Hardware Control, Image Display, Image Processing, Image Analysis, and 3D Visualization. Images were enhanced and analyzed using Adobe Photoshop before being printed on an Epson Stylus Colour 900 printer.

2.6 Quantification of Immunocytochemically Labeled Neuromuscular Junctions

All NMJs on every slide were counted and analysed. Each NMJ was analysed by the proportion of postsynaptic terminals contacted by presynaptic terminals, and divided into one of the following categories: 0% vacant, 1%-25% occupied,

26%-50% occupied, 51%-75% occupied, 76%-99% occupied, 100% fully occupied. All data were inserted into a Microsoft Excel spreadsheet for further analysis, and graphs were produced in Excel and GraphPad Prism.

2.6.1 Method of Quantification of Synaptic Degeneration

Scion Image programme (based on NIH image and downloaded from www.scioncorp.com) was used to measure the occupancy of the nerve terminals. First, two different channels (green/red) of synaptic terminals were taken under confocal microscopy (Figure 2.5 A). Second, the number of pixels in each of different channel images over the defined endplate area was measured by using Scion image programme (Figure B&C). Third, the occupancy of each endplate was calculated: Occupancy% = Green Pixel/ Red Pixel*100. In practice, the semi-quantitative assessment of endplate occupancy formed a sufficient basis for most of the analysis.

Figure 2.5 Scion Image Quantification of Nerve Terminals

(A) Confocal images of a NMJ in the green and red channels, alongside a merged image.

(B) An image of a single nerve terminal from the green channel exposed into Scion Image.

(C) An image of a single nerve terminal from the red channel exposed into Scion Image.

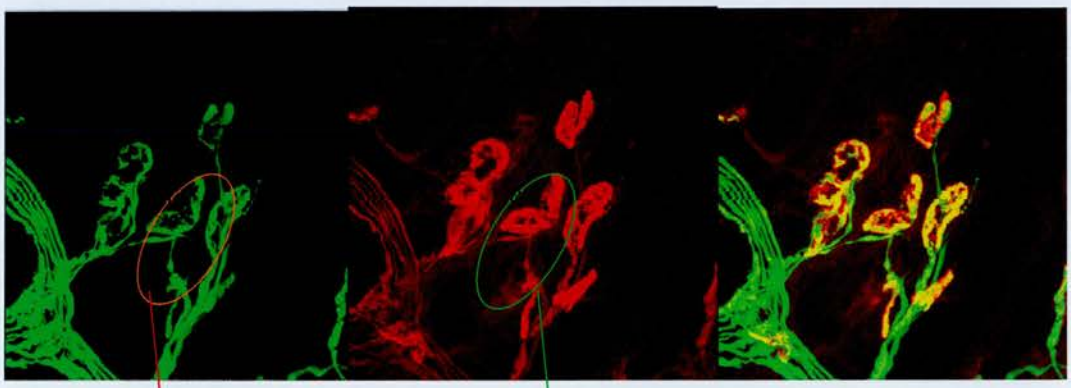

(A)

(B)

(C)

2.6.2 Polyhedral Degeneration Diagram (PDD)

Further analysis of the possible relationships between states of innervations was attempted using a model geometric method. I first classified the state of innervation and occupancy of neuromuscular junctions in different types of animals following axotomy, I then constructed diagram to represent these states. In my PDD method, circles were placed at the apices of polyhedra, each representing a different state of synaptic degeneration. Using Microscope PowerPoint, the diameter of the circles was defined by the percentage (scaled to 1/32 i.e. 1%=1/32) of neuromuscular junctions in each category.[1] Arrows pointed out the possible links between the different states. The relative proportion of terminal in the given states at different time points allowed me to infer the most likely 'trajectories' of degeneration from the fully occupied to the vacant states. See Chapter 6 for more details.

2.7 Immunofluorescent Staining for Wld^S Protein on Cerebellum Slices

Following killing the animals, the skull was cut open with scissors and the brains were removed and rapidly transfer into cold oxygenated ACSF (See Appendix I for composition). To form a flat edge, one side of the brain was removed, and the flat edge was stuck with superglue at the bottom of a slicing chamber. Sagital slices

[1] The PowerPoint version used for that measurement employ inches as a unit of length rather than centimeter, but since the calculation gave a dimensionless result this did not matter.

100μm thick were cut, and immediately placed in 4% paraformaldehyde solution to fix for 20 mins. Section were then twice washed in 0.1M PBS, the brain slices were incubated in freshly-made blocking solution overnight in cold-room (4°C), and the solution was placed on a rocking platform to agitate the solution. After discarding the blocking solution, the brain slices were incubated overnight in rabbit-primary antibody Wld^{18} (generous gift from Dr. M P Coleman). This antibody recognizes the Wld^{s} protein uniquely and with high affinity. The epitope corresponds to an 18 amino acid polypeptide linking the N70 Ube4b and Nmnat region, corresponding to an mRNA which is not normally translated in wild-type mice. The primary antibody was then labeled with TRITC or FITC labeled anti-rabbit secondary antibody overnight. After a quick wash in 0.1 M PBS three times, Topro-3 was applied into the solution for 10 mins to label nuclear DNA. After a quick wash in 0.1M PBS, the brain slices were mounted in mowiol (Calbiochem) for confocal imaging. See the end of chapter for detailed protocol.

2.8 Statistical Analysis

Unless otherwise stated, the statistical tests were unpaired t-tests for continous parametric data and unpaired Mann-Whitney test for discrete or categorical (i.e. non-parametric) data. The analysis was performed using Prism (Graphpad Software) running on windows XP on a Dell computer. Detailed protocols for immunostaining and image analysis are listed in Appendix I.

3. Analysis of Neuromuscular Synaptic Degeneration in Homozygous and Heterozygous young *Wld*^{s} mice

3.1 Introduction

Wallerian degeneration refers to the distal axonal fragmentation and degeneration that occur after an axon is separated from its cell soma (Vial, 1958; Nicholls et al., 1992). In the mammalian neuromuscular junction, the degeneration of nerve terminals occurs earlier than the degeneration of axons induced by axotomy (Birks et al., 1960; Miledi and Slater, 1970). In the spontaneous mutant *Wld*^{s} mouse, degeneration of axons and synaptic terminals is significantly delayed after axotomy (Lunn et al., 1989; Ribchester et al., 1995). Using vital dye labeling, immunocytochemistry, and electrophysiology, it has been shown that axotomised *Wld*^{s} motor nerve terminals, as well as axons, undergo a process described as piecemeal withdrawal, which appears to be distinct from classical Wallerian degeneration (Mattison et al., 1996; Parson et al., 1998; Ribchester et al., 1999).

In 1998, Coleman et al first showed that the *Wld*^{s} mutation comprises an 85 kb tandem triplication of genes, containing exons of three different genes, Ube4b (the mammalian homologue of ubiquitin fusion degradation protein 2(Ufd2)), Nmnat (nicotinamide mononucleotide adenylyl transferase), and a novel member of the cellular retinoid-binding protein family (Rbp7). One end of *Ube4b* (the code for the N-terminal 70 amino acids) and the complete sequence of *Nmnat* form a chimeric gene with an open reading frame coding for a 43 kDa fusion protein. Subsequently Mack et al (2001) showed, using transgenic lines with different levels of *Wld*^{s}

expression, that the extent of axon preservation is strongly dependent on the expression level of the chimeric *Wld*^{S} protein. However, heterozgyous *Wld*^{S} mice, which have half the 'gene-dose', and express about half as much *Wld*^{S} protein as homozygotes, show little difference in protection of their axons compared to the young homozygous *Wld*^{S} mice. On the other hand, motor nerve terminals appear to degenerate rapidly in *Wld*^{S} heterozygotes (Gillingwater et al 2002). In this chapter, I set out to measure and analyse the sensitivity of synaptic degeneration in greater detail.

3.2 Results

3.2.1 Morphology of the Neuromuscular Junctions in *Wld*^{S} Mice

Time course of synaptic degeneration in young homozygous *Wld*^{S} mice

Sixty-four lumbrical muscles were taken at 5, 7, 9 and 11 days post bilateral tibial axotomy in CFP/*Wld*^{S} mice (N=9 mice). The postsynaptic ACh receptors were labeled with TRITC-α-BTX (Figure 3.1). In order to obtain a clear image and more accurate data, every NMJ in each muscle that presented en face was individually assessed as to the level of occupancy, confocal microscopy and Scion Image software were used (see chapter 2). Confocal projection images facilitate this process by compressing all the endplates into a single digital focal plane; avoid the need to

image each endplate, most of which were in different optical sections. At each successive time point following axotomy, the number of vacant endplates was increased (Figure 3.2). For example, at 7days axotomy 34.61% mean ± 8.25 S.E.M of endplates were vacant; and by 9 days 55.08% ± 8.58 were vacant (Figure 3.3).

The data confirms previous findings reported by Gillingwater et al (2002). Therefore, all subsequent analyses were carried out using mice expressing fluorescence protein in motor neurons.

3.2.2 Morphology of Neuromuscular Junctions in Different Types of Mice

Axons and NMJs show different sensitivities to *Wld*^{S} gene dose

Tibial nerve labeled by YFP expression was taken from each of wild-type, *Wld*^{S} heterozygous, and *Wld*^{S} homozygous mice at 4 days following axotomy, and compared with unoperated mice. Images are shown in the Figure 3.4. Axons degenerated rapidly in wild-type mice (Figure3.4 B), but were well protected from degeneration in both heterozygous and homozygous *Wld*^{S} mice 4 days after axotomy (Figure 3.4 C, D). In contrast to axon preservation, NMJ preservation was different. NMJs are from one young heterozygous *Wld*^{S} and one wild-type at 1 day after axotomy, and one young *Wld*^{S} mouse at 5 days after axotomy are shown in Figure 3.5. Endplates in unoperated muscles were fully occupied by their motor nerve

terminals (Figure A). Motor nerve terminals degenerate rapidly and synchronously in *Wld*^{S} heterozygotes and wild-type mice (Figure 3.5 B, C), but progressively vacated motor endplates following axotomy in *Wld*^{S} homozygotes (Figure 3.5 D). Interestingly, these images also suggest that intramuscular axonal branches are more vulnerable to degeneration than their parent axons in the tibial nerve (see below Figure 3.10).

3.2.3 Quantification of Endplate Occupancy in Wild-type, Heterozygous and Homozygous *Wld*^{S} mice

Wild-type mice

NMJs from 9 unilateral sciatic axotomised wild-type mice were studied at 6 hours, 12 hours, and 14.5 hours and 17 hours respectively. In total thirty-three deep lumbrical muscles were dissected from these mice. Nerve terminal morphology was assessed from the endogenous YFP fluorescence and endplates were counterstained with TRITC-α-BTX. Nerve terminals and axons degenerated quickly in these mice. After 14.5 hours fewer than 10% of endplates were occupied, At 17 hours, all nerve terminals had degenerated completely. The complete motor innervation in wild type mice was reconstructed by The Adobe Photoshop at 6 hours post unilateral sciatic nerve section. Some nerve terminals started to degenerate, but axons remained intact (Fig 3.7).

Heterozygous *Wld*^{S} mice

Fifth-six muscles were taken from sixteen YFP16 Balbc/*Wld*^{S} mice (5-8 weeks old). The left sciatic nerve in these mice was cut unilaterally at different time points: 6 hours, 12 hours, 17hours, 20 hours and 24 hours before sacrificing the mice. All muscles were labeled with TRITC α- BTX. From 6 hours to 24 hours, a few endplates started to degenerate at 6 hours axotomy, after then the nerve terminals degenerated dramatically, fully occupied and vacant endplates could be found, but very few endplates were partially occupied and all endplates became vacant 3 days after axotomy (Figure 3.5-3.9). Some axons branching on the NMJs had become fragmented. The biggest change in the number of occupied endplates occurred between 12 and 20 hours after axotomy. Remarkably, the sensory axons were better protected by *Wld*^{S} gene than the motor axons in heterozygous YFP16/*Wld*^{S}/Balbc mice (Fig 3.10). Montage pictures showed that in the whole NMJ of YFP16/*Wld*^{S}/Balbc mice, axons were still intact even after 4 days axotomy, while both synapses and the branches connected with synapses had already completely degenerated.

Confocal montage pictures allowed comparison of the patterns of degeneration in young heterozygous *Wld*^{S} mice and wild-type mice at different time points. It appeared that synaptic degeneration in heterozygous *Wld*^{S} mice was only slightly delayed by the *Wld*^{S} protein in comparison to wild type mice (Figure3.7-3.10).

Quantification of synaptic degeneration in the three different types of mice is shown in the Figure 3.11. There were only slight differences in the degeneration of nerve terminals in the heterozygous *Wld*^{s} mice and wild-type mice, and synaptic degeneration in homozygous *Wld*^{s} mice was much slower. In heterozygotes, it appeared that in addition to motor nerve terminals, intramuscular axon branches also degenerated within 24 hours in most cases, in contrast to the preservation of axons in the tibial nerve in heterozygous *Wld*^{s} mice. This difference is evident also in Fig 3.10, and merits further investigation in future studies.

Homozygous *Wld*^{s} mice

In young YFP16/*Wld*^{s} mice, twenty-nine lumbrical muscles were taken after 3, 5, 7, and 9 days post unilateral sciatic nerve section. The nerve terminals degenerated gradually. Most endplates were fully occupied or partially occupied after axotomy. Data in Figure 3.8 show the time course of synaptic degeneration in *Wld*^{s} homozygous mice. In 3 days axotomised lumbrical muscle preparations, 10.77% ± 4.04 of endplates were vacant by 5 days vacancy had increased to 28.22% ± 5.77 of endplates, then 59.32% ±3.84 at 7days, and to 75.53% ± 2.3% at 9 days.

The results of time course of synaptic degeneration in these three different axotomised mice lines showed that Wld^{s} protein does have a protective effect on synaptic degeneration, even when the dose is reduced. For example, the amount of synaptic degeneration at 17 hours was slightly lower in heterozygous *Wld*^{s} mice

compared with wild type mice (Fig 3.11). Perhaps more compelling, occasionally there were terminals that were well-preserved at 36hrs axotomy in *Wld*^{S} heterozygotes when this occurred, the preservation seems to affect all the terminals in the protected motor unit. Perhaps this indicates that there is some variability in the level of *Wld*^{S} gene expression between motor neurons.

However, there was a large difference in synaptic protection comparing either heterozygous or wild-type mice with *Wld*^{S} homozgyotes. Degeneration of synapses was almost 10 times slower in the homozygous *Wld*^{S} mice. Whereas in wild-type or heterozygous mice, the nerve terminals degenerated completely after 17 hours in wild-type mice. However, I did occasionally observe protection, as a few nerve terminals were occupied 24 hours after axotomy in heterozygous *Wld*^{S} mice. Therefore, in comparison to the axons, NMJs are clearly very sensitive to the gene dose.

3.2.4 Analysis Using Polyhedral Degeneration Diagram (PDD)

The above analysis gave a good indication of differences in the rate of synaptic degeneration in the different groups of mice that were studied. Polyhedral Degeneration Diagrams (PDD) was used to examine for difference in the pattern of synaptic degeneration. Confocal micrographs show the definitions of the five states of axonal and synaptic degeneration (Fig 3.12). Innervation states of axons and synapses during neuronal degeneration were defined as follows: O represents an

intact axon connected with a fully occupied endplate ; CP represent partial occupancy with the synaptic terminal still connected to the axon; CF represents synapses becoming fragmented after nerve section, but with at least one fragmented still connected with an intact axon; DF represents both axons and synapses becoming fragmented following axotomy; V represents both axons and synapses degenerating completely after nerve section. Using PDD analysis, the diameters of circles positioned at the apices of polyhedra representing their states, were set by the proportions of neuromuscular junctions in each category. Blue circles represent the fully occupied (O) state, red circles represent the disconnected fragemented (DF) state, pink circles represent connected partial (CP) state, green circle represents the connected fragmented (CF) state, and yellow circles represent vacant (V) state. I used these diagrams to infer the most likely trajectories between states. Altogether, I identified five degeneration states (O, DF, CP, CF, V) during synaptic degeneration, with 7 possible trajectories from fully occupied endplates to vacant endplates, namely, 1) O→DF→V; 2) O→CP→V; 3) O→CF→V; 4) O→CP→DF→V; 5) O→CP→CF→V; 6) O→CF→DF→V; 7) O→CP→CF→DF→V (See CD Rom for animation). There is no possible endplate degeneration pathway from O state to V state directly in any type of axotomised *Wld*^{s} mice. In each type of mouse, synaptic terminals theoretically could follow any of these trajectories to degenerate. However, the PDD analysis suggests that, in heterozygous *Wld*^{s} mice (Fig 3.13), most synaptic terminals became DF and very few were CP at different time points, and therefore it

can be concluded that the majority of endplates follow the process (O→DF→V), while a few endplates go through other processes (O-CP-DF→V or O→CP→V). In wild-type mice (Fig 3.14), the main process of synaptic degeneration was similar to heterozygous *Wld*^{s} (O→DF→V) and few endplates go through the CP or CF states before degenerating completely.

However, in the homozygous *Wld*^{s} mice (Fig 3.15), the degeneration patterns are evidently different, most endplates go through CP state before degenerating (O→CP→V), while very few endplates degenerate from O state to DF state (O→CF→V or O→CP→CF→V). This suggests that synaptic terminals progressively retract following axotomy in homozygous *Wld*^{s} mice but undergo fragmentation and synchronous degeneration in wild-type mice. A single copy of the *Wld*^{s} gene (i.e. *Wld*^{s} heterozygous) is not sufficient to mitigate or convert the mode of degeneration, from that of the wild type to that of homozygous type. Thus, the pattern of synaptic degeneration in heterozygous *Wld*^{s} mice is more similar to wild-type than to the slow retraction of motor nerve terminal degeneration observed in homozygous *Wld*^{s} mice. However, from the PDD analysis, the rate of synaptic degeneration in heterozygotes is slower than in wild-type mice. For example, at 17 hours, some endplates in heterozygous were still occupied in heterozygotes, while all endplates in wild-type degenerated completely. Therefore PDD analysis provides the main evidence that NMJs degeneration in heterozygous *Wld*^{s} mice is delayed compared with wild-type mice.

Although the PDD analysis suggests there were significant qualitative differences in the pattern of synaptic degeneration in *Wld*^{S} homozygotes compared with heterozygotes or wild-type, alternative interpretation can not be ruled out at present. For instance, the CP (and /or CF) states could be quite common but rapidly transient in wild-type and heterozygotes. Such issues may only be unequivocally resolved using techniques such as repeated visualization in vitro (e.g. Walsh & Lichtman, 2003).

Figure 3.1 Morphological Evidence for Different Degeneration Patterns of Neuromuscular Junctions.

All NMJs are from lumbrical muscles of axotomised young CFP/*Wld*^{S} mice (2 month old) and stained for TRITC-α-bungarotoxin. Figures (A, B, C, D) show the different percentage occupancy of endplates after axotomy using confocal microscopy. (A) Confocal image showing vacant endplates (0%); (B, D, E) Confocal images showing the partially occupied endplates, for example, 25% partially occupied endplates (B); 50% partially occupied endplates (D); and 75% partially occupied endplates (E); (C) Confoçal image showing fully occupied endplates. This analysis method of synaptic degeneration is also used in CFP and YFP16 *Wld*^{S} mice in the following experiments. Scale bar=30μm.

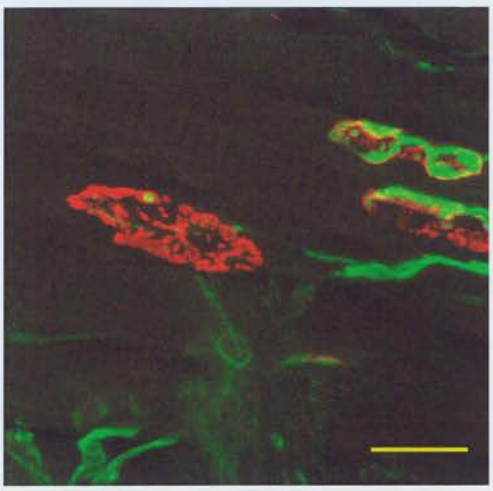

(A) 0% occupancy

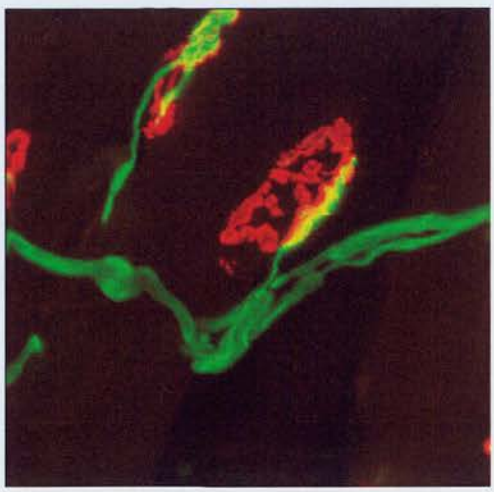

(B) 25% occupancy

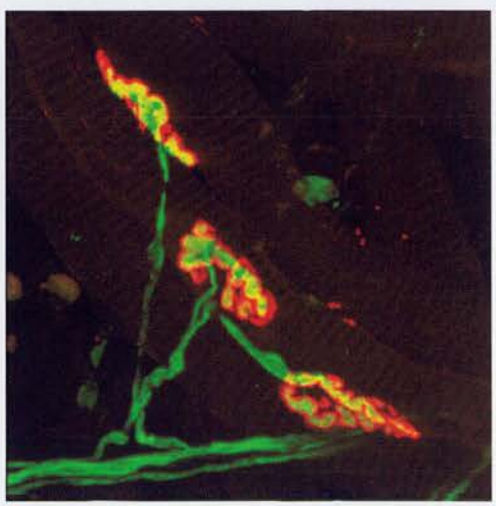

(C) 100% occupancy

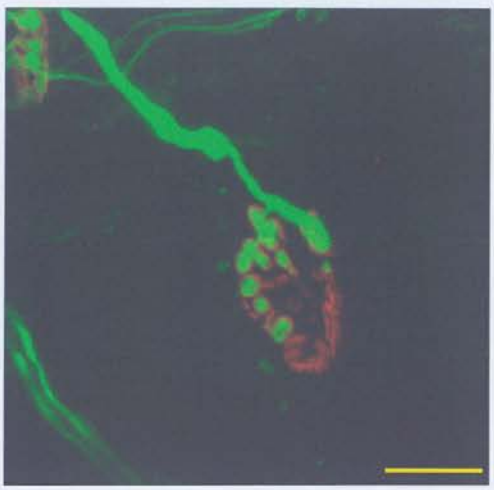

(D) 50% occupancy

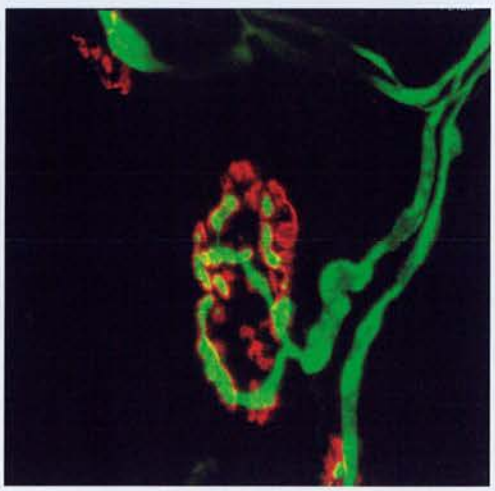

(E) 75% occupancy

Figure 3.2 Synapses Retract in Axotomised *Wld*^{S} Homozygotes

Standard confocal microscopy images of NMJs from young CFP/*Wld*^{S} mice (2 month old) deep lumbrical muscles (labelled with TRITC α-BTX). (A, B, C & D) Scale bar = 30μm.

(A) Confocal images of NMJs from a CFP/*Wld*^{S} mouse at 3 days following nerve section.

(B) Confocal images of NMJs from a CFP/*Wld*^{S} mouse at 5 days following nerve section.

(C) Confocal images of NMJs from a CFP/*Wld*^{S} mouse at 7days following nerve section.

(D) Confocal images of NMJs from a CFP/*Wld*^{S} mouse at 9 days following nerve section.

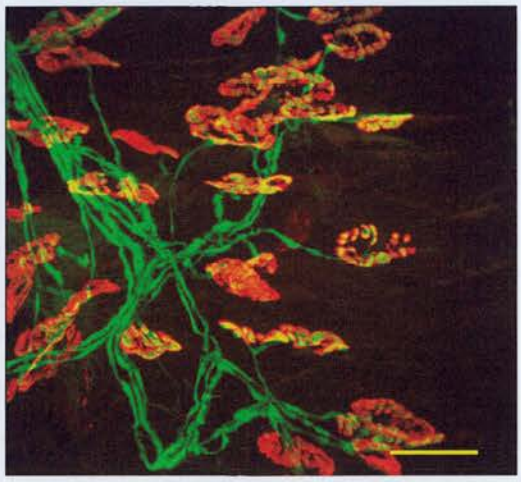

(A) 3dx

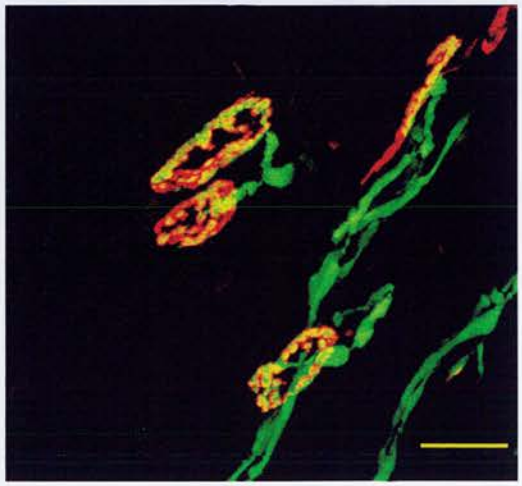

(B) 5dx

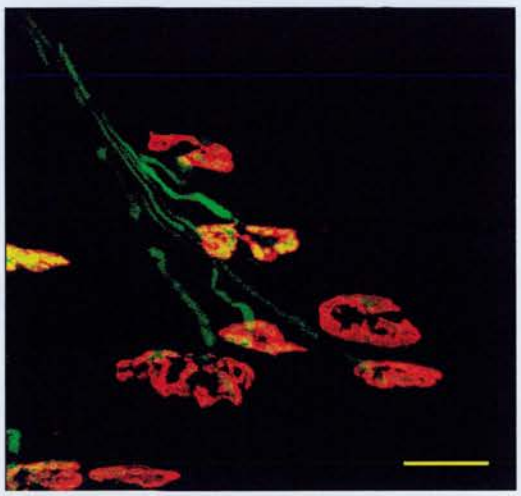

(C) 7dx

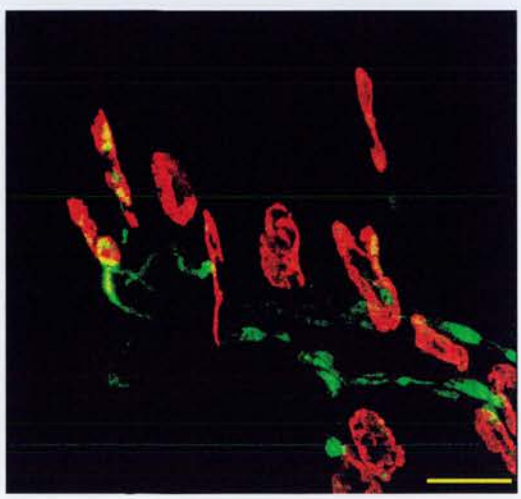

(D) 9dx

Figure 3.3

Graphs showing the time course of synaptic degeneration in the deep lumbrical muscles of CFP/*Wld*^{S} mice after 5, 7, and 9 days axotomy. (Graph A, B, C) Error bars represent ±SEM

(A) Each column represents the percentage of total number of endplates in each occupancy group in young *Wld*^{S} mice 5 days after axotomy.

(B) Each column represents the percentage of total number of endplates in each occupancy group in young *Wld*^{S} mice 7 days after axotomy.

(C) Each column represents the percentage of total number of endplates in each occupancy group in young *Wld*^{S} mice 9 days axotomy.

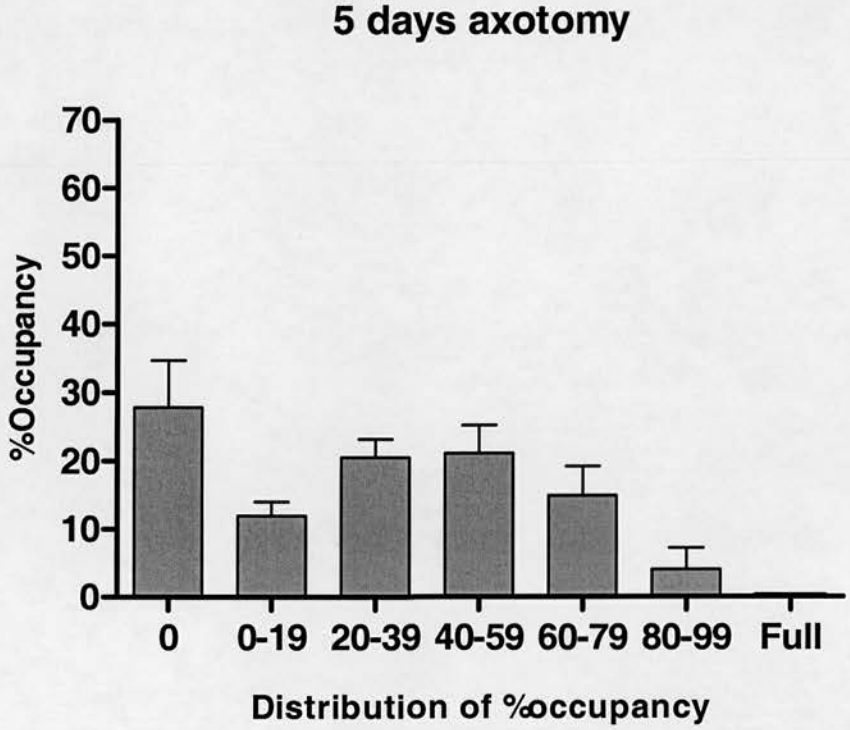
5 days axotomy
%Occupancy
70
60
50
40
30
20
10
0
0
0-19
20-39
40-59
60-79
80-99
Full
Distribution of %occupancy

(A)

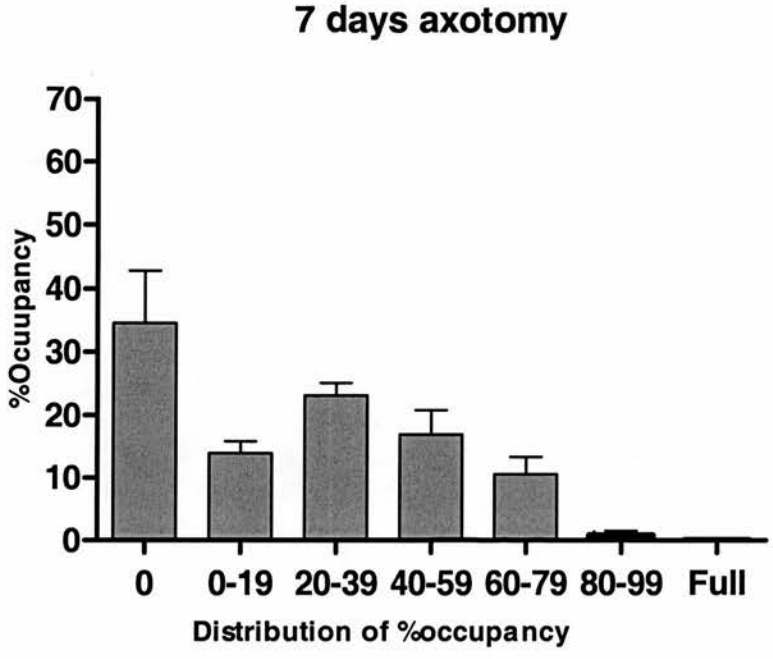
7 days axotomy
70
60
50
40
30
20
10
0
%Ocuupancy
0
0-19
20-39
40-59
60-79
80-99
Full
Distribution of %occupancy

(B)

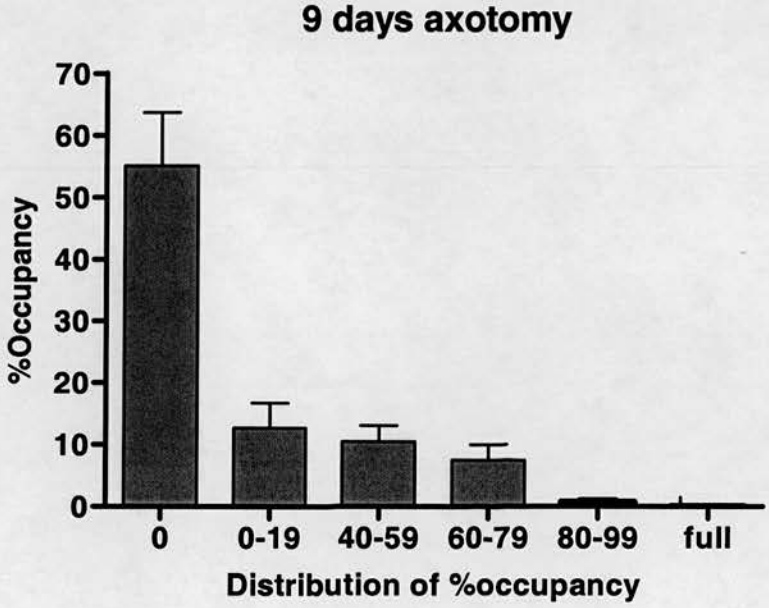
9 days axotomy
%Occupancy
70
60
50
40
30
20
10
0
0
0-19
40-59
60-79
80-99
full
Distribution of %occupancy

(C)

Figure 3.4 Morphological Evidence for Preservation of Axons

(A, B, C & D) Confocal micrograph of tibial nerves from three different types of YFP16 transgenic mice (Heterozygous *Wld*^{S}, Wild-type, Homozygous *Wld*^{S}) at 4 days after unilateral sciatic nerve section. Note that some axons show some evidence of vacuolation inclusions. The reasons for this are unknown but could be related to the way YFP in distributed in the cytoplasm. Scale bar= 30μm

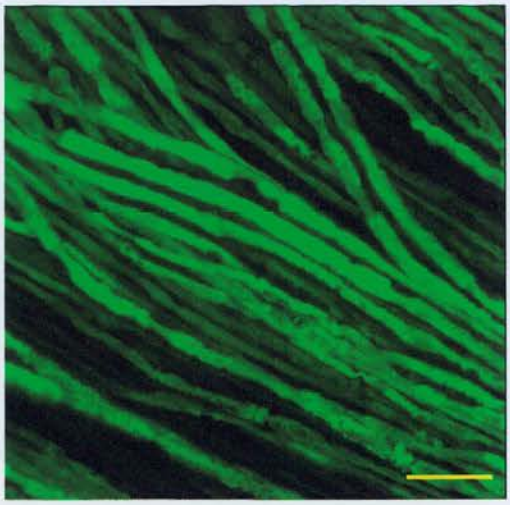

(A) Control

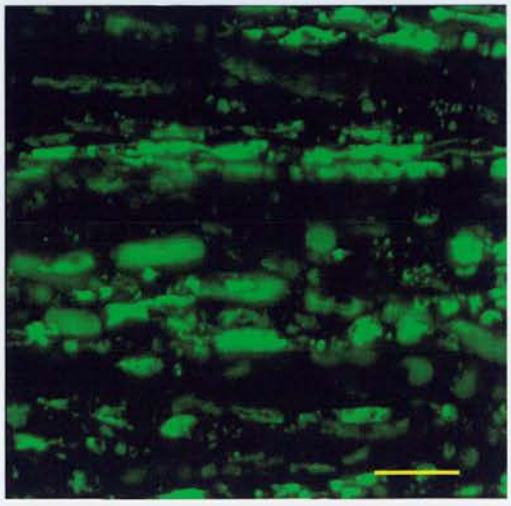

(B) C57Bl6 4dx

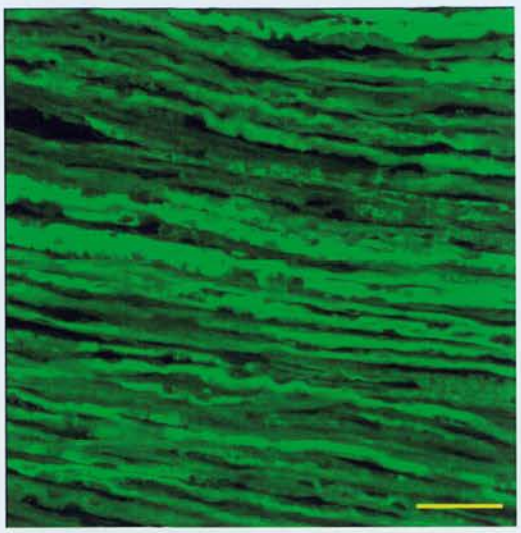

(C) Wlds 4dx

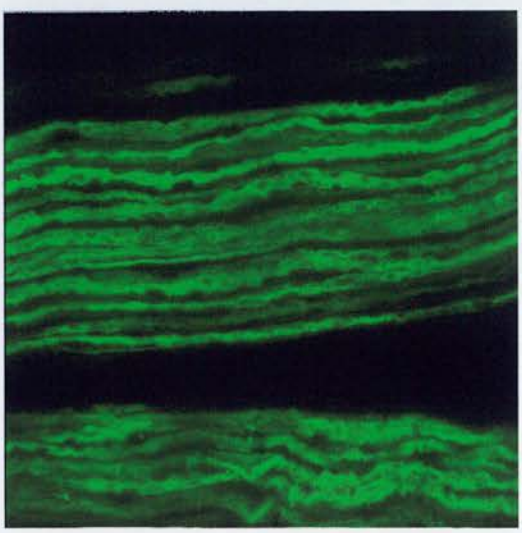

(D) Balbc/Wld 4dx

Figure 3.5 Morphological Evidence for Preservation of Neuromuscular Junctions

Confocal micrograph from 2 month YFP16 *Wld*^{S}/*Wld*^{S} mice NMJs, 1 day or 3 days post axotomy. (labelled with TRITC α-BTX)

(A) Unoperated lumbrical muscles, showing fully occupied endplates and intact axon.

(B) Heterozygous lumbrical muscles after 3 days, showing vacant endplates

(C) Wild-type lumbrical muscles after 1day, showing vacant endplates

(D) Homozygous lumbrical muscles after 3 days, showing almost all endplates remain fully occupied. Scale bar=30μm

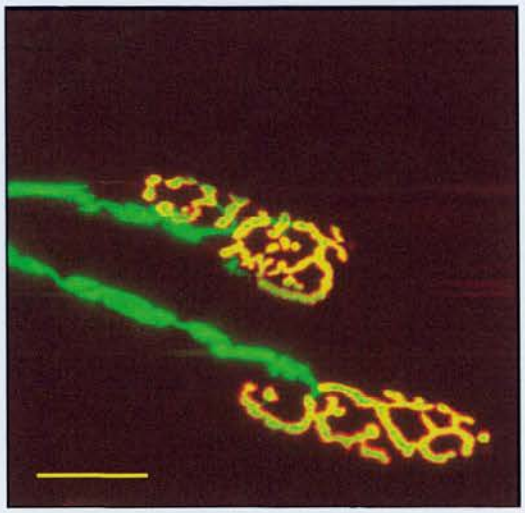

(A) Control

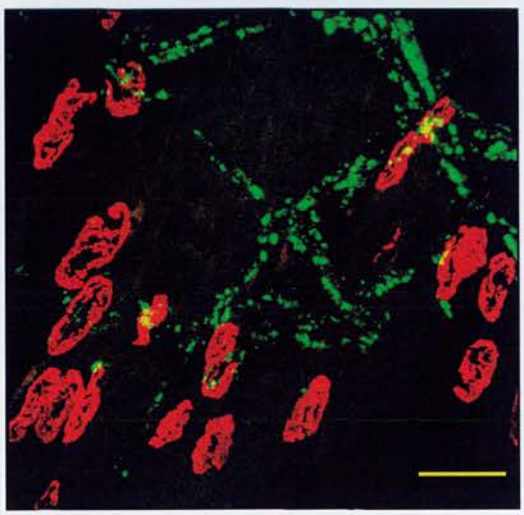

(B) Balbc/*Wld*^{s} 3dx

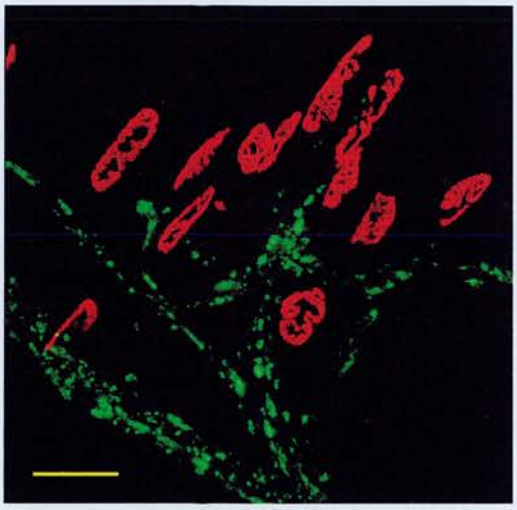

(C) C57/Bl6 1dx

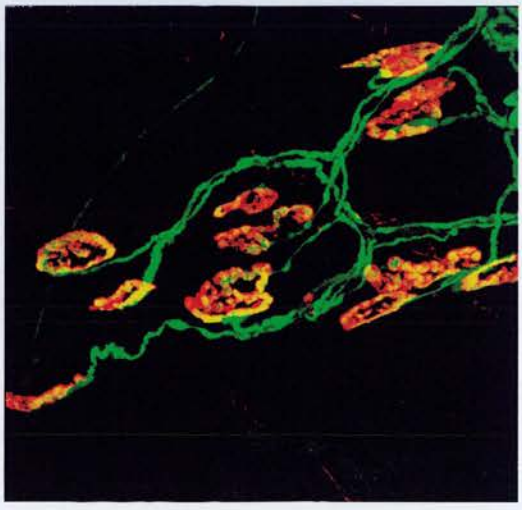

(D) *Wld*^{S}/*Wld*^{S}- 3dx

Figure 3.6 Synaptic Degeneration in Young YFP16 Homozygous *Wld*^{S} Mice after Axotomy

Quantitative analysis of synaptic degeneration in the axotomised NMJs from YFP16 *Wld*^{S}/*Wld*^{S} mice. Bar charts show the percentage of vacant endplates at 3, 5, 7, and 9 days post axotomy. Means and standard errors are shown.

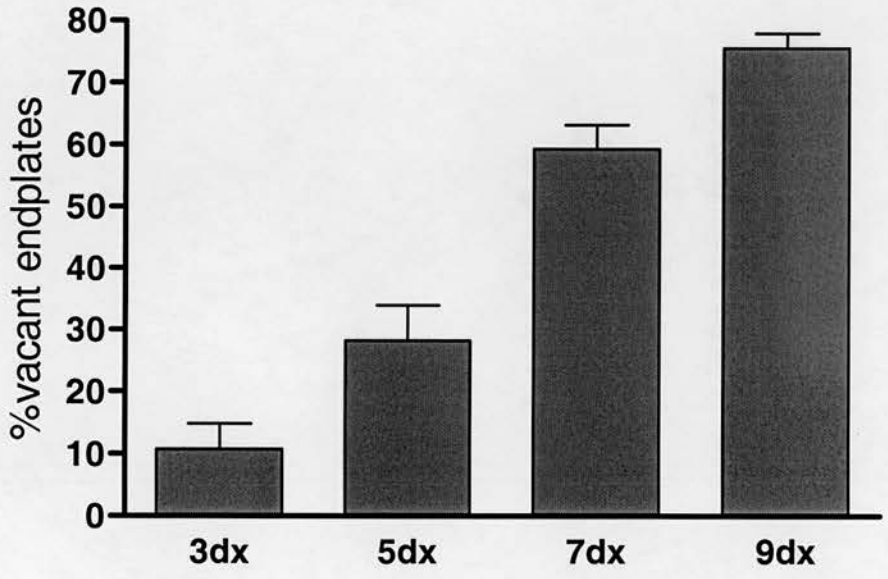

Figure 3.6

Figure 3.7 Complete Reconstruction of the Neuromuscular Innervation in young YFP16/C57Bl6 (wild-type) Lumbrical Muscles at 6 Hours after nerve section

(A) Montage of confocal micrographs of YFP16 C57/Bl6 mice 6 hours after axotomy, many nerve terminals (AChRs labeled red) are occupied by intact YFP16-labeled axons (green). Scale bar=200μm

(B) Confocal image showing some neuromuscular junctions at higher magnification. Scale bar=40μm

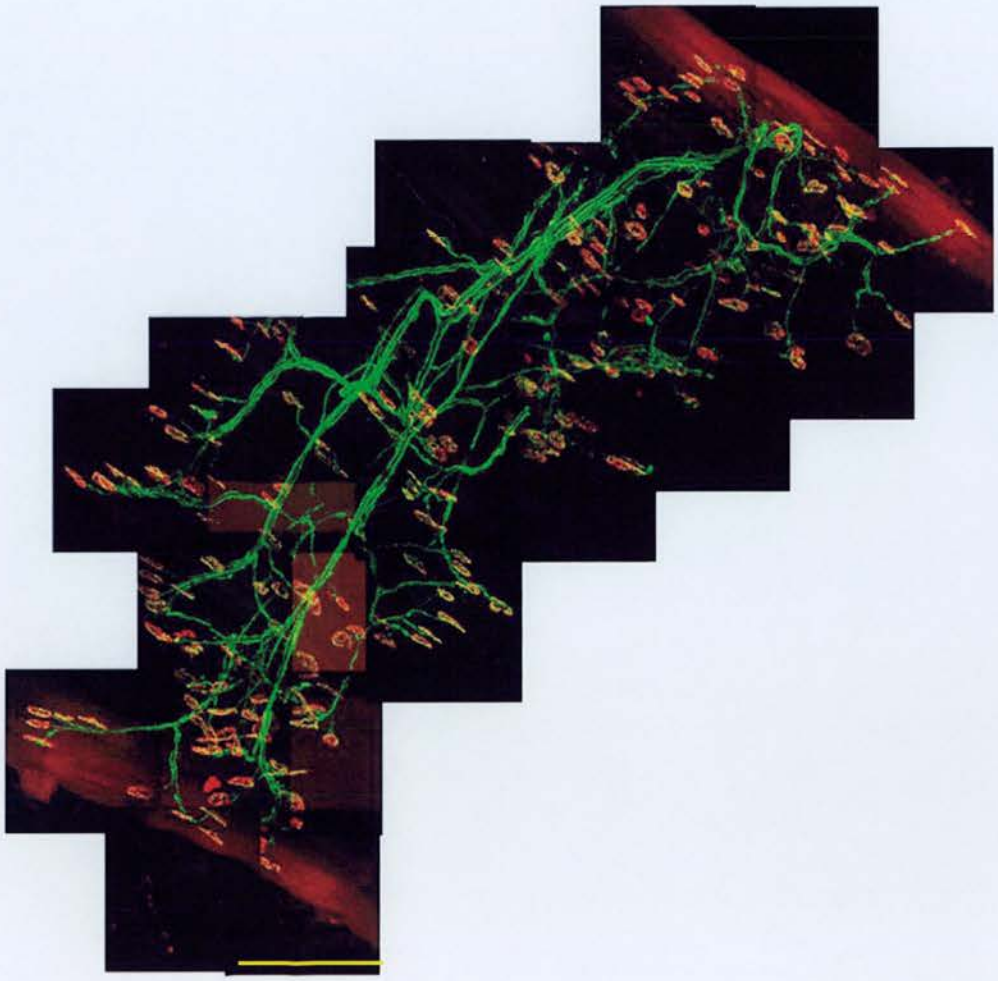

(A)

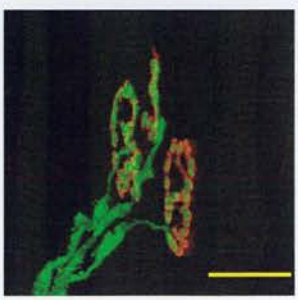

(B)

Figure 3.8 Reconstruction of Neuromuscular Innervation in Lumbrical Muscles of Young Heterozygous *Wld*^{S} Mice (2 months old) at 12 hours after nerve section

Montage showing 40 times objective confocal micrograph of YFP16 Balbc/*Wld*^{S} mouse lumbrical muscles 12 hours after axotomy, Most endplates (AChRs labeled red) remain occupied, and YFP16-labeled axons (green) and nerve terminals (yellow) are intact. Scale bar= 200μm

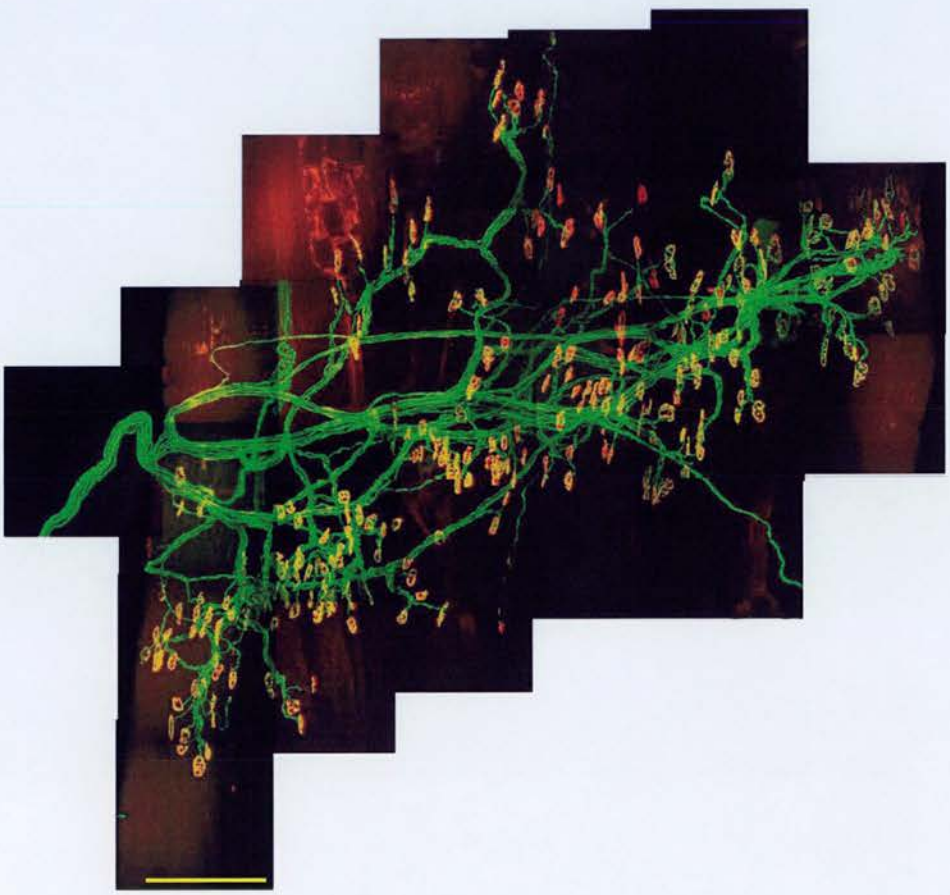

Figure 3.8

Figure 3.9 Reconstruction of the Neuromuscular Innervation in Lumbrical Muscles of Young Heterozygous *Wld*^{S} Mice (2 months old) at 20 Hours after nerve section

(A) Montage of confocal micrographs of YFP16 Balbc/*Wld*^{S} mice 20 hours after axotomy, neuromuscular junctions (AChRs labeled red) and YFP16-labeled axons (green) degenerate. Scale bar=200μm (Fig B&C). Confocal image showing different degeneration patterns of nerve terminals and axons at higher magnification. (B) Confocal image showing fully occupied endplate (white arrow) and vacant endplate (blue arrow). (C) Showing some fragmented and intact YFP-16 labeled axons. Scale bar=40μm

(A)

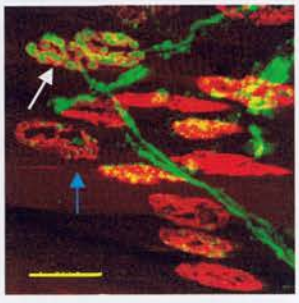

(B)

(C)

Figure 3.10 Reconstruction of the Neuromuscular Innervation in the Lumbrical Muscles of Young Heterozygous *Wld*^{S} mice 4 days after axotomy

Montage showing 40 times objective confocal micrograph of cross-bred Balb/c mice with YFP16 *Wld*^{S} mice 4 days after axotomy. Scale bar=200μm. Almost all the motor nerve terminals have degenerated but sensory axons supplying to muscle spindles remain preserved (arrows).

Figure 3.10

Figure 3.11 Time Course of Nerve Terminal Degeneration in Different Types of Mice after Axotomy

Graph of the various time courses of nerve terminal degeneration in 2 months old heterozgyous, homozygous *Wld*^{s} mice and C57/Bl6 mice following unilateral sciatic nerve section. The data show the percentage of vacant endplates in different mice (see Fig 3.5) Black triangles represent data from 2 months old C57/Bl6 mice, and black inverted triangle represents data from 2 months old homozygous *Wld*^{s} mice. White circle represents data from 2 months old heterozygous *Wld*^{s} mice. A statistical analysis of these data was considered unnecessary.

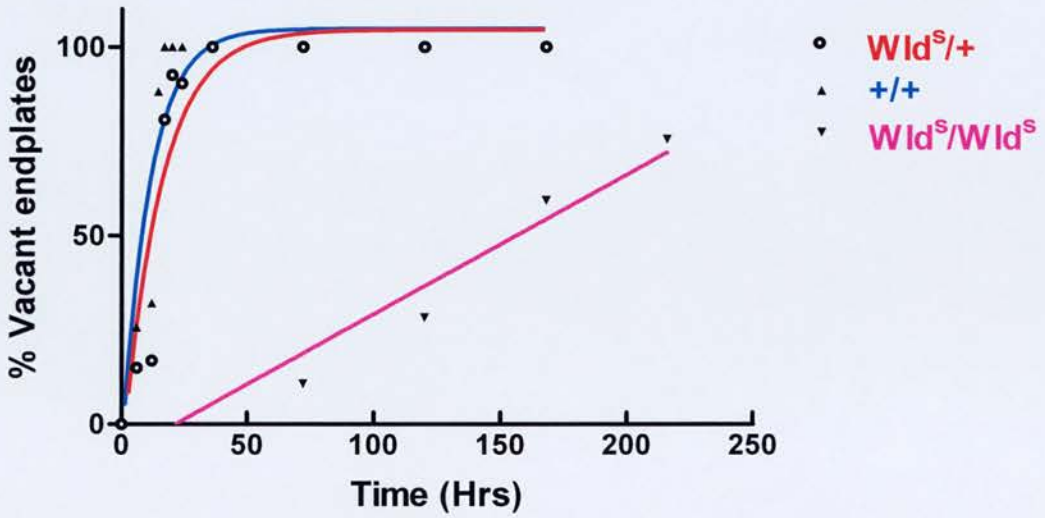
% Vacant endplates
100
50
0
0
50
100
150
200
250
Time (Hrs)
Wld^S/+
+/+
Wld^S/Wld^S

Figure 3.11

Figure 3.12 Confocal Micrographs Illustrate the Five States of Axonal and Synaptic Degeneration

O represents fully occupied endplates, at which the terminal is connected to intact axons; CP represents partially occupied endplates which are connected with intact axon; CF represents fragmented endplates at which at least one fragement is connected with an intact axon; DF represents endplates with synaptic boutons disconnected from axons, both axons and terminals are fragmented, that is, where there was no discernable continuity between the axon and the motor nerve terminal. V represents endplates where terminals and axons were both degenerated completely. Two other possible states are a fully occupied endplate with the terminal disconnected from its axon ("DO"); and a partially occupied endplate with the terminal disconnected from its axon ("DP"). Neither state was ever seen in my experiments.

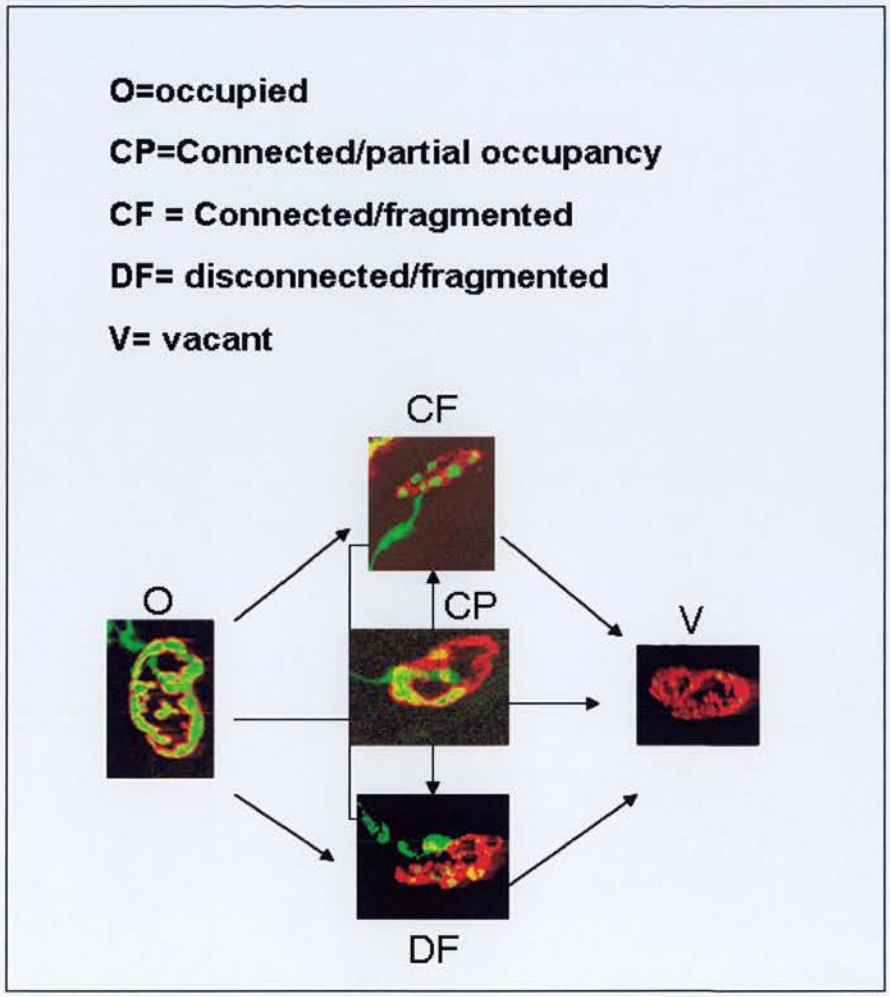
O=occupied
CP=Connected/partial occupancy
CF = Connected/fragmented
DF= disconnected/fragmented
V= vacant
CF
O
CP
V
DF

Figure 3.12

Figure 3.13 PDD Analysis on Young Heterozygous *Wld*^{S} Mice

The PDD shows the states of axonal and synaptic degeneration in the young heterozygous *Wld*^{S} mice. All five states (O, DF, CP, CF, V) of synaptic degeneration were found. Blue circles represent fully occupied endplates (O). Purple circles represent partially occupied endplates connected with intact axons (CP). Green circles represent fragmented endplates connected with intact axons (CF). Red circles represent fragmented endplates disconnected from the axon (DF). Yellow circles represent vacant endplates without axonal connection (V). Arrows represent the possible trajectories of axonal and synaptic degeneration at different time points in the young axotomised heterozygous *Wld*^{S} mice.

The chart shows the percentages of different states of axons and synapses during the degeneration process in axotomised heterozygous *Wld*^{S} mice at 6-hours, 12-hours, 17-hours, 20-hours and 24-hours time points, and standard error estimates with every percentage of endplates. Endplates degenerated dramatically between 12 hours and 17 hours post-axotomy.

The variable signs of the CF and CP states probably reflect individual variation in the rate and /or pattern of degeneration in the individual muscle samples at the different time points.

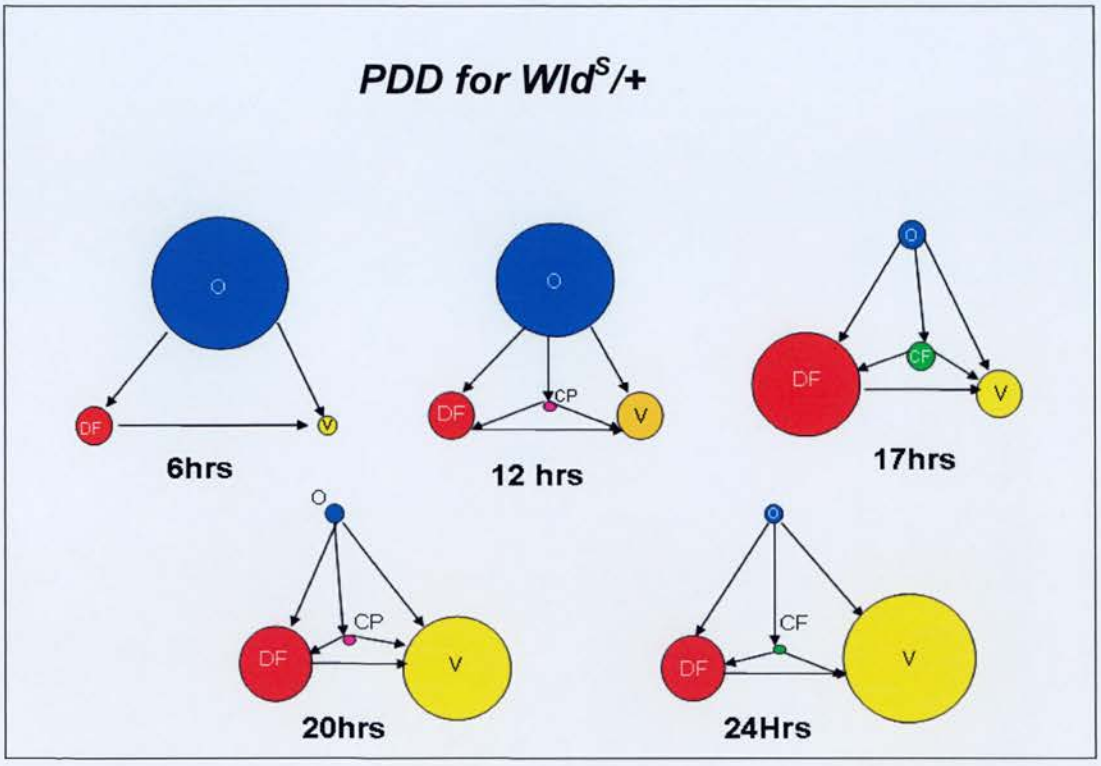

Figure 3.13

Time / States (%endplates)	6 hours	12 hours	17 hours	20 hours	24 hours
O	85.21±2.34	81.02±2.60	15.41±2.44	6.28±1.39	11.66±4.19
CP		1.64		1.76±0.19	
CF			7.48±1.62		1.66±0.35
DF	12.44±1.79	12.85±2.89	57.24±2.51	36.86±6.38	32.13±5.40
V	8.62±2.63	13.07±3.26	23.19±3.78	63.74±9.15	58.01±5.25

Figure 3.14 PDD Analysis on Young Wild-Type Mice

The PDD shows the states of axonal and synaptic degeneration in young wild-type mice. All five states (O, DF, CP, CF, V) of synaptic degeneration were found. Blue circles represent fully occupied endplates (O), Purple circles represent partially occupied endplates connected with intact axons (CP). Green circles represent fragmented endplates connected with intact axons (CF). Red circles represent fragmented endplates disconnected from the axon (DF). Yellow circles represent vacant endplates without axons connected (V). All arrows represent the possible trajectories of axonal and synaptic degeneration at different time points in the axotomised young wild-type mice.

The chart shows the percentages of different states of axons and synapses during the degeneration process in axotomised wild-type mice at 6-hours, 12-hours, 14.5-hours, and 17-hours time points, and standard error estimates with every percentage.

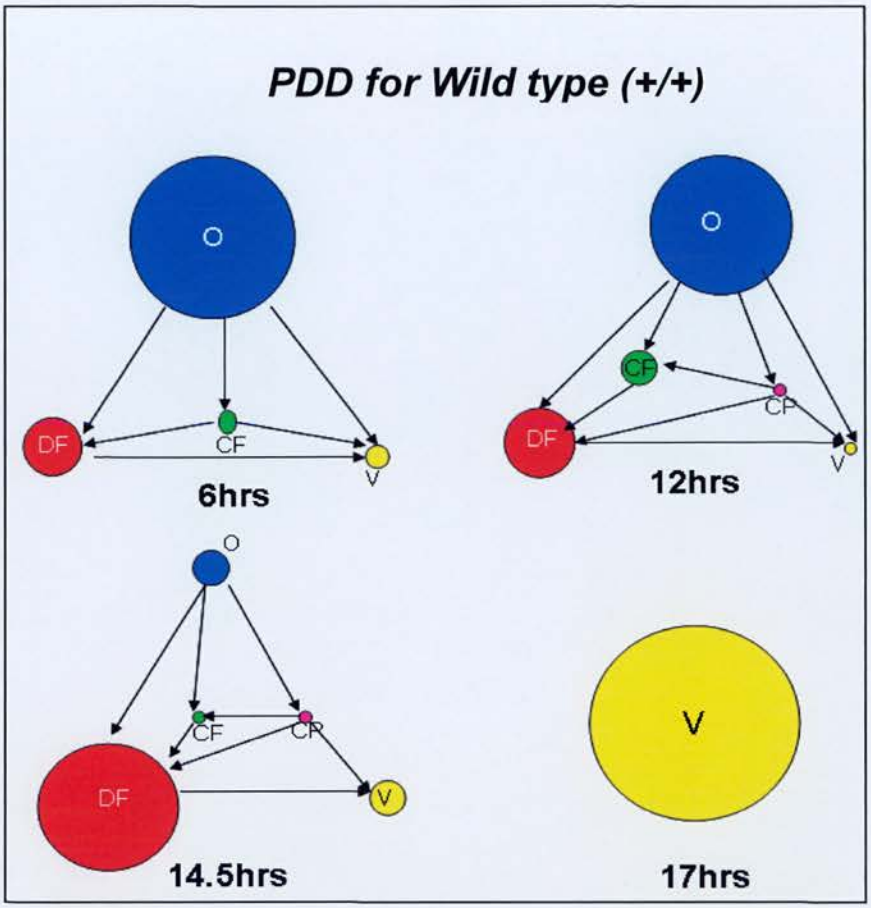

Figure 3.14

Time / States (%endplates)	6 hours	12 hours	14.5 hours	17 hours
O	72.91±2.22	64.90±6.21	10.74±3.61	0
CP			0.49	0
CF	2.8±1.68	9.01±3.88	0.49	0
DF	25.69±2.43	32±7.09	85.34±4.25	0
V	3.25±0.94	2.29±0.26	12.151±6.55	0

Figure 3.15 PDD Analysis on Young Homozygous *Wld*^{S} Mice

The PDD shows the states of axonal and synaptic degeneration in homozygous *Wld*^{S} mice. Four states (O, DF, CP, V) of synaptic degeneration were found. Blue circles represent fully occupied endplates (O), Purple circles represent partially occupied endplates connected with intact axons (CP). Red circles represent fragmented endplates disconnected with axon (DF). Yellow circles represent vacant endplates without axons connection (V). All arrows represent the possible trajectories of axonal and synaptic degeneration at different time points in the axotomised homozygous *Wld*^{S} mice.

The chart shows the percentages of different states of axons and synapses during the degeneration process in homozygous *Wld*^{S} mice following at 3 days, 5 days, 7 days and 9 days following axotomy, and standard error estimate with every percentage of endplates.

In this sample, almost 10% of endplates were vacant only 3 days after axotomy, whereas previous data suggest that all endplates were occupied up to almost 4 days after axotomy. The difference could be explained perhaps either by sample variation, or perhaps the more detailed analysis performed here gives a more accurate indication of the true rate/pattern of degeneration in homozygotes.

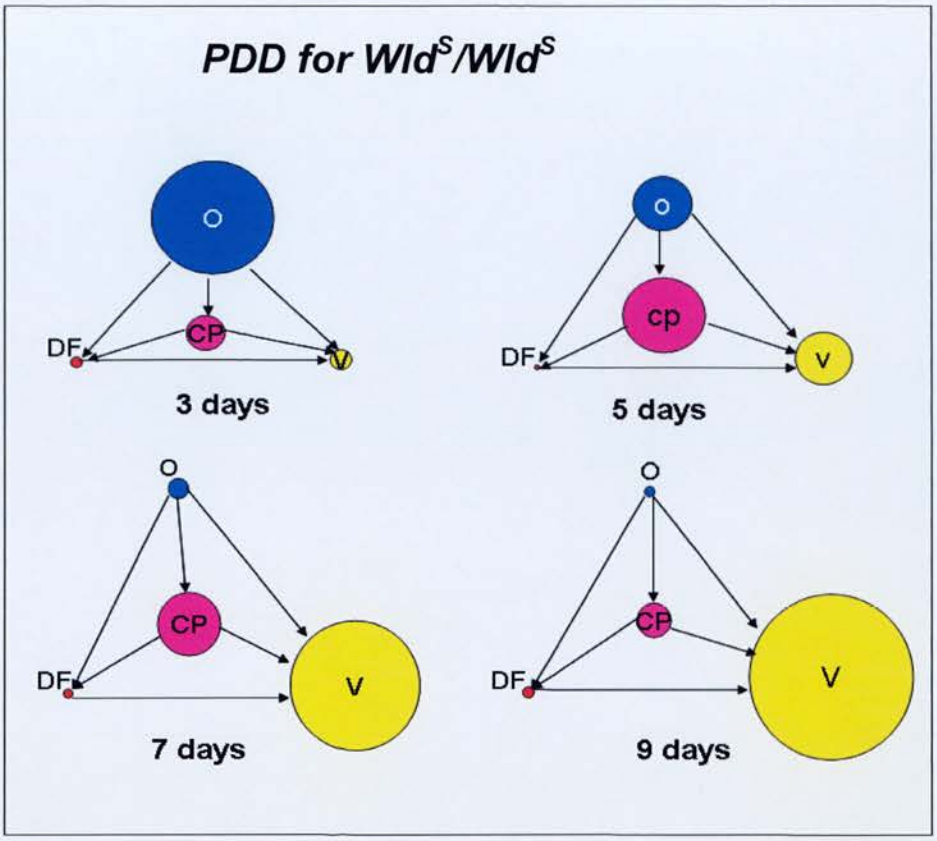

Figure 3.15

Time / States (%endplate)	3 days	5 days	7 days	9 days
O	61.28±4.95	29.07±4.47	9.17±1.84	4.62±0.85
CP	19.00±2.57	40.87±1.98	28.81±2.96	15.36±2.04
CF	1.82±0.33			0.90±0.15
DF	5.49±2.28	2.30±0.38	3.85±0.78	5.02±0.76
V	10.78±4.04	28.32±5.78	59.32±3.85	75.53±2.38

Summary

Previous studies have shown that the degeneration of axons and synaptic terminals is much delayed by the *Wld*^{s} gene in the mutant *Wld*^{s} mice, in contrast to wild type mice. Moreover, Mack et al (2001) have shown that axon degeneration is gene dose-dependent in *Wld*^{s} transgenic mice. Therefore, the main effort in this chapter was focused on measuring the *Wld*^{s} gene effect on synaptic terminal degeneration within wild type, heterozygous, and homozygous *Wld*^{s} mice. (The *Wld*^{s} gene dose is only half in heterozygous *Wld*^{s} mice). There are three main findings in this chapter.

First, synapses are more sensitive than axons to the *Wld*^{s} gene than axons. In heterozygous *Wld*^{s} mice (Figure 3.2 & 3.4), I showed that axons remained intact in heterozygous *Wld*^{s} mice as well as in young homozygous *Wld*^{s} mice following nerve section. However, the data demonstrated that synapse degeneration in heterozyougs *Wld*^{s} mice was although slightly slower than wild type mice, was faster than in young homozygous *Wld*^{s} mice.

Second, the morphology of synaptic degeneration in these different types of mice, as measured by both immunocytochemical staining and fluorescent protein expression, showed that the synaptic degeneration pattern in heterozygous *Wld*^{s} mice was distinct from that in young homozygous *Wld*^{s} mice, and more similar to that in wild type mice. That is, the majority of synaptic degeneration in the axotomised heterozygous *Wld*^{s} mice was more like the Wallerian degeneration process in wild type mice. However, axons still remain intact.

Third, PDD analysis revealed distinct difference in the patterns of synapse degeneration in wild-type mice, young heterozygous, and young homozygous *Wld*^{S} mice. The analysis implied the possible trajectories in wild-type mice, young homozygous and heterozygous *Wld*^{S} mice. In homozygous *Wld*^{S} mice, the main process appear to be O→CP→V, and a few endplates go through O→CF→V or O→CP→CF→V. In heterozygous *Wld*^{S} mice, the main process is O→DF→V, and a few endplates go through O→CP→DF→V or O→CP→V trajectories. Finally, in wild-type mice, additional to processes similar to those in heterozygous *Wld*^{S} mice, other processes that a few endplates go through are O→CP→CF→V; O→CF→V; O→CP→DF→V; O→CP→CF→DF→V. It is unlikely that the difference could be explained by difference in the time intervals between samples. If that were the case, the slow rate of degeneration in homozygous *Wld*^{S} mice should also have enabled visualization of those other states as well.

4. Analysis of Synaptic Degeneration in Old *Wld*^{S} Mice and *Wld*^{S} Protein Expression in Cerebellar Granule Cells

4.1 Introduction

The previous chapter showed that nerve terminals are progressively withdrawn from axotomised endplates in young *Wld*^{s} mice. In more mature mice (age >7 months old), this synaptic degeneration pattern is absent, although axons are still protected from axotomy (Gillingwater et al., 2002). That is, in older mice, motor nerve terminals appear to degenerate almost as rapidly as in wild-type mice. Classical degenerative signs appear in most synaptic terminals after axotomy, such as swollen and disrupted mitochondria, reduced synaptic vesicle densities, intra-terminal membrane whorls, fragmented terminal membranes and terminal Schwann cell phagocytosis.

In chapter 3, I showed that synaptic protection is weak when the *Wld*^{s} gene dose is halved. Thus a plausible hypothesis to account for the loss of synaptic protection with age in *Wld*^{s} mice, is that expression of the protective Wld^s protein declines with age. However, in previous work, levels of expression of the chimeric protein as indicated by western blotting of homozygous *Wld*^{s} mouse brain tissue, suggested that Wld^s protein expression did not diminish significantly with age (Gillingwater et al., 2002).

In this chapter, I examined the time course of axotomy-induced synaptic degeneration in old *Wld*^{s} mice. I utilised the same PDD analysis to depict the pattern of degeneration in old homozygous *Wld*^{s} mice as that which was used in wild-type

and young heterozygous and homozygous *Wld*^{s} mice (see Chapter 3). In order to evaluate whether the morphology of synaptic degeneration could be due to a change in Wld^{s} protein expression level in young homozygous and heterozygous and old homozygous *Wld*^{s} mice, I used quantitative immunocytochemistry to measure Wld^{s} protein expression in cerebellar granule cells, stained with Wld^{18} antibody. It is debatable whether immunocytochemistry is a better or more reliable method for quanlifying protein expression. However, inmmuocytochemistry certainly provides better optical resolution (at a cellular level) compared with, say, western blot analysis.

4.2 Methods

The methods used in the majority of experiments within this chapter were described in Chapter 2. The following section describes methods which are specific to this chapter. *Wld*^{s} protein was labeled with TRITC-Secondary antibodies and imaged with the HeNe laser and nuclei were counterstained using Topro 3 and visualize using the red diode laser on the BioRad radiance 2000 confocal microscope.

4.2.1 Wld^{s} Protein Expression Analysis

Cerebellar slice images were obtained using confocal microscopy, images of slice preparations were taken at two different channels at each laser power (HeNe laser power 20%, 30%, 40%, 50%, 60% of maximum), because the nuclei were

labeled by Topro-3 (red diode laser used to visualize Topro staining of nuclei) and *Wld*^{s} genes were labeled by Wld^{18} ab, and then the two images were merged using the integrated BioRad software to form an image of Wld^{s} protein expression on cerebellum granule cells. Pixel intensities were measured using the Image J programme. First, images in the red channel were loaded in order of laser power from the lowest to the highest laser power in the stack (20, 30, 40, 50, 60 etc). Several Wld^{s} protein spots were selected and the pixel intensity of each spot was measured using the Image J programme, next, the same method was used to measure background regions in each slice (i.e. regions between Topro-stained nuclei), the corrected brightness of spots was obtained by subtracting background intensities from each of them. Thirdly, the means and standard deviations of spot brightness at each laser power were calculated. Lastly, a graph of laser power vs. corrected brightness of spots was produced.

Similar techniques were attempted in the spinal cord. However technical difficulties yielded unsuitable material for analysis. Thus I used cerebellum to test the hypothesis instead.

4.3 Results

4.3.1 The Morphology of Neuromuscular Junctions in Old *Wld*^{s} Mice

Confocal images of neuromuscular Junctions were taken from YFP16 *Wld*^{s}

mice aged 7-12 months old, 3 days after unilateral sciatic nerve section. All muscles were labeled with TRITC α- BTX, and fixed in 4% paraformadehyde. Unlike young *Wld*^{s} mice, the pattern of endplate degeneration suggests that synapses were removed more quickly in these old *Wld*^{s} mice. Figure 4.1 A shows three different patterns of endplate innervation during degeneration (Blue arrow= fully occupied endplate, Purple arrow= vacant endplates, White arrow= fragmented endplates compared with Fig 3.5 D). However, as in young *Wld*^{s} mice, the axons of old *Wld*^{s} mice degenerated slowly following axotomy (Fig 4.1 B), they appeared completely intact 3 days after unilateral sciatic nerve section.

4.3.2 PDD analysis of axotomised NMJ in old *Wld*^{s} mice

I classified the states of innervation and occupancy of neuromuscular junctions sampled in old *Wld*^{s} mice (N= 6) to assess the patterns of synaptic degeneration. In the previous chapter, I identified five different states of axonal and synaptic degeneration in wild type, young heterozygous, and homozygous *Wld*^{s} mice during axotomy, they are: O state which represents fully occupied endplates connected with intact axons, CP state which represents partially occupied endplates connected with intact axons. CF state which represents fragmented endplates connected with intact axons. DF state which represents fragmented endplates with disconnected axons, and V states which represents vacant endplates. There are 7 possible trajectories of axonal and synaptic degeneration, namely 1) O→DF→V; 2) O→CP→V; 3)

O→CF→V; 4) O→CP→DF→V; 5) O→CP→CF→V; 6) O→CF→DF→V; and 7) O→CP→CF→DF→V. Using this same classification, I found only four main distinct states of axonal and synaptic degeneration in old axotomised *Wld*^{s} mice. They were: fully occupied (O), disconnected fragmented (DF), vacant (V), and very few connected partial (CP) at 17 hours, 24 hours, and 48 hours post axotomy. More specifically at 17 hours after axotomy, 78.72%±3.7 NMJs were fully occupied endplates with intact axons. 16.60%±2.25 NMJs appeared fragmented both in axons and synapses, and only 7.02%±0.88 NMJs had degenerated completely (Figure 4.2). Therefore, taking all data together, I conclude that the main trajectory of synaptic degeneration is O→DF→V, and few synapses also go through O→CP→DF→V or O→CP→V trajectories. This pattern is remarkably similar to that observed in young heterozygous *Wld*^{s} mice and completely different from that observed in young homozygotes. However the synaptic degeneration in axotomised old *Wld*^{s} mice is slower than heterozygous *Wld*^{s} mice.

4.3.3 Protein Expression in the Cerebellum of *Wld*^{s} Mice

Cerebellar slices were taken from three young (1-2 months) YFP16 *Wld*^{s} mice, three young YFP16 heterozygous *Wld*^{s} mice, and three old (>8 month) YFP16 *Wld*^{s} mice. Wld^{s} proteins in these slices were labeled immunocytochemically with the Wld^{18} antibody. Figures 4.3 & 4.4 show the Wld^{s} protein expression in cerebellar granule cells (CGC) of young and old homozygous and young heterozygous *Wld*^{s}

mice. It appears from these images that in heterozygous *Wld*^{s} mice, fewer CGC appeared to express Wld^{s} protein (TRITC immunostaining, red) in their nuclei (blue; Topro stain), compared to the young homozygous (2 month-old) *Wld*^{s} mice and old (7 month-old) homozygous *Wld*^{s} mice. However, using progressively increasing excitation laser power (HeNe laser power 20%, 30%, 40%, 50%, 60% of maximum) number of cells with spots in their nuclei gradually increased (Figure 4.5 & 4.6). These two groups of images were from a homozygous *Wld*^{s} mouse and a heterozygous *Wld*^{s} mouse. In the heterozygotes, the amount of Wld^{s} protein detected was significantly greater with a laser power setting of 60% (Fig 4.5; 4.7D $P<0.05$, ANOVA). This finding suggests that varying the excitation laser power is a useful way to detect differences in *Wld*^{s} protein expression.

In this experiment, at the same laser power setting, Wld^{s} protein expression differed in young homozygous, heterozygous and old homozygous *Wld*^{s} mice. Wld^{s} protein seemed to be expressed in most cerebellar granule cells in *Wld*^{s} mice, whereas the amount of Wld^{s} protein was obviously reduced in the young heterozygous *Wld*^{s} mice. However, in the old *Wld*^{s} mice, the Wld^{s} proteins expression was not consistent, the amount expressed in some of cerebellum granule cells were more in some areas than in other areas (Fig 4.4), Indeed, at low laser power, it did not seem that Wld^{s} proteins were expressed in most of the cerebellum granule cells as in young heterozygotes. In order to analyse the differences in Wld^{s} protein expression in young homozygous and old homozygous *Wld*^{s} mice, and young

heterozygous *Wld*^{s} mice, the mean intensity of proteins expressed in the CGC were tested in the each type of mouse at varying laser powers (20%, 30%, 40%, 50%, 60%). Fig4.7, A, B, C shows that in each type of mice, the mean intensity of immunofluorescence gradually increased with following the increasing laser powers. Moreover, Wld^{s} proteins showed stronger expression in young homozygous *Wld*^{s} mice than in young heterozygous and old homozygous *Wld*^{s} mice. The increases in mean intensity of Wld^{s} proteins fluorescence in both heterozygous and old homozygous *Wld*^{s} mice were not as obvious as in young homozygous *Wld*^{s} mice, even though the mean intensity of Wld^{s} protein in old *Wld*^{s} mice was relatively higher than in heterozygous *Wld*^{s} mice. The difference was most apparent at 60% laser power, figure 4.7, D shows the distinct mean intensity of each type of mouse at 60% laser power. A (young *Wld*^{s}) = 9.907 ± 0.657, B (heterozygotes) = 5.1385 ± 0.6165, C (old *Wld*^{s}) = 6.5957 ± 0.4517 ($P<0.001$; A vs B, $P<0.01$; A vs C, one-way ANOVA, Dunnett's post hoc test). This analysis therefore suggests that mouse age could be another intrinsic factor affecting Wld^{s} protein expression. The level of protein expression in old heterozygous *Wld*^{s} mice was not examined in the present study. *Wld*^{s} mice have a normal life span, thus the reason for the apparent selective decline of Wld^{s} protein examination in some neurons is also unknown but potentially of great interest for future research.

Figure 4.1 Morphology of NMJs of Old *Wld*^{S} Mice after Axotomy

(A) Confocal image of NMJs from an Old YFP16 *Wld*^{S} mouse 3 days after axotomy. Postsynaptic terminals stained by α-BTX.

Three different colour arrows showing the various states of nerve terminals, fully occupied endplates (blue arrow) fragmented endplates (white arrow) and vacant endplates (pink arrow). Scale bar = 30μm.

(B) Confocal image of axons from an old YFP16 *Wld*^{S} mouse 2 days after unilateral sciatic nerve section. Scale bar = 30μm.

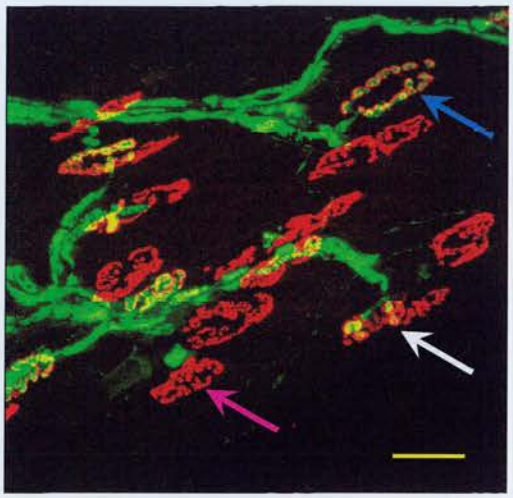

(A)

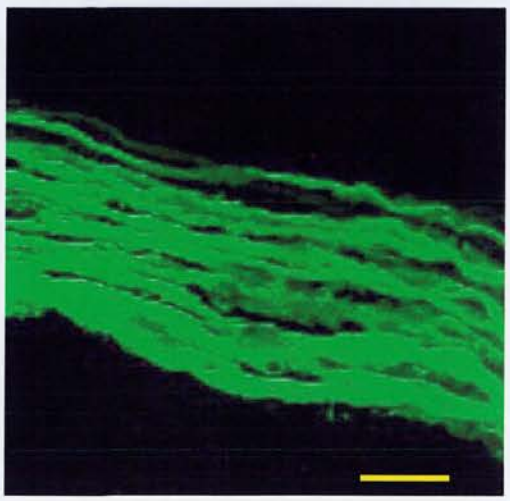

(B)

Figure 4.2 Polyhedral Degeneration Diagram (PDD) Analysis of Synaptic Degeneration in Old *Wld*^{S} Mice

The PDDs show the process of axonal and synaptic degeneration in the axotomised old (>8 months) *Wld*^{S} mice. Letters are used to represent the states of axons and synapses during neuronal degeneration after axotomy. That is, O represents fully occupied endplate; connected with intact axons, CP represents partially occupied endplate which is connected to an intact axon; CF represents fragmented endplate that is connected to intact axons; DF represents terminal disconnected from axons, where both of them are fragmented, V represents that endplates and axons are both degenerated completely. Blue circles represent the fully occupied (O) state, red circles represent the disconnected fragmented (DF) state, pink circles represent connected partial (CP) state, and yellow circles represent vacant (V) state.

The chart shows the percentages of different states of axons and synapses during the degeneration process in axotomised old (> 8 months) *Wld*^{S} mice at 17-hours, 24-hours and 48-hours time points, and standard error estimates with every percentage of endplates.

PDD diagram of old Wld^S mice

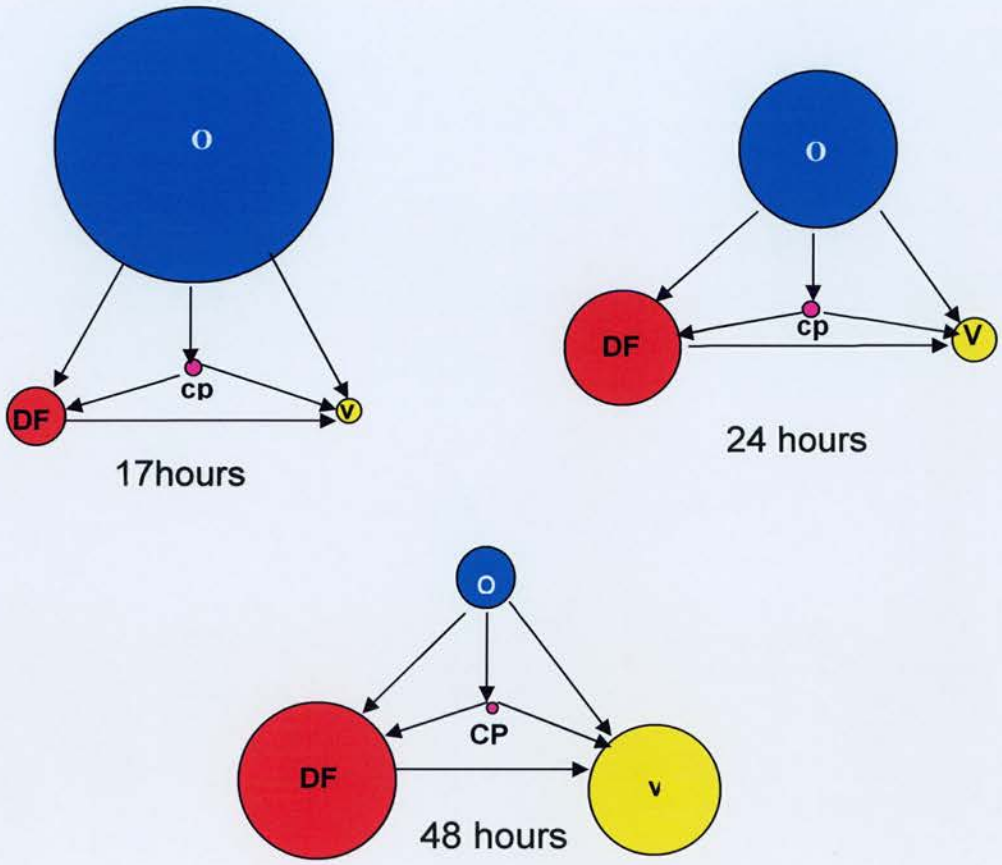

Time / Pattern (%endplates)	17 hours	24 hours	48 hours
O	78.72±3.70	54.432±8.25	16.43±3.62
CP	4.65±2.22	4.95±1.95	2.324±0.36
CF			
DF	16.60±2.25	32.84±3.93	44.82±4.23
V	7.02±0.88	12.41±3.60	37.34±5.14

Figure 4.3 Protein Expression in the Cerebellar Granule Cells (CGC) of *Wld*^{S} mice

(A-B) Confocal images of cerebellar granule cells from the *Wld*^{S} mice at zoom 2.5. Wld^{S} protein immunostained with Wld^{18} (red), and nuclei stained with Topro-3. Scale bar = 5μm

(A) Cerebellar granule cells from a 2 months old homozygous *Wld*^{S} mouse

(B) Cerebellar granule cells from a 2 months old heterozygous *Wld*^{S} mouse

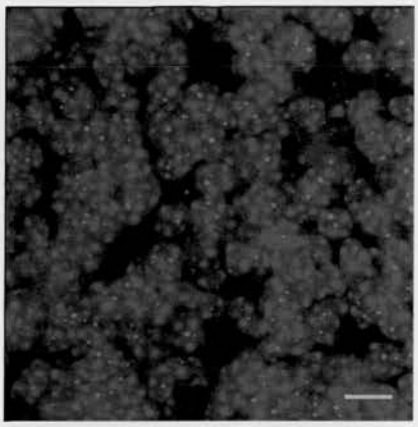

(A) Young *Wld*^{S}

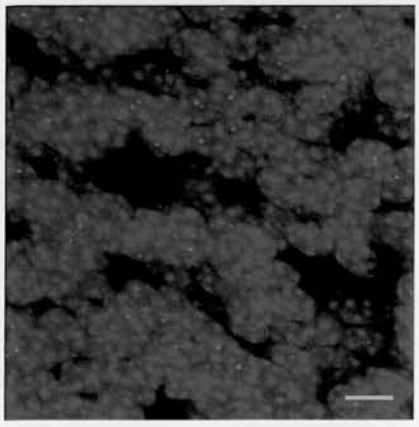

(B) Heterozygous *Wld*^{S}

Figure 4.4 Protein Expression in the Cerebellar Granule Cells (CGC) of Old *Wld*^{S} Mice

(A-B) Confocal images of cerebellar granule cells from old *Wld*^{S} mice at zoom 5.0. Wld^S protein immunostained with Wld^{18} (red), and the nuclei stained with Topro-3 (blue). Different regions of the cerebellum appear to show different levels of *Wld*^{S} protein expression. Scale bar = 5μm

Old *Wld*^{S} mice

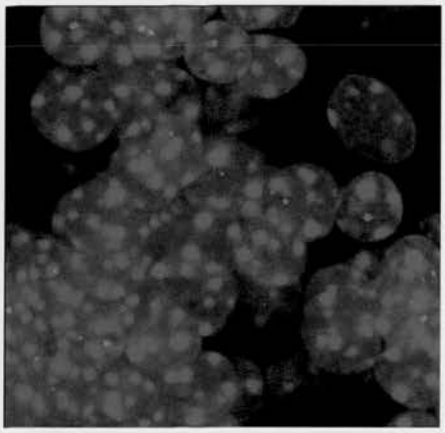

(A)

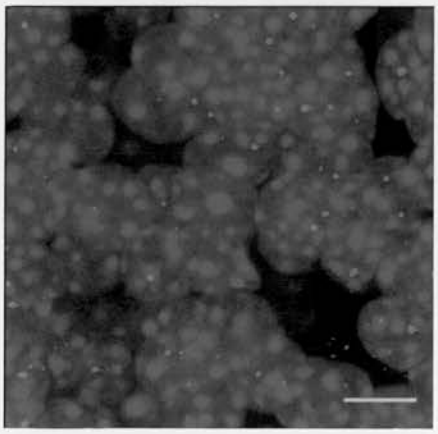

(B)

Figure 4.5 *Wld*^{S} Protein Expression in Different Laser Powers in Heterozygous and Young Homozygous *Wld*^{S} mice

(A-B) Confocal images of cerebellar granule cells from young heterozygous & homozygous *Wld*^{S} mice (8 weeks old) with increasing laser power (HeNe laserpower 20%, 30%, 40%, 50%, 60% of maximum). The nuclei of cerebellar granule cells immunostained with Topro-3 (blue) and *Wld*^{S} proteins immunostained with Wld[18] antibody. Scale bar = 5μm

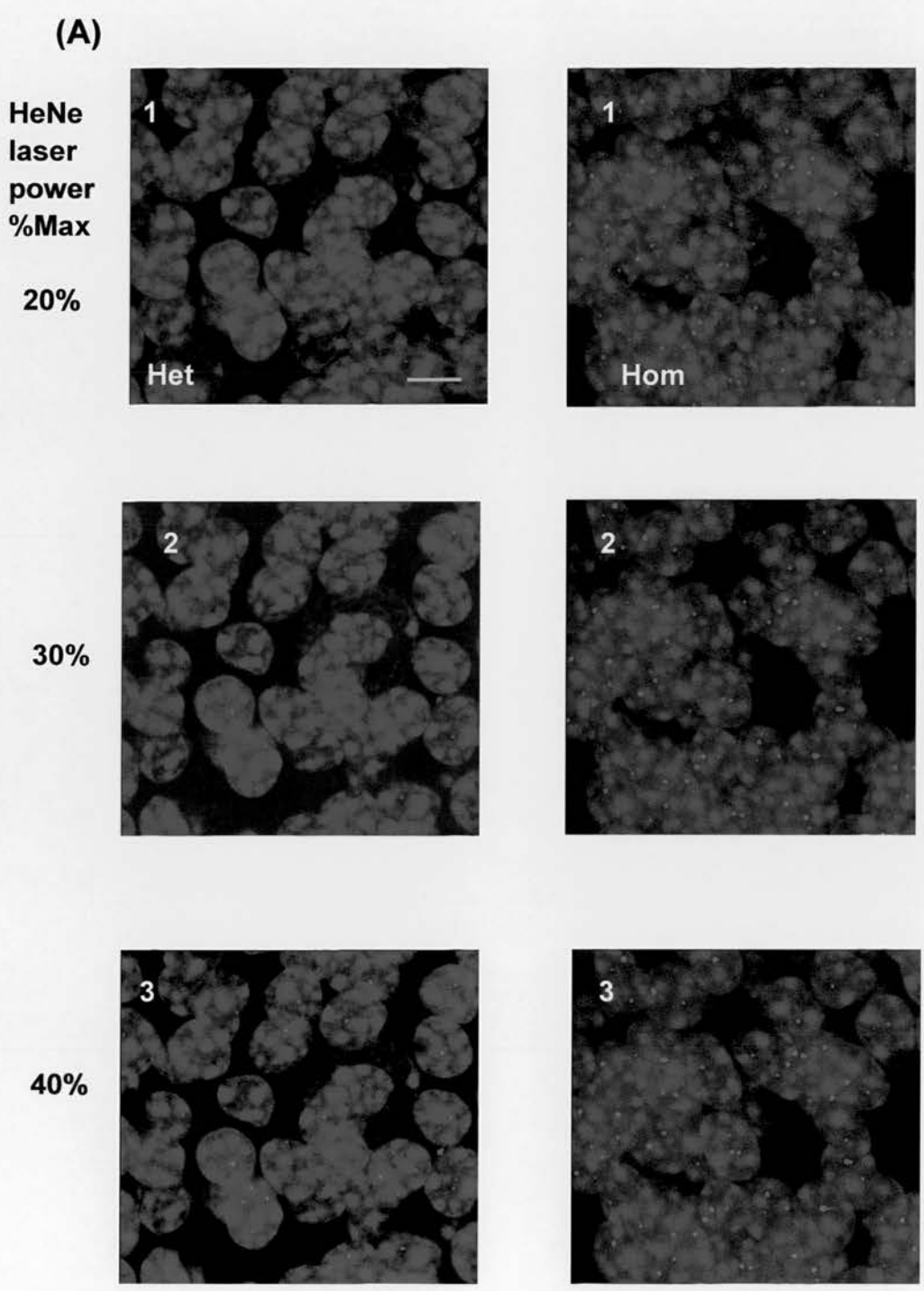
(A)
HeNe laser power %Max
20%
30%
40%
1
Het
1
Hom
2
2
3
3

(B)

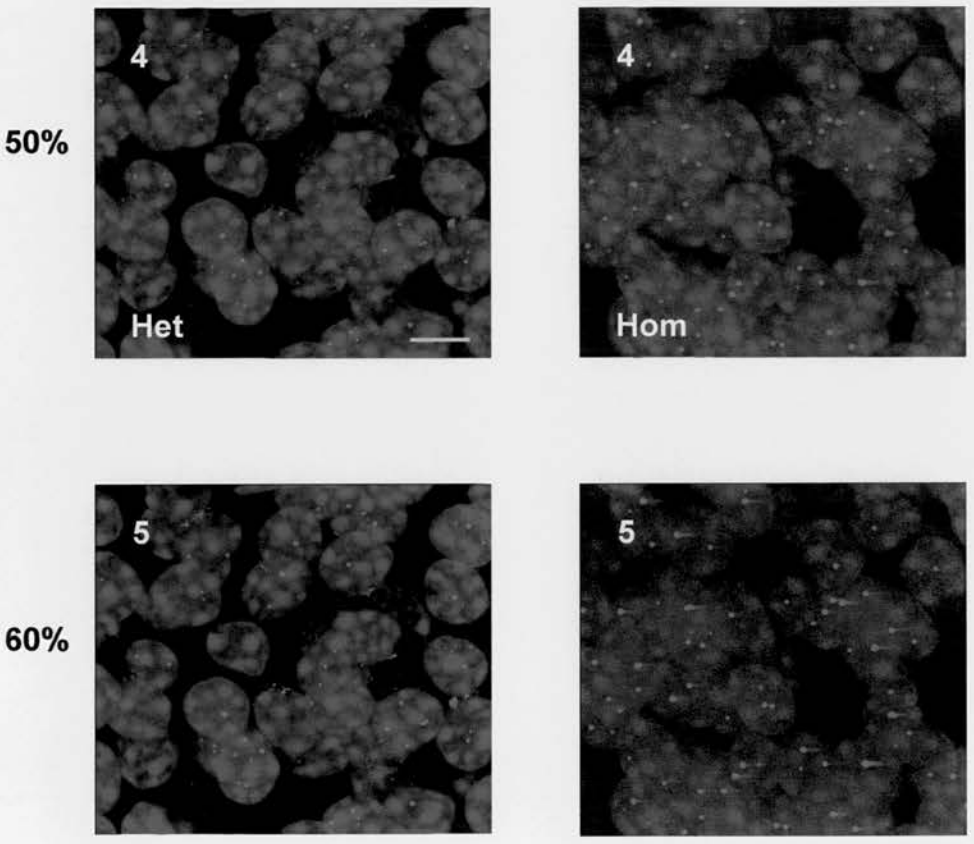

Figure 4.6 *Wld*^{S} Protein fluorescence at Different Laser Powers in Old *Wld*^{S} Mice

(A) Confocal images of cerebellar granule cells from Old *Wld*^{S} mice (>7 months old) with increasing laser power (HeNe laserpower 20%, 30%, 40%, 50%, 60% of maximum). The nuclei of cerebellar granule cells immunostained with Topro-3 (blue) and *Wld*^{S} proteins immunostained with Wld^{18} antibody. Scale bar = 5μm

(A)

HeNe laser power %Max

20%

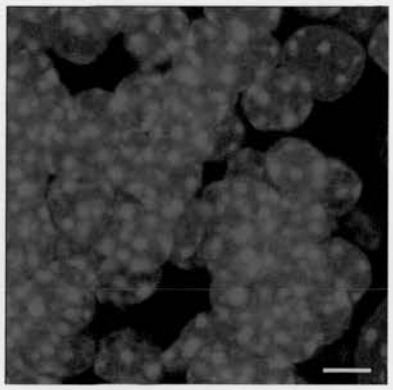

30%

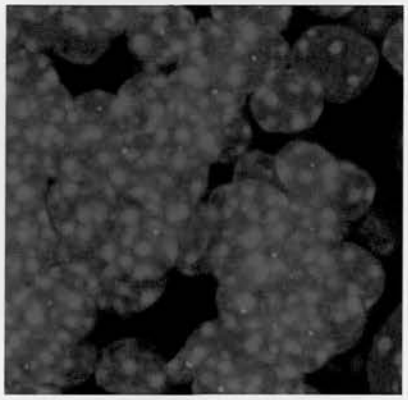

40%

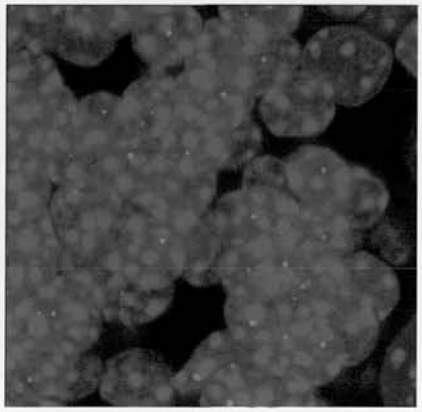

50%

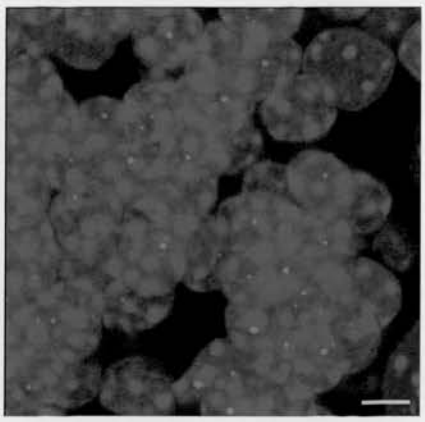

60%

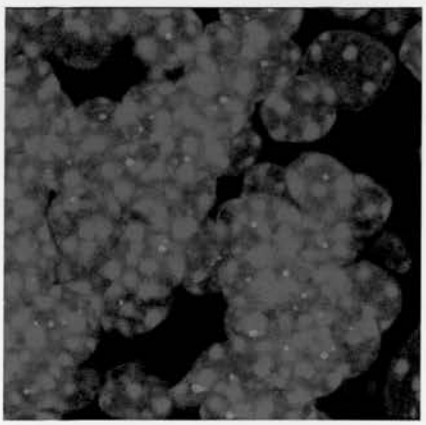

Figure 4.7 Intensity of Wld^s Protein Expression in Heterozygous *Wld^s* and Homozygous *Wld^s* Mice

(A) Graph of laser power versus mean spot intensity in 2 month-old *Wld^s* mice as calculated from counts of immunocytochemically stained (Topro-3, Wld^{18} antibody) cerebellar granule cells. Black squares represent data from three 2 months old homozygous *Wld^s* mice.

(B) Graph of laser power versus mean spot intensity in 2 months old heterozygous *Wld^s* mice as calculated by counts of immunocytochemically stained (Topro-3, Wld^{18} antibody) cerebellar granule cells. Squares represent data from three 2 month-old *Wld^s* heterozygous mice.

(C) Graph of laser power versus mean spots intensity in 7 months old *Wld^s* mice as calculated by counts of immunocytochemically stained (Topro-3, Wld^{18} antibody) cerebellar granule cells. Black squares represent data from three 7 month-old *Wld^s* mice.

(D) Mean intensity of Wld^s protein in young homozygous and heterozygous *Wld^s* mice, and old homozygous *Wld^s* mice respectively at 60% laser power. column A represents young *Wld^s* mice; column B represents young heterozygous *Wld^s* mice; column C represents old homozygous *Wd^s* mice (ANOVA test: $P<0.0001$; A vs B, $P<0.01$; A vs C, $P<0.01$; Dunnett's post hoc test).

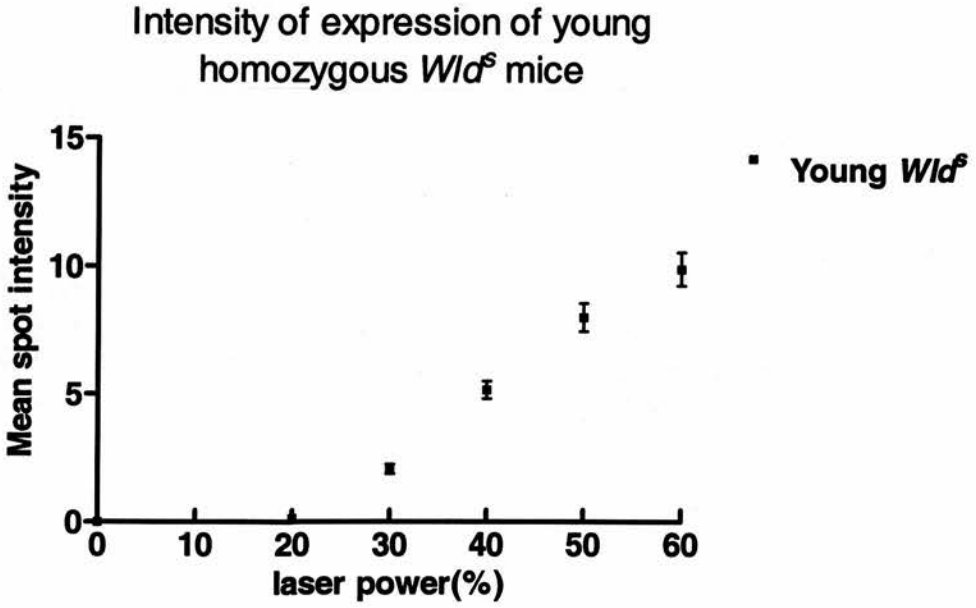
Intensity of expression of young homozygous Wld^S mice
Mean spot intensity
15
10
5
0
0
10
20
30
40
50
60
laser power(%)
Young Wld^S

(A)

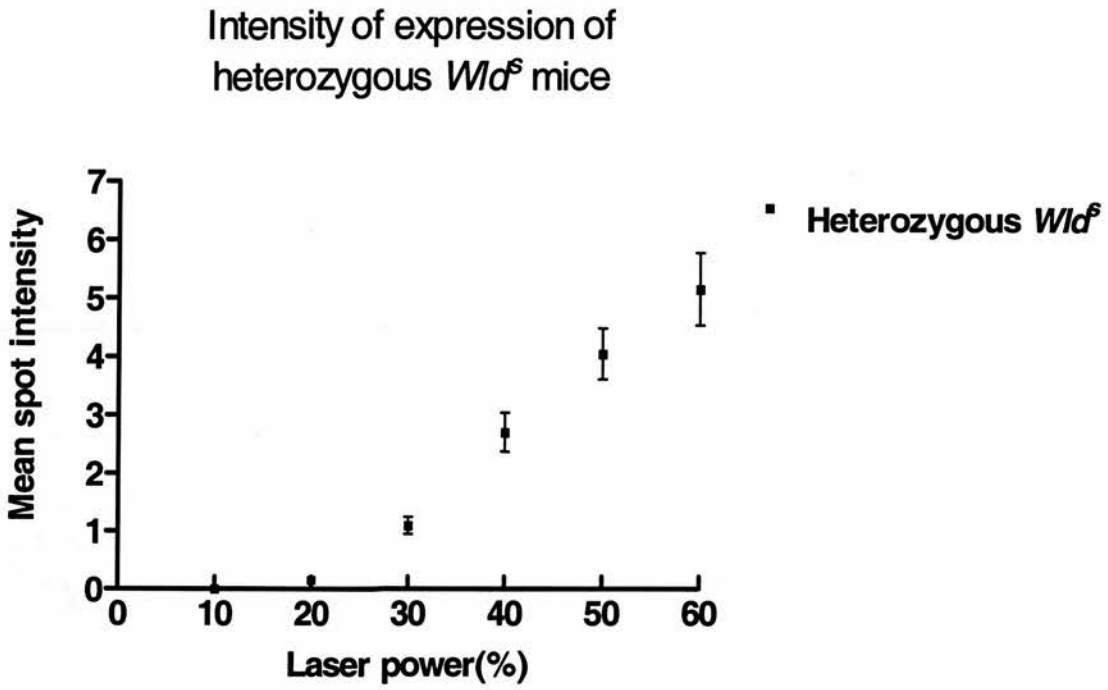
Intensity of expression of
heterozygous Wld^S mice
Mean spot intensity
0
1
2
3
4
5
6
7
0
10
20
30
40
50
60
Laser power(%)
Heterozygous Wld^S

(B)

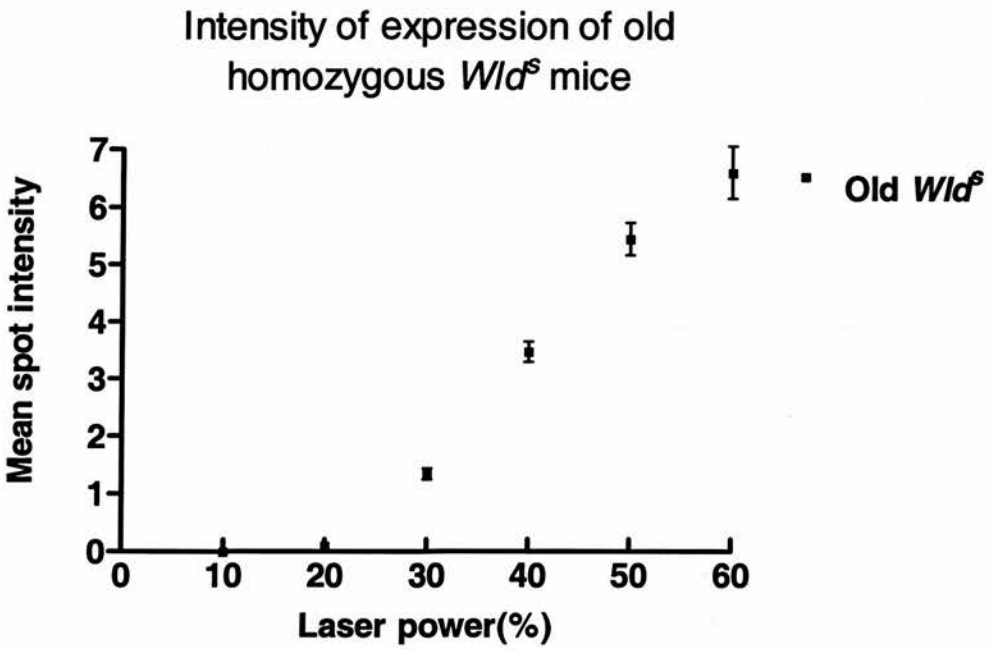
Intensity of expression of old homozygous Wlds mice
Mean spot intensity
0
1
2
3
4
5
6
7
0
10
20
30
40
50
60
Laser power(%)
Old Wlds

(C)

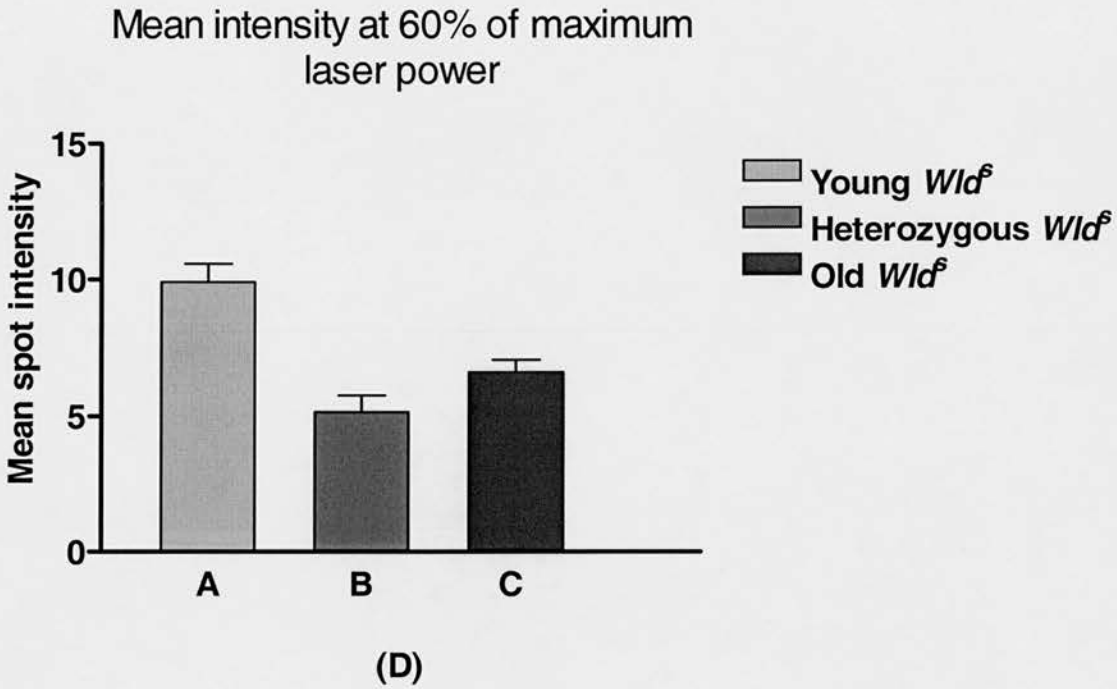
Mean intensity at 60% of maximum laser power
Mean spot intensity
15
10
5
0
A
B
C
Young Wld^S
Heterozygous Wld^S
Old Wld^S

(D)

Summary

In the previous chapter, I showed that the *Wld*^{S} gene plays an important role in delaying the degeneration in axons and synaptic terminals. Moreover, gene dose, a genetic intrinsic factor, influences the degeneration pattern of axons and synapses in the axotomised *Wld*^{S} mice.

Age is another intrinsic factor affecting nerve terminal degeneration, and has been presented by Gillingwater et al (2002). They showed that when mice were over 4 months old, synaptic degeneration reverted back to a Wallerian-like process, but with axons still intact. The PDD analysis method I applied to old *Wld*^{S} mice extends their findings (Figure 4.2). Wld^S protein expression in the cerebellar granule cells in young heterozygous *Wld*^{S} mice and old homozygous *Wld*^{S} mice suggested that *Wld*^{S} protein expression is decreased in many neurons of the axotomy-induced old *Wld*^{S} mice, in contrast to the young axotomised homozygous *Wld*^{S} mice.

Therefore, reduced protein expression in old *Wld*^{S} mice may explain the distinct axon and synaptic protection as old *Wld*^{S} mice age, at least in some neurons.

5. Effect of Botulinum Toxin and Nerve Stump Length on Synaptic Degeneration in *Wld*^{S} Mice

5.1 Introduction

Botulinum toxin is a neurotoxic protein produced by the bacterium Clostridium botulinum. It is one of the most poisonous naturally occuring substances known. Its highly toxic property has been used in minute doses to treat many nervous system diseases: muscle spasms, uncontrolled blinking, headache disorders and musculoskeletal pain (Bhidayasiri et al., 2005). It even improves sialorrhoea in Amyotrophic Lateral Sclerosis (ALS) (Giess et al., 2002), however, recently the most popular use of botulinum toxin (BoTox) in many parts of the world has become in the field of cosmetic treatment. For instance, de-wrinkling properties are due to its action as muscle relaxant. BoTox also promote nerve sprouting as well as inhibitory Ca^{2+} influx into motor nerve terminals during activities. It was therefore of interest to ask whether it might delay synaptic degeneration as well.

Botulinum toxin is a two-chain polypeptide which contains a 100-kDa chain and a 50-kDa light chain joined by a disulphide bond. The light chain is a protease whose action prevents vesicles from anchoring to the nerve terminal membrane to release actetylcholine, This action is mediated by one of the fusion proteins targeted by BoTox (see below) at a neuromuscular junction. The toxin must enter the nerve terminals in order to cause paralysis. This requirement is mediated by the heavy chain of the toxin which targets the toxin to specific types of axonal terminals.

After attachment of the toxin heavy chain onto proteins on the surface of nerve

terminals, the entire molecule is taken up into neurons by endocytosis. The light chain which has the protease activity, leaves endocytotic vesicles and enters the cytoplasm. Botulinum neurotoxin type A (BoTox/A) blocks the exocytosis of acetylcholine (Ach) by its intracelluar proteolytic cleavage of synaptosomal-associated protein, with a molecular mass of 25 kDa (SNAP-25), a vesicular type of SNARE protein (Schiavo et al., 1993; Blasi, 1993). Interestingly, botulinum neurotoxin type A also stimulates sprouting of nerve endings at the neuromuscular junction after blocking neurotransmission (de Paiva et al; 1999). The process takes a few days and appears to be a consequence of muscle paralysis (Brown et al., 1977; 1980; 1982; Caroni et al., 1994).

Neither the mechanism of synaptic degeneration nor regulation has been fully clarified, finding compounds that slow down synaptic degeneration is another objective of neurodegenerative disease research. Botulinum toxin A was used to test whether blocking transmitter release could protect synaptic terminals from degeneration after axotomy.

Nerve Stump Length

Miledi & Slater (1970) used rats to test the effect of nerve stump length on synaptic degeneration by cutting a short stump and a long stump of phrenic nerve. They examined synaptic transmission using electrophysiology and ultrastructural techniques up to 48 hours later. They showed that the rate of synaptic degeneration

varied with the different lengths of nerve stump. This finding confirmed previous studies by Luco & Eyzaguirre (1955) on the tenuissimus of a cat. Moreover, in 1995, Ribchester et al used *Wld*^{s} mice to study the effect of nerve stump length on synaptic degeneration. The results suggested that an increase of 1cm in the length of the distal stump delayed degeneration by about 1- 2 days. However, this conclusion was drawn from physiological analysis, I therefore repeated these experiments using morphological analysis to examine the outcome.

5.2 Method

Chronologically, the experiments described in this chapter were carried out before colonies of *Thy1.2* YFP mice became established. Hence, immunostaining of axons and endplates was used to visualize the neuronal processes. Six young female *Wld*^{s} mice (2 months old) were used in the experiments. 5µl botulinum toxin type A (from Sigma) was injected into one hind foot of each of 3 mice before cutting the sciatic nerve in the mid-thigh region. Each injection contained 1.0-1.5 ng BoTox. As a control, the hind feet on the contralateral side of three other *Wld*^{s} mice were injected with 3-5 µl of the non-sprouting buffer only[1] (for composition see Appendix I) Similar injections were made in three *Wld*^{s} mice in which the tibial nerve was cut instead of the sciatic nerve (Distance between sciatic and tibial nerve lesion sites was almost 2 cm). Five days after axotomy, the animals were killed, the

[1] Conventional physiology saline buffer is reported to produce a small amount of sprouting (W. Thompson, personal communication to R.R Ribchester).
" Non-sprouting" buffer has composition that avoids this.

tibial nerve was stimulated with 10V, 1ms pulses. Absence of contraction confirmed neuromuscular paralysis on the injected side. The lumbrical muscles were isolated and stained with the TRITC α- Bungatrotoxin, and immunostained with NF and SV2. The images were viewed and analysed by conventional fluorescence microscopy.

In addition, three old *Wld*^{s} mice (7 months old) with unilateral section of the sciatic nerve were studied. Each operated foot of the three mice was injected with 3μl BoTox (c=0.05 ng/μl), (since I found that the old mice did not survive when injected with the same volume of BoTox as in young mice) and the contralateral leg injected with 3μl non-sprouting buffer as the sham control. Lumbrical muscles were isolated from two of the mice 3 days after axotomy. Lumbrical muscles were isolated from the third mouse 7 days after axotomy. Immunostained preparations were viewed and analysed by fluorescence microscopy.

5.3 Results

5.3.1 Morphologic Evidence for Preservation of Synaptic Terminals in *Wld*^{s} Mice after BoTox Injection in young *Wld*^{s} mice

Lumbrical muscles 1, 2, 3, 4 (n=16) from 5 days axotomised 2 months old *Wld*^{s} mice (n=6) were immunocytomchemically labeled (NF, SV2 and α- BTX). Quantitative analysis suggests that BoTox had a small additive effect on the protection from synaptic degeneration (Figure 5.1). The occupancy of NMJs gave

the simplest measure of any effect. In BoTox injected muscles occupancy was 92.76%±1.4, while the occupancy of NMJs without BoTox injection was 80.038%±7.826 ($P< 0.05$, Mann-Whitney test). It was significantly different from muscles injection with non-sprouting buffer solution

5.3.2 Botox has no Effect on Synaptic Degeneration in Old *Wld*^{s} Mice

Lumbrical muscles 1, 2, 3, 4 (n=12) from 3 days (N=2) and 7 days (N=1) axotomised 7 months old *Wld*^{s} mice (n=6) were immunocytomchemically labeled (NF, SV2 and α- BTX) and the NMJs individually assessed as to their level of occupancy. Qualitative analysis of lumbrical muscles preparations showed that BoTox had little effect on the protection of synaptic degeneration (Figure 5.2). Almost all endplates were vacant by 3 days, the percentage of vacant endplates after BoTox injection was 88.48%±4.356 at this time, and increased to 98.87%±0.603 by 7 days after axotomy. This was not significantly different from control muscles, injected with non-sprouting buffer solution. (Percentage vacancy data was plotted here rather than percentage occupancy simply to facilitate visual comparison of the data.

5.3.3 Morphologic Evidence for Preservation of Synaptic Terminals in the *Wld*^{s} Mice after Axotomy: Effect of Nerve Stump Length

Lumbrical muscles 1, 2, 3, 4 (n=16) from 5 days axotomised 2 months old *Wld*^{s} mice (n=6) were immunocytomchemically labeled (NF, SV2 and α- BTX) and the NMJs individually assessed as to their level of occupancy.

Qualitative analysis of lumbrical muscle preparations suggests that nerve terminals degenerated slightly slower in the sciatic nerve-cut compared to the tibial nerve-cut groups. (Figure 5.3) However, quantitative analysis indicated that the difference was not statistically different. The occupancy of endplates after axotomy was 84.196% ±15.77, while the occupancy after tibial axotomy was 80.038% ± 17.50 ($P>0.05$; Mann-Whitney test).

Fig 5.1 BoTox Effects on Synaptic Degeneration

(A) Conventional fluorescence microscopy images of NMJs from young *Wld*^{S} mice (8 weeks old) with BoTox injection (immunostained with NF and SV2 antibodies and ACh receptors labelled with TRITC α-BTX). Scale bar = 30μm.

(B) Bar chart showing the percentage occupancy of endplates stained by α-BTX in the lumbrical muscles 5 days after axotomy, from 2 months old *Wld*^{S} mice which were injected with BoTox after sciatic or tibial nerve axotomy.

There was a small statistically significant additional delay in nerve terminal degeneration following the Botox injection ($P < 0.05$; Mann-Whitney).

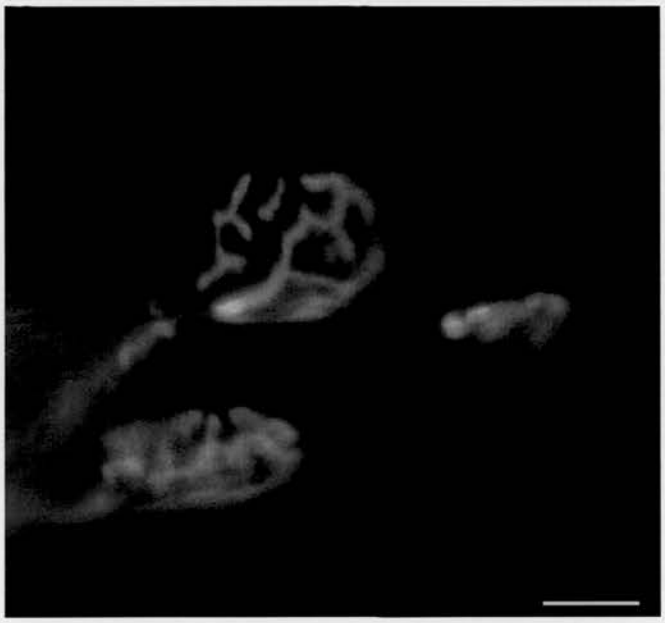

(A)

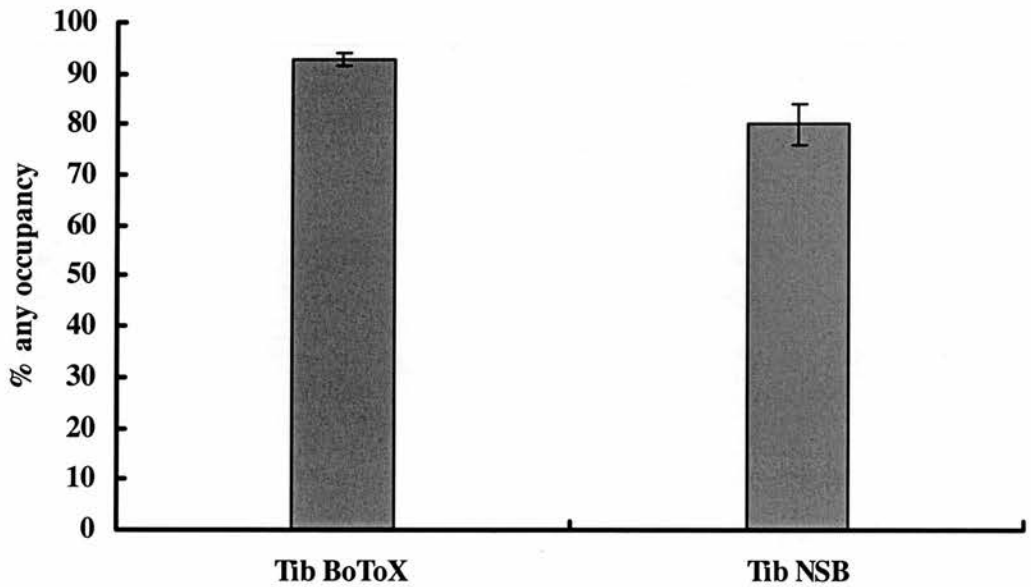

(B)

Fig 5.2 BoTox Effect on the Old *Wld*^{s} Mice after Axotomy

(A) Conventional fluorescence microscopy image of NMJs from old *Wld*^{s} mice (>7 months old) with BoTox injection (immunostained with NF and SV2 antibodies and labelled with TRITC α-BTX). Scale bar = 30μm.

(B) Bar chart showing the percentage of nerve terminals stained by α-BTX in the lumbrical muscles 3 and 7 days after axotomy, from 7 months old *Wld*^{s} mice which were injected with Botox after sciatic and tibial nerve axotomy. A few endplates remained occupied 3 days after injection, but almost all nerve terminals had degenerated completely 7 days after injection.

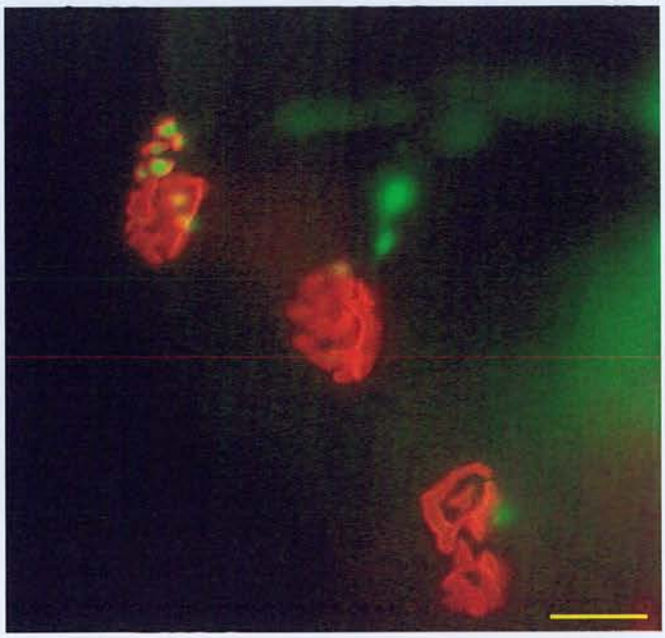

(A)

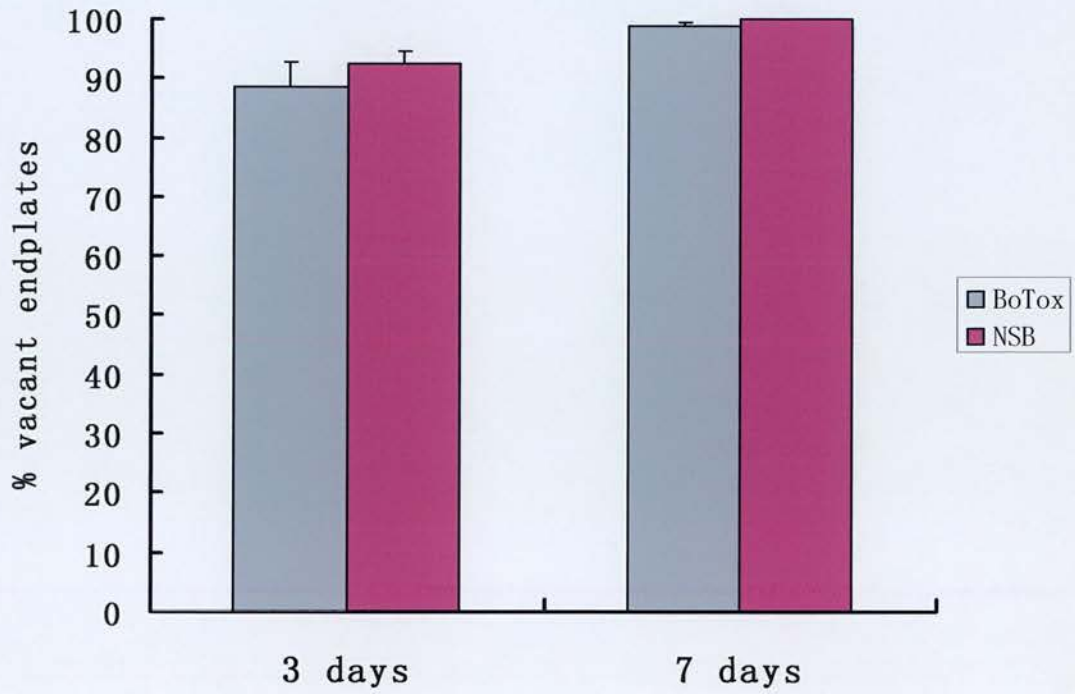
100
90
80
70
60
50
40
30
20
10
0
% vacant endplates
3 days
7 days
BoTox
NSB

(B)

Fig 5.3 Nerve stump length experiment

(A) Bar chart showing the percentage of occupied endplates in the lumbrical muscles 5 days after axotomy, from 2 months old *Wld*^{s} mice, injected with non-sprouting buffer solution after sciatic and tibial nerve axotomy. The AChRs in the postsynaptic membranes were stained by TRITC-α-BTX. The protection of synaptic terminals in the sciatic nerve axotomy was not statistically significant ($P > 0.05$; Mann-Whitney).

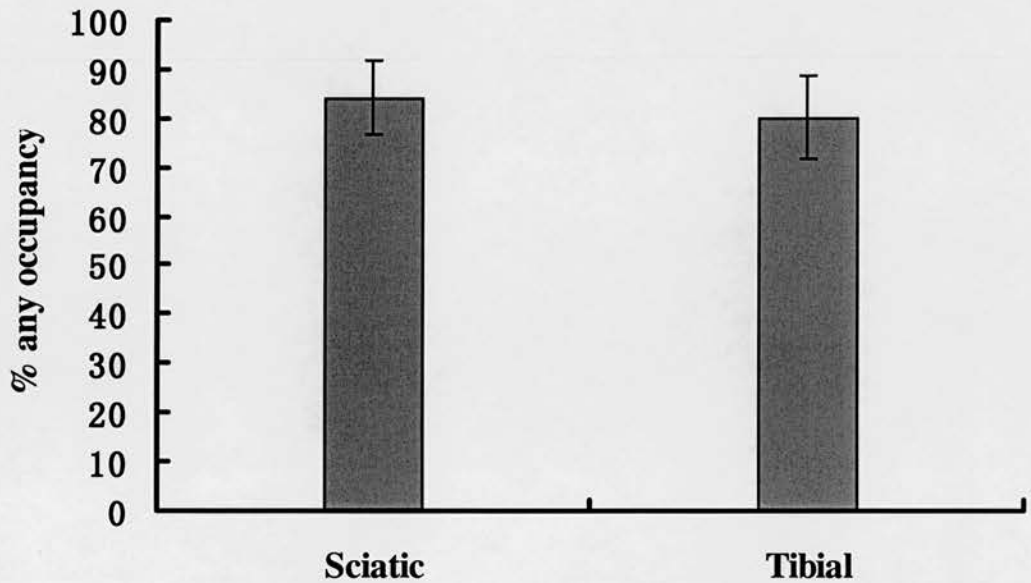

(A)

Summary

Wld^S gene dose and age of mice influence the patterns and rate of axons and synaptic degeneration after axotomy in *Wld*^{S} mice. It was interesting to ask whether extrinsic factors could also influence these processes, adding to the protective *Wld*^{S} phenotype. Here, I examined two potential influences that have been shown previously to influence synaptic form and function in wild-type mice, namely muscle paralysis and nerve stump length.

Although, previous studies suggested that blocking vesicle release may delay degeneration of synapses (Mattison, 1999, PhD Thesis University of Edinburgh) in my studies the degeneration of synaptic terminals was only slightly delayed following BoTox injection in young *Wld*^{S} mice 5 days after axotomy. Moreover, this protective effect on synaptic terminals was lost in old *Wld*^{S} mice 3 days after axotomy, in these mice all terminals had degenerated either in the presence or absence of BoTox. The different nerve stump lengths between sciatic nerve section and tibial nerve section did not yield a significant difference in synaptic degeneration.

These largely negative findings underscore the potency of the protective effect of the *Wld*^{S} gene, and the powerful effect of age in abolishing it, at least at the synaptic level.

6. Discussion

The main findings of the present study are threefold: Firstly, synaptic protection by *Wld*^{s} gene is more sensitive to reduced gene dose and mice age than axons or synapses in axotomised young homozygous *Wld*^{s} mice. This finding is supported by PDD analysis, which provides a new way of systematically and comprehensively representing their pattern and "trajectory" of axonal and synaptic degeneration in axotomy-induced wild type, young homozygous, young heterozygous and old homozygous *Wld*^{s} mice. Using PDD analysis, we can see how similar patterns of synaptic terminal degeneration occur in both young axotomised heterozygous and old homozygous *Wld*^{s} mice, and this was distinctly different from the way synapses degenerate in young homozygous *Wld*^{s} mice.

Next, I presented evidence that variation of synaptic degeneration in heterozygous *Wld*^{s} mice may be due to its reduced expression of Wld^{s} protein with age in some neurons, suggesting that synaptic degeneration in old axotomised *Wld*^{s} mice may also be modulated by a gene-dose effect. I measured Wld^{s} protein expression in cerebellar granule cells of young homozygous and heterozygous and old homozygous *Wld*^{s} mice. I found a reduction of Wld^{s} protein expression in all neurons of young heterozygous mice and in at least some neurons in old homozygous *Wld*^{s} mice. This decrease may therefore explain the distinct pattern of synaptic degeneration in old *Wld*^{s} mice.

Thirdly, besides gene-dose and age, I examined the effect of two other potential

influences: nerve stump length and neuromuscular transmission. However, I did not find any compelling evidence that these significantly affect the rate of synaptic degeneration. The results of leaving a long nerve stump did not confer any additional protection, and blocking neuromuscular transmission with Botox only slightly enhanced synaptic protection in young *Wld*^{s} mice, whilst there was no effective protection in old (7 months old) *Wld*^{s} mice

6.1 The *Wld*^{s} Gene Strongly Protects Axons

In wild-type mice, Wallerian degeneration is normally complete within 24 to 48 hours of axotomy, the primary event in Wallerian degeneration is axonal fragmentation and degeneration, which is accompanied by a failure of the nerve to conduct in mice, at 1 to 2 days axotomy, the sciatic nerve becomes incapable of conducting compound action potentials. (Vial, 1958; McDoald, 1972; Allt, 1976; Nicholls et al., 1992)

In contrast, in the mutant *Wld*^{s} mice, the lesioned axon is preserved for several weeks before eventually degenerating (Lunn et al., 1989; Tsao et al., 1994). In other words, the *Wld*^{s} mutant has about a 10-fold delay in axonal degeneration after nerve injury (Gillingwater et al., 2003). Furthermore, Mack et al 2001 suggested that axons were still protected well in heterozygous *Wld*^{s} mice after axotomy, in despite of the reduced gene dose. They used different lines of transgenic mice after the same axotomy to demonstrate that axonal protection is gene dose –dependent. Their result

showed that axonal preservation in the transgenic line $4836^{Tg/+}$ (81.7 ± 2.2; n=3) is similar to the $Wld^{s/+}$ (86.2±1.2; n=3) and Wld^{s}/Wld^{s} (90.0±4.7; n=3) at the same time after axotomy, by observing that the transgene expression level in line 4836 is similar to that in Wld^{s}/Wld^{s} mice. Subsequently, Gillingwater et al (2002) demonstrated that axons were also preserved by the Wld^{s} gene in mature Wld^{s} mice (> 4 months old).

The findings of the present study on axon degeneration in these four different types of mice have confirmed these previous studies. Confocal micrographs of tibial nerves following sciatic nerve lesions have shown that in unilateral sciatic nerve section, there was no obvious difference in axonal degeneration among young heterozygous Wld^{s}, homozygous Wld^{s}, and old homozygous Wld^{s} mice, but in wild type mice, the axons totally degenerated within the same period post axotomy. (Figure 3.4 B, C, D & Figure 4.1 B). However, in further time course studies on NMJs among young heterozygous, homozygous and old homozygous Wld^{s} mice, this intramuscular axonal protection by the Wld^{s} gene following nerve section appeared somewhat different. Further analysis of this will be discussed in the following PDD analysis section.

6.2 NMJs are Very Sensitive to Gene Dose

In Mack et al's work, most studies focused on whether a change in Wld^{s} gene dose affects axonal degeneration. As I pointed out in the Introduction comparing homozygous and heterozygous Wld^{s} mice, provides a simple way to testing the effect

of gene dose. Regarding the Wld^S protein effect on synaptic degeneration, Mack et al (2001) only mentioned that in transgenic heterozygous *Wld*^{S} mice after 3 days, some synaptic terminals were still occupied (Mack et al., 2001). Through morphological and ultrastructural studies, Gillingwater et al (2002) suggested that age is another factor which influences the synaptic degeneration. Consequently, the present study was mainly focused on the synaptic degeneration as affected by both *Wld*^{S} gene dose and age in different types of mice following axotomy.

There are two copies of the chimeric *Wld*^{S} gene in heterozygous *Wld*^{S} mice and 4 copies in homozygotes. Young wild type mice, heterozygous and homozygous *Wld*^{S} mice were used to form a sample group with varying *Wld*^{S} gene dose in the study. Moreover, in order to investigate further the relationships of synaptic degeneration among these types, the time courses of synaptic degeneration were studied in young *YFP16* homozygous and*YFP16* heterozygous *Wld*^{S} mice, and in *YFP16* wild type (C57/Bl6) mice, following the unilateral sciatic nerve section.

6.2.1 Wild-Type Mice

It has been shown that, in wild type mice, nerve terminals normally degenerate within 24-26 hours, which is earlier than their motor axons (Birks et al. 1960; Miledi & Slater 1970; Gillingwater et al., 2001). The process of synaptic degeneration is synchronous in axotomised wild-type mice, both axons and synaptic terminals degenerate rapidly following axotomy (Miledi and Slater, 1968; 1970; Winlow and

Usherwood, 1975). In my present experiments, in *YFP16* wild type mice, nerve terminals began to degenerate rapidly and apparently simultaneously (i.c. more synchronously than in homozygous *Wld*^{S} mice) from 6 hours post axotomy and no synaptic terminals were occupied at exactly 17 hours post axotomy. This is much less than the 24-26 hours in previous work, and in total six YFP16 *Wld*^{S} mice (8 weeks) were used. My data and other evidence from studying rats and mice suggest that degeneration of synaptic terminal precedes axon degeneration (Miledi and Slater, 1970; Beirowski et al., 2003). That is, axon fragmentation does not normally begin until about 36 hours in peripheral nerves, whereas nerve terminals degeneration was complete in my study by 17 hours.

6.2.2 Young Homozygous *Wld*^{S} Mice

In mutant *Wld*^{S} mice, Ribchester et al (1995) showed that *Wld*^{S} NMJs are preserved and able to release neurotransmitter and recycle synaptic vesicle membrane for at least 3 days, and in some cases as long as 2 weeks, following nerve section. Moreover, vital dye labeling, immunocytochemistry and electrophysiology suggest that while nerve terminals degenerate synchronously in axotomised wild-type mice, progressive piecemeal synapse withdrawal is induced by axotomy in *Wld*^{S} mice. It was suggested that nerve terminals retract from the endplate, bouton by bouton, to form a swelling bulb at the distal end of the axon, which is detached from the endplate (Mattison, 1999; Gillingwater and Ribchester et al., 2001). This pattern

of terminal withdrawal occurs in a similar fashion during synapse elimination, which takes place in neonatal mammals to form the neuromuscular innervation pattern in postnatal development (Sanes and Lichtman, 1999; Keller-Peck et al., 2001; Gillingwater et al., 2002; 2003).

In young homozygous *Wld*^{s} mice, the present findings showed that synaptic degeneration have an appearance similar to that in previous studies which used FM1-43 to label nerve terminals (Parson et al., 1998; Ribchester et al, 1999). In Fig3.3 (A, B, C) with increasing days post axotomy, fully occupied endplates became partially occupied endplates and eventually became vacant, the different percentage patterns of partially occupied endplates at different times have suggested that the axotomy-induced synaptic elimination in *Wld*^{s} mice is a gradual withdrawal process in *Wld*^{s} mice. These data strongly support previous finding of a progressive withdrawal pattern of synaptic degeneration in axotomised homozygous *Wld*^{s} mice. Thus the hallmark of homozygous *Wld*^{s} mice is piecemeal, asynchronously and slow synaptic retraction; whereas in heterozygotes or wild-type mice it is rapid, uniform and much more synchronous. These differences suggest that the mechanisms are different.

During the time course of studying synaptic terminal degeneration in young homozygous *Wld*^{s} mice, two different staining methods were used, one used CFP transgenic mice and another *Thy1*-YFP16 transgenic mice, since the Cyan and

Yellow Fluorescence Protein in these lines express fluorochrome in all motor neurons (Feng et al, 2000). The latter method is widely used in many recent NMJ experiments, due to its accurate and good quality staining, so it was also used in the majority of my studies. However, compared with *CFP* and *YFP16* mice synaptic degeneration data (Fig3.6) suggest there are differences in % vacant endplates in the young Wld^S mice after the equivalent number of days post axotomy. The reason for this difference is two-fold. Firstly, the first group of mice underwent tibial nerve section, while the second group of mice had sciatic nerve section. With regards to the nerve stump dependence hypothesis, in the sciatic nerve section experiment, synaptic degeneration was slightly slower than that in the tibial nerve section experiment. However, in my morphological experiment, there is no significant difference between the sciatic and tibial nerve section. Secondly, the different transgenic mice lines used in these two groups could be another reason for this difference. However, recent studies show no effect of fluorescence protein examined on the rate of synaptic degeneration in Wld^S mice (Bridge et al., 2007 Figure 6.1)

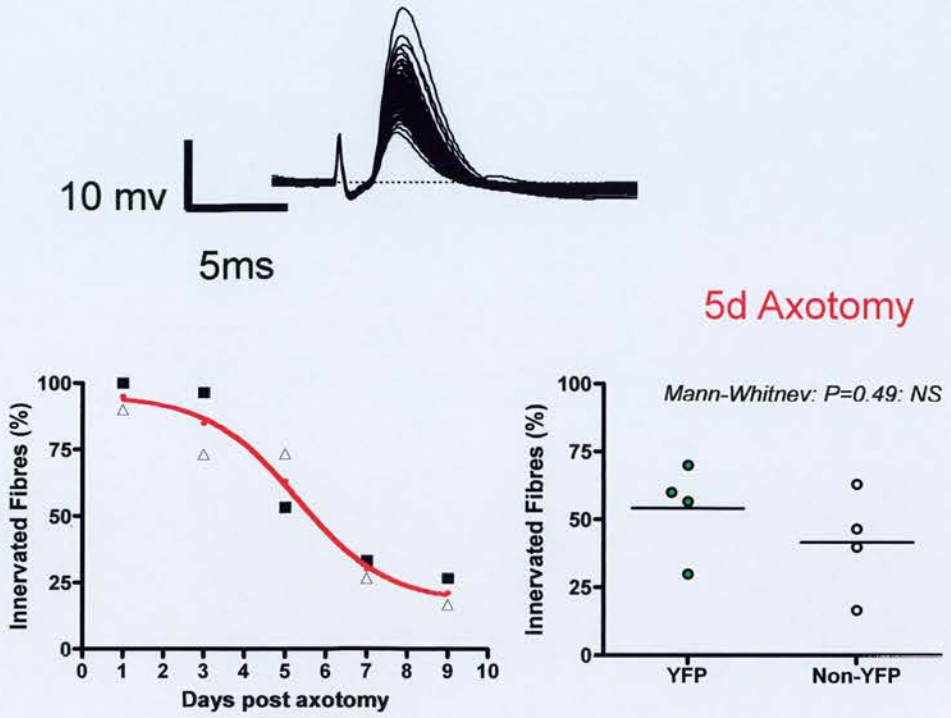

From Bridge et al (2007) Neurobiology of Aging. In Press.

Figure 6.1 YFP does not interfere with *Wld*^{S}

From Bridge et al (2007) showing that the rate and amount of synaptic degeneration measured electrophysiologically from end-plate potential recording (upper traces) is not significantly different comparing *Wld*^{S} mice expressing the YFP transgene with those that do not express this transgene (graph).

6.2.3 Young Heterozygous *Wld*^{S} Mice

Mack et al (2001) demonstrated that the number of occupied endplates decreased in the 4836 hemizygous transgenic mice, compared with those in the 4836 homozygous transgenic mice. The 4836 transgenic line expresses similar level of Wld^S protein to natural mutant *Wld*^{S} mice. The study of nerve terminal degeneration in young heterozygous *Wld*^{S} mice therefore supports this previous finding, and also suggested that the *Wld*^{S} gene does have a protection effect on synaptic degeneration in the axotomised heterozygous *Wld*^{S} mice, compared to wild type mice, although the effect is much less than that in young homozygous *Wld*^{S} mice.

The present study of heterozygous *Wld*^{S} mice provided evidence that the protection of motor nerve terminals by the *Wld*^{S} gene was weaker and also more sensitive to gene dose than axons. Few studies to date have studied nerve terminals on naturally heterozygous *Wld*^{S} mice. Mack et al (2001) provided data to show that synaptic degeneration in transgenic heterozygous *Wld*^{S} mice is faster than that in the transgenic homozygous *Wld*^{S} mice. The heterozygous *Wld*^{S} mice were produced by crossed-breeding C57/*Wld*^{S} mice cross-breeding with Balbc/Bl6 mice. At one day following unilateral sciatic nerve section, most endplates were vacant, while very few were fully occupied. (Figure 3.13.B) Moreover, in comparison with the homozygous *Wld*^{S} mice, the pattern of synaptic degeneration appeared to be distinct. Neither piecemeal withdrawal of nerve terminals nor retraction boutons

(Gillingwater et al., 2002) could be found during the degeneration process, and the rate of degeneration of NMJs was faster than in the homozygous *Wld*^{s} mice. Taking these studies, it can be concluded that in heterozygous *Wld*^{s} mice, the reduced dose of the *Wld*^{s} gene in a weak protection of synaptic degeneration.

6.2.4 Old Homozygous *Wld*^{s} Mice

The present experiment shows that only a few synaptic terminals could be found after axotomy in old *Wld*^{s} mice, most endplates were vacant, a few were fully occupied, and very few were partially occupied. This finding confirms the previous findings of Gillingwater et al (2002) who used the electrophysiology, vital staining with FM1-43, immunocyto-chemistry and electron microscopy to demonstrate that unlike axonal degeneration, the degeneration of synaptic terminals in *Wld*^{s} mice is age dependent. When mice are over 4 months old, the morphology of nerve terminal degeneration reverts to that in wild-type mice. According to their morphological analysis in old mice, very few partially occupied endplates were seen, and most endplates were either fully occupied or vacant. In 4 months old *Wld*^{s} mice about 35% of endplates were occupied 3 days axotomy. In 7 months old *Wld*^{s} mice, however, fewer than 5% occupied endplates remained by 3 days. Electrophysiological analysis suggested that in 4 month old mice, only approximately 20% of fibres showed EPPs 3 days following axotomy. In 7 months old mice less than 5% showed evoked EPPs. The present results of morphological analysis in axons and synaptic degeneration

also supported the group's findings, for example, in *Wld*^{s} mice over 7 months old, < 20 % synaptic terminals were occupied at 2 days after axotomy (Figure 4.2), and due to both intramuscular axons and synaptic terminals fragmenting, no EPPs could be evoked when nerve fibres were stimulated.

6.3 Polyhedral Degeneration Diagram (PDD)

6.3.1 Pattern of Synaptic Degeneration

My studies suggest that there are at least two patterns of axons and nerve terminals degeneration after axotomy in the wild-type mice and young *Wld*^{s} mice. That is to say, both axons and nerve terminals undergo classical Wallerian degeneration in wild-type mice. In young *Wld*^{s} mice, the synapses degenerate in a retraction pattern similar to neonatal elimination (Gillingwater and Ribchester, 2003) and axons are protected well by the *Wld*^{s} gene in young *Wld*^{s} mice.

However, when the time courses of synaptic degeneration in wild-type, heterozygous and young and old homozygous *Wld*^{s} mice were studied and the degeneration of synaptic terminals further quantified different results were showed by the present studies. The patterns of axonal and synaptic degeneration were more complicated than the two mentioned above.

All states of innervation and occupancy of neuromuscular junctions were classified into five patterns in young and old *Wld*^{s} homozygous, heterozygous and

wild-type mice to assess the patterns of axonal and synaptic degeneration. These were occupied (O), connected/partial occupancy (CP), Connected/fragmented (CF), Disconnected/fragmented (DF), Vacant (V) (See chapter 3 & chapter 4 for the explanation for each state). We used these to infer the most likely trajectories between states, including 7 possible degeneration trajectories of axonal and synaptic degeneration, in wild type, heterozygous, and young and old homozygous *Wld*^{S} following axotomy, such as, 1) O→DF→V; 2) O→CP→V; 3) O→CF→V; 4)O→CP→DF→V; 5) O→CP→CF→V; 6) O→CF→DF→V; and 7) O→CP→CF→DF→V; in wild-type, heterozygous, and young and old homozygous *Wld*^{S} following axotomy. In all these trajectories, axons as well as synaptic terminals take different tracks to degenerate from fully occupied endplates to various states before degenerating completely. Apart from trajectory 2 (O→CP→V), which has already been confirmed in young *Wld*^{S} mice, all trajectories remain merely speculative. My hypothesis is that all of these are possible in the degeneration process in axotomised mice; in reality, however, there may only be one, two or more trajectories that exist. Based on time course data in young homozygous *Wld*^{S} mice, CP state is the only state found during the degeneration process, therefore, O→CP→V is the only one possible degeneration trajectory in axotomised homozygous *Wld*^{S} mice.

Of course, the limitation of the PDD method is that it does not take into account any variability in the denervation of each state which could also be a variable that

explains the difference in the PDD trajectories. Nevertheless quantitative kinetic analysis (e.g. Ribchester, 1988) may be necessary to resolve this issue.

My conclusion are consistent with the previous finding that synaptic degeneration is a progressive withdrawal process in young axotomised homozygous *Wld*^{s} mice, with presynaptic terminals gradually retracting from postsynaptic terminals while the axons still entirely connect with them. However, in the young axotomised heterozygous and wild-type mice, there were five states of axonal and synaptic degeneration were found in the degeneration process, they are O (occupied), V (vacant), CP(connected partial), CF(connected fragmented),and DF(disconnected fragmented) respectively. Thus, it may be speculated that there were 7 possible trajectories during the degeneration process, which are: 1) O→DF→V; 2) O→CP→V; 3)O→CF→V; 4)O→CP→DF→V; 5)O→CP→CF→V; 6)O→CF→DF→V; and 7)O→CP→CF→DF→V respectively. If fully occupied endplates (O) started to degenerate following axotomy, they could go through any one of CP, CF and DF states at the early degeneration stage. Then if fully occupied endplates (O) went through the connected partial (CP) state first, there would be three possible tracks for degeneration, firstly, CP→CF→V, where partially occupied endplates become fragmented, with axons still entirely connected to fragmented synaptic terminals, then the synaptic terminals disappear followed by the axons breaking into small segments. A second pathway is CP→DF→V: the partially occupied endplates degenerate into fragmented endplates and axons break into small

segments before degenerating completely. The third is CP→CF→DF→V: partially occupied endplates become fragmented with axons still entirely connected to synaptic terminals, axons then become fragmented followed by both synaptic terminals and axons disappearing in the later degeneration stage.

If fully occupied endplates (O) went through CF at the early degeneration stage, two possible following subsequent trajectories exist: One is CF→V, where fully occupied endplates become fragmented endplates following axotomy, with axons still completely connected to endplates, then axons break in to small segments before endplates degenerate completely, another trajectory is CF→DF→V; where partially occupied endplates become fragmented followed by intact axons disconnecting, from these fragmented endplates, and finally these axons break into small segments before disappearing entirely.

Lastly, if fully occupied endplates (O) went through DF state at the early degeneration stage, only one trajectory would happen, namely O→DF→V, in this fully occupied endplates first become fragmented endplates, followed by axons breaking into small segments in the early stage, and afterward both of them degenerating completely in the later degeneration stage.

Analysis of PDD was used in the axonal and synaptic degeneration of the old axotomised *Wld*^{S} mice. There were four possible states at each time point, which are fully occupied (O), disconnected fragmented (DF), connected partial (CP), and

vacant (V). With increasing hours after axotomy, such as, at 17 hours and 24hours, the majority of synaptic states were either fully occupied endplates connected to axons (O) or fragmented endplates disconnected to axons, very few degeneration pattern were partially occupied endplates connected to intact axons (CP).Therefore it is speculated that there are three possible axonal and synaptic degeneration states in old *Wld*^{s} mice, most nerve terminals degenerate from fully occupied endplates to disconnected fragmented endplates (O→DF→V), and very few endplates were partially occupied before all nerve terminals degenerated completely (O→CP→DF→V or O→CP→V). PDD analysis of wild-type, young heterozygous, homozygous and old homozygous *Wld*^{s} mice provides a useful way to comprehend the mechanism of NMJ degeneration following nerve section. From PDD, we ascertained that the degeneration patterns of synaptic terminals were affected by varying gene dose and mouse age. For instance, most synapses become fragmented at each axotomised hours in young axotomised heterozygous *Wld*^{s} mice, this phenomena resembles Wallerian degeneration in wild type mice, and is different from progressive asynchronous and piecemeal synaptic withdrawal in homozygous *Wld*^{s} mice.

From PDD analysis of these contrasting groups, it is possible to conclude that reduced gene dose influences both degeneration pattern and degeneration rate of synaptic terminals after axotomy. The Wallerian-like degeneration widely found in axotomised heterozygous *Wld*^{s} mice demonstrated that the pattern of synaptic

degeneration reverted back to the wild type fashion. Electrophysiologically, fragmented synapses can not evoke EPPs if axons are disconnected from these synapses. Moreover, the rate of synaptic degeneration increases dramatically with reduced gene dose, in contrast to young homozygous *Wld*^{s} mice.

In old homozygous *Wld*^{s} mice, two different states exist during degeneration, the majority of synapses become fragmented (DF) after axotomy, and a few synapses were in retracted fashion (CP), resembling synaptic degeneration in young heterozygous *Wld*^{s} mice. Therefore, it could also be hypothesized that mouse age plays a role in influencing Wld^{s} protein expression, given the similarity of morphological situations were found in the wild type, heterozygous and old homozygous *Wld*^{s} mice.

6.3.2 Rate of Synaptic Degeneration

The rate, as well as pattern, of degeneration of nerve terminals is influenced by gene dose and mouse age. For instance, the rate of synapse degeneration in both axotomised young heterozygous and old homozygous *Wld*^{s} mice was faster than in young axotomised homozygous *Wld*^{s} mice. Moreover, some occupied endplates were still found in young heterozygous *Wld*^{s} mice 1 day after axotomy and in old homozygous *Wld*^{s} mice 2 days after axotomy, while in wild-type mice, synaptic terminals degenerated completely at 17 hours post axotomy, in contrast, synaptic degeneration can last nearly two weeks in young axotomised homozygous *Wld*^{s}

mice.

6.3.3 Pattern and Rate of Axonal Degeneration

PDD analysis shows that the degeneration pattern and rate of proximal axons, as well as synaptic terminals, are also influenced by gene dose and mouse age. The rate of proximal axons degeneration was fast in axotomised heterozygous and old homozygous *Wld*^{s} mice, in comparison to homozygous *Wld*^{s} mice. In wild-type mice, since the majority of NMJs were in DF state following axtomy, it can be speculated that the degeneration mechanism of axons which are connected to these synaptic terminals is a Wallerian-like degeneration. This mechanism was also found in axotomised heterozygous *Wld*^{s} mice, where most intramuscular axons broke into small segments either before or following synaptic terminals fragmentation (e.g. see Fig 3.10). In contrast, no intramuscular axonal segments were found in homozygous *Wld*^{s} mice up to 3 days after axotomy, the pattern observed is similar to progressive withdrawal following synapses retraction. However, in old homozygous *Wld*^{s} mice, these two different mechanisms may exist simultaneously during the proximal axon degeneration process, given the DF state majority and a few CP states found throughout this process. To date, as axonal mechanism still remains unclear in the recent studies, thus, it is difficult to know whether the Wallerian-like degeneration of intramuscular axons in both young heterozygous and old homozygous *Wld*^{s} mice is indeed similar to the mechanism in wild-type mice. This merits further investigation

in future studies.

Beirowski et al (2005) suggested that different degeneration mechanisms of distal axons occured in wild-type and *Wld*^{S} mice, thus, my present findings in proximal axons may facilitate elucidation of the genuine mechanism of axonal degeneration after nerve injury in the future.

In summary, PDD analysis suggests that the degeneration patterns of both axons and synaptic terminals are influenced by both of *Wld*^{S} gene-dose level and mice of age.

6.3.4 PDD Analysis in Neonates

Usage of PDD analysis is not restricted to the above type of mice, but may also be extended to other types to study the time course of synaptic degeneration. For instance, as an example, I applied PDD analysis to a study of neonatal elimination (See PDD schematic picture below, the data from Keller-Peck et al 2001 Figure 6.2). During synapse elimination in neonates, only the CP state is found, thus the pathway O→CP→V alone may be speculated. Nerve terminals retract by a progressive withdrawal process during synapse elimination, and axons are retracted after that (Korneliussen and Jansen, 1976; Walsh and Lichtman, 2003). This result strongly supports the previous findings that synapse elimination is a progressive withdrawal process during innervation (Gillingwater & Ribchester, 2001; Gillingwater et al., 2002).

Furthermore this PDD could perhaps be applied to animal models or biopsy material from patients with motor neuron diseases, such as Amyotrophic lateral sclerosis (ALS) and used to measure the progression of diseases. By comparing with *Wld*^{S} mice, it may be possible to uncover similar degeneration trajectories in NMJ, or discover new patterns of axonal and synaptic degeneration in this disease model. Greater knowledge of the mechanism of motor neuron degeneration may lead to more effective treatments of motor neuron diseases. PDD is thus a potentially useful analysis model in furthering our understanding of NMJ degeneration and advancing motor neuron disease research in the future.

Figure 6.2 Polyhedral Degeneration Diagram (PDD) Analysis the Mechanism of Synaptic Degeneration Mechanism in neonates

The PDD shows the process of axonal and synaptic degeneration in the young (8 days after birth) mice. Letters are used to represent the states of axons and synapses during neuronal degeneration after axotomy. That is, O represents fully occupied endplate; connected with intact axons, CP represents partially occupied endplate which is connected to an intact axon; V represents that endplates and axons are both degenerated completely.

The chart shows the percentages of different states of axons and synapses during the degeneration process in young (8 days after birth) mice.

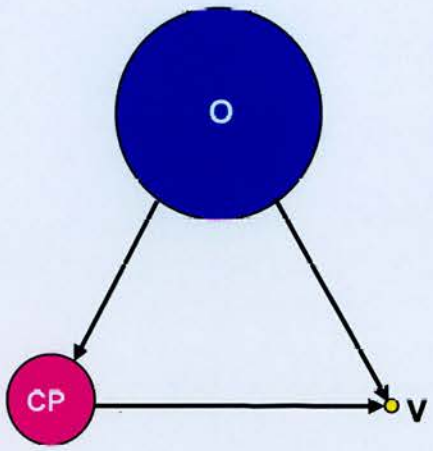

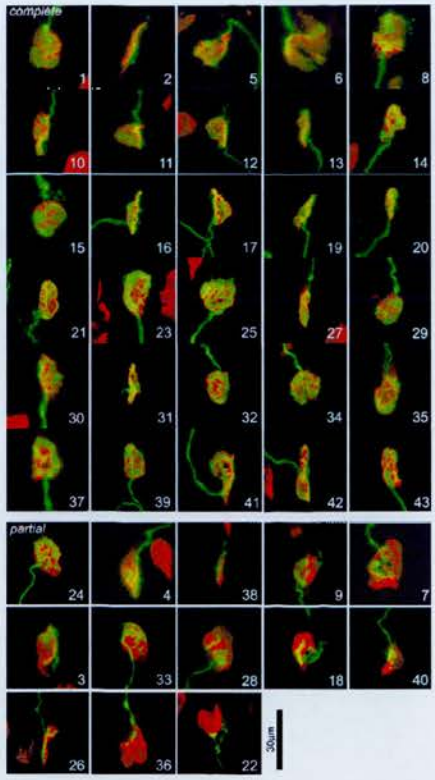

(Reproduce Figure from Keller-Peck et al 2001)

Time / Pattern (%endplates)	8 days
O	61. 36
CP	29.13
V	9.09

(Based on Keller-Peck et al 2001)

6.4 Wld^s Protein Expression in Cerebellar Granule Cells

As discussed in chapter 3 & 4, the Wallerian-like mechanism of synaptic degeneration in heterozygous *Wld^s* mice can be attributed to a decreased gene dose, and similar degeneration pattern was also found in axotomised old *Wld^s* mice.

The question remains whether the observed synaptic protection in old homozygous *Wld^s* mice and the similar mechanism of synaptic protection in young heterozygous *Wld^s* mice may be accounted for by one single explanation. Could it be all down to the age-dependence of *Wld^s* protein expression? Wld^s protein is localized to cell nuclei and is absent from neuronal cytoplasm, therefore Wld^s protein localized in the neuronal nuclei is sufficient to protect against PNS axonal degeneration, and CNS synaptic degeneration from injury, and disease-induced neuro-degenerative stimuli (Lunn et al., 1989; Gillingwater and Ribchester, 2001; Wang et al., 2001; 2002). Wld^s protein expression was measured in cerebellar granule cells in order to test this hypothesis, since cerebellar granule cells in the *Wld^s* mouse have a consistent and high level of expression of Wld^s protein with about 90% of the population containing at least one large nuclear spot bearing Wld^s protein (T. Wishart PhD thesis, University of Edinburgh). Overexpression of Wld^s protein either in the cerebellum or in transfected cell lines in vitro leads to downregulation and upregulation of several other genes. However we do not yet know any of these always required for expression of the protective *Wld^s* phenotype (Gillingwater et al 2006b).

Antibody Wld-18 targets a unique 18 amino-acid peptide in the Wld^S protein in this experiment. This peptide is coded by DNA normally contained within the 5' untranslated region of Nmnatl, expressed between the Ube4b and Nmnat portion of the *Wld*^{S} chimeric gene. This Wld-18 antibody is both specific and versatile, hence immunocytochemistry can be used to visualize the Wld^S protein expression level. Protein expression varied within cell types, some neurons showed intense particulate Wld^{18} protein staining, while others showed very fine speckling staining (Fig 4.1). In my study, Wld^S protein expression in cerebellar granule cells showed strong punctate expression of the mutant protein using an immunocytochemical method. All cells were visualized by immunofluorescence using a *Wld*^{S}-specific primary antibody, TRITC-conjugated secondary antibody, and topro-3 for the nuclei.

The mean intensity of rhodamine fluorescence was measured by confocal microscopy. In homozygous *Wld*^{S} mice, Fang et al (2005) also showed that Wld^S protein is expressed in the nuclei of both neuronal and non-neuronal cells in the brain and the spinal cord, the intensity of protein expression varied from cell to cell and the size and shape of Wld^S proteins were different, Another factor might be that more protein expression can be observed with increasing of the laser power, for instance, with varying laser power, the intensity and size of *Wld*^{S} dots became brighter and larger in the young heterozygous, homozygous and old homozygous *Wld*^{S} cerebellum preparation as visualized by confocal microscopy. In order to analyse variation in Wld^S protein expression in different types of *Wld*^{S} mice, the intensity of protein

expression was measured at varying laser powers, namely 20%, 30%, 40%, 50%, and 60% of the maximum. The immunocytochemical data (Graph 4.7 B, C, D) demonstrate that firstly, the intensity levels of *Wld*^{s} protein expression were evidently reduced in both young heterozygous and old homozygous *Wld*^{s} mice following increasing laser power, compared with the intensity expression in young homozygous *Wld*^{s} mice.

Regarding the influence of mouse age, this finding does not prove but is consistent with the cause of Wallerian-like degeneration in old axotomised *Wld*^{s} mice being a reduction in protein expression level. By analysis, my immunocytochemical suggests protein expression level was relatively higher in old *Wld*^{s} mice, in comparison to young heterozygous *Wld*^{s} mice, due to a few partially occupied endplates remaining during the degeneration process in old *Wld*^{s} mice. It can hence be postulated that this protein expression level in old *Wld*^{s} mice should still prevent some neurons from degenerating. Fang et al (2005) have shown that the intensity of protein expression varies in different cells in the brain and spinal cord of *Wld*^{s} mice. Therefore, we can speculate that the intensity of Wld^{s} protein expression in some neurons is higher than in other neurons, and that these would have stronger protection from axonal and synaptic degeneration than others. Nevertheless, these various responses are not evident in young homozygous *Wld*^{s} mice, perhaps for the reason that the *Wld*^{s} protein level is more than sufficient in these mice to prevent axons and synapses from degeneration, whereas, following decreasing gene dose and

increasing mice age, these various responses become apparent, This hypothesis could help us to explain the different degeneration states in young heterozygous and old homozygous *Wld*^{s} mice after axotomy.

However, this finding is incompatible with earlier western blotting analysis of Wld^{s} protein expression in brain, which suggested that expression level of the mutant protein does not change with age (Gillingwater et al, 2002). On the other hand, the immunostaining method is has a better spatial resolution compared to western blotting. For instance, when performing western blotting, the whole population of cells from the tissue sample is homogenized, proteins are extracted, run on a denaturing gel, transferred to a blot and detected by specific antibodies. The intensity of the detected band on a western blot therefore reflects the average expression level of the protein in that population of cells. In immunohistochemistry, tissues are sectioned, cells are fixed, (permeabilized) and stained *in situ*. The intensity of staining (i.e. dots) indicates the expression level of that protein in particular cells.

The *Wld*^{s} gene has been sited in the region of the distal mouse chromosome 4 (Lyon, 1993), and subsequently identified to be an 85-kb tandem triplication (Coleman, 1998). This finding led to the discovery of a chimeric gene which contains the 5' end of Ube4b and the Nmnat (Conforti, 2000; Emanuelli et al., 2001), a key enzyme which plays an important role in the synthetic pathway of NAD+. The third gene, Rbp7, is a novel member of the cellular retinoid-binding protein family that is

highly expressed in white adipose tissue and mammary glands. The protection mechanism of the *Wld*^{s} gene has not yet been delineated, although some studies have suggested that Nmnat could play a critical role in the neuro-protective effect in neuron in the *Wld*^{s} mice.

This immunostaining finding may therefore help to explain that morphological phenomenon of axotomised synaptic degeneration in the young heterozygous and old homozygous *Wld*^{s} mice found in the previous work, namely, the weaker synaptic protection by Wld^{s} protein compared to axonal protection in both young heterozygous and old homozygous *Wld*^{s} mice following nerve section, and the similar appearance of synaptic degeneration patterns in axotomised young heterozygous and old homozygous *Wld*^{s} mice.

Furthermore, it confirmed that Wld^{s} protein has a strong influence in axonal degeneration in *Wld*^{s} mice. Naturally, the results of the CNS Wld^{s} protein expression may not provide enough evidence to explain the morphological results in the PNS, thus, both western blotting and immonstaining on Wld^{s} protein of spinal cord of heterozygous and old homozygous *Wld*^{s} mice would be logical next step to further test this hypothesis in the future.

6.5 Effect of Extrinsic Factors on Synaptic Degeneration

6.5.1 The Effect of Length of Nerve Stump

The sciatic nerve is the largest single nerve in the mammal; it runs from each side of the lower spine down through the posterior thigh, and all the way down to the foot, connecting the spinal cord with the leg and foot muscles. The tibial nerve is one of two major divisions of the sciatic nerve, supplying the hamstring muscles, the muscles of the back of the leg, the muscles of the plantar aspect of the foot, and the skin on the back of the leg and on the sole of the foot. The distance from the injury sites in the sciatic and tibial nerves was almost 2cm, roughly the same distance from the tibal nerve lesion site to the lumbrical muscles. Since the distance from the tibial nerve to the foot is shorter than that from the sciatic nerve, synaptic degeneration following tibial nerve section was expected to be more rapid than that following sciatic nerve section. However, in the equivalent period following tibial nerve axotomy, synaptic terminals degenerated slightly slower than that followed sciatic nerve surgery. The data didn't show the significant difference between sciatic nerve surgery and tibial nerve surgery. Previous studies suggested that increasing the length of the distal axonal stump alters the rate of degeneration in wild-type mice (Luco and Eyzaguirne, 1955; Birks et al., 1960; Miledi and Slater, 1970). Moreover,

Ribchester et al (1995) suggested that an increase of 1 cm in the length of the distal stump delayed degeneration by about 1～2 days in *Wld*^{s} mice.

The present data are at variance with these findings. Of note, previous studies based their conduction on physiological measurement, whereas my study used anatomical measurement. It is possible that the physiological integrity of axons and synapses is more sensitive to nerve stump length than in their structural presence. Differences in the rate of degeneration measured physiologically and anatomically have also been reported (Ribchester et al., 1995; Gillingwater et al., 2002; 2003).

6.5.2 Dose and Injection Site

Botulinum toxin was used to test the possible role of synaptic activity in degeneration, since this toxin blocks all neurotransmitter release (Bhidayasiri et al., 2005; Rossetto et al., 2001). The dose and injection site of the botulinum A are critical factors which directly affect the experiment result outcome. Since botulinum toxin A is highly toxic, too high a dose of toxin would cause the animal to die, while too small a dose would be ineffective in blocking synaptic transmission and hence, preclude any effective result. Moreover, Borodic et al (1994) suggested that, the higher the dose and volumes of BoTox Injection, the greater the penetration of the toxin through muscle fascia, yet the lesser the spread which is reduced by approximately 20-25% (Shaari et al., 1991). The dose used in my experiment was a 3-5μl injection containing 1-1.5 ng Botulinum Toxin Type A in mice. This range was

sufficient to block neuromuscular transmission (see methods P146) in the injected groups of mice (Variation in the volume and amount of BoTox injection were required to avoid toxicity).

Likewise, to obtain a maximal effect of BoTox, the injection site is another major determinant. In the present experiments I compared the effects of BoTox injection into young mice and mature mice. Since the purpose of this experiment was to test the effect of BoTox on synaptic degeneration in the NMJs of the foot, the center of the sole seemed an ideal injection site. Stimulation of the tibial was done before isolating the lumbrical preparation, and an absence of contractile response was taken to indicate that the dose and route of administration were appropriate for the present experiments.

6.5.3 BoTox Effects on Synaptic Degeneration

Following local injection into muscles, the BoTox enters the nerve terminal via endocytosis, interacts with intracellular proteins SNAP-25 and inhibits the neuromuscular junction. Inhibiting Ach release produces paralysis of the affected muscles (Bhidayasiri et al., 2005; Rossetto et al., 2001).The characteristic of *Wld*^{s} mice is slow Wallerian degeneration following the nerve injury, five days after tibial nerve injury in *Wld*^{s} mice many endplates were still occupied, indicating protection by the *Wld*^{s} gene was not reduced by BoTox injection. Given the inhibiting effect of BoTox, the inactivity of synapses may well provide additional

protective stimulus. Thesleff et al (1990) suggested that BoTox blockade delays and prevents the retraction of synaptic terminals and motor neuron death during development. It has also been shown that the pattern of synaptic degeneration in *Wld*^{s} mice is similar to that in neonates (Mattison et al., 1996; Parson et al., 1998; Ribchester et al., 1999).

The results show in Fig 5.10, therefore suggest that BoTox could possibly provide some protection against synaptic degeneration, in addition to the protective effects of the Wld^s gene, but the effect is rather slight. Since BoTox also blocks synaptic transmission, its utility as a neuroprotective agent is likely to be minimal.

6.5.4 BoTox Effect on the Mature *Wld*^{s} Mice

In the previous chapters, I showed that synaptic terminals are slowly withdrawn from axotomised endplates in young *Wld*^{s} mice, yet this synaptic protection phenotype is absent following axotomy in mature mice, despite the *axons* being still protected from degeneration by the *Wld*^{s} gene (Gilllingwater et al., 2002). In my experiments on 7 months old *Wld*^{s} muscles, at 2 days post axotomy, most terminals had showed fragmented and degenerative signs. In the present study, 3µl BoTox was injected in the mice's hind feet, however, the data as presented in Figure 5.3 that this was not sufficient to prevent rapid degeneration of synaptic terminals in mature *Wld*^{s} mice. It is hence difficult to conclude that synapses are protected strongly from degeneration by BoTox at 3 days post axotomy, although a few endplates remain

partial or fully occupied at this time point, Nonetheless. However, it is clear that BoTox did not affect synaptic degeneration at 7 days post axotomy, since by this time 100% endplates had degenerated completely.

6.6 Compartmental neurodegeneration

Previous studies of the reaction of cell bodies, axons and synaptic terminals in axotomised *Wld*^{s} mice suggests, that mechanisms of degeneration are compartmentalised in neurons (Gillingwater and Ribchester, 2001). My current findings, in the morphological study rather than the molecular mechanism study have given some evidence to confirm this. For example, the time course analysis of NMJs in these mice has shown that the rate and pattern of synaptic degeneration after axotomy are apparently influenced by gene dose and mouse age in *Wld*^{s} mice, while the axons are only affected slightly. Moreover, in axotomised heterozygous and old homozygous *Wld*^{s} mice, DF and CP states were found to exist simultaneously during the synaptic degeneration process, that is, synaptic terminals could take more than one pathway to degenerate in young heterozygous and old homozygous *Wld*^{s} mice after axotomy. One is similar to wallerian degeneration, and the other is a withdrawal process similar to developmental synapse elimination in neonates. Therefore, from the morphological study, it may be suggested that, in motor neurons, synapses have an independent mechanism to degeneration, compared with axons and their cell bodies.

6.7 Neurodegenerative diseases

Synaptic degeneration is the early stage of neuron degeneration in many neurodegenerative diseases. For example, Alzheimer's disease is considered to be mainly a kind of disease of synapses (Selkoe, 2002; Gillingwater and Ribchester, 2003). In Huntington's disease, synapse abnormalities are related with the deterioration of motor and cognitive abilities in the central nervous system (Wishart et al., 2006). In motor neuron disease, synapse loss is known to occur during the early stages of Amyotrophic lateral sclerosis in the SOD1 transgenic mice model, and the degeneration pattern of synapses is via piecemeal retraction, which is similar to the pattern in young axotomised *Wld*^{S} mice and mice neonate (Maselli et al., 1993; Frey et al., 2000; Schaefer et al., 2002; Gillingwater and Ribchester, 2003). However, it should perhaps be always borne in mind that synapses may be extremely vulnerable to any malfunction, wherever it may occur in a neuron. For example, it is otherwise healthy synapses that degenerate first after axotomy, as this thesis and previous studies have shown. This does not mean, of course that protecting synapses should not be the goal of treatment for neurodegenerative diseases.

Further studies of axotomy-induced synaptic degeneration in the PNS could also provide more insight to help us understand and examine axotomy-induced synaptic withdrawal in the CNS and the mechanisms of remodeling in central connections, such as that in the developmental organization of the visual system and the

cerebellum. Gillingwater et al (2006a) who studied synaptic degeneration of the CNS in young *Wld*^{s} mice showed that the synaptic degeneration pattern is distinct from the PNS. In the CNS, the onset of synaptic degeneration is delayed by the *Wld*^{s} gene, but once it occurs, the form of degeneration appears similar to wild type.

A recent study showed that the *Wld*^{s} gene has a stronger protection on synaptic degeneration in axotomy-induced transgenic rat than in *Wld*^{s} mice. Moreover, the rat model has advantages over the mouse model for studying neurodegenerative disease (Adalbert et al., 2005). Some of the limitations studying mouse model disease will also be overcome in other mammalian species models (Gillingwater et al., 2006a). The PDD analysis method is of benefit not only in *Wld*^{s} mice studies, but also for *Wld*^{s} transgenic rats and other *Wld*^{s} transgenic mammalian species studies.

Although the mechanism by which *Wld*^{s} delays degeneration in synaptic terminals remains unclear, the present study extends the limits of our knowledge regarding synaptic degeneration in mutant *Wld*^{s} mice. It is known that there are morphological and physiological similarities among naturally-occurring synapse elimination in neonates, asynchronous withdrawal in young *Wld*^{s} mice, and the retraction pattern occurring in many forms of neuromuscular disease (Gillingwater and Ribchester, 2003). Given the diversity of synaptic degeneration patterns in axotomy- induced *Wld*^{s} mice under the influence of gene dose and mice age, *Wld*^{s} mice would be a suitable target for studying the mechanism of synaptic degeneration

in different neurodegenerative diseases. Therefore, the present findings may facilitate us to extend the current knowledge of synaptic degeneration. Some of these provide effective methods to study the mechanism of synaptic degeneration in *Wld*^{s} mice, such as PDD analysis of NMJs and Wld^{s} protein expression in cerebellar granule cells. Others provide a way to delay the synaptic degeneration, such as, blocking transmission by botulinum toxin. Thus, all data could possibly lead to useful advances in the treatment of Alzheimeri's disease and other CNS diseases, such as Parkinson's and Huntington's diseases, as well as PNS diseases like Amyotrophic lateral sclerosis in the future.

7. Conclusion

In this thesis, Thy1-YFP16 *Wld*^{S} mice were cross-bred with Balbc/bl6 mice to produce heterozygous *Wld*^{S} mice with fluorescently-labeled motor neurons. Synaptic degeneration after axotomy in these mice was compared with that in *Wld*^{S} homozygous and wild-type mice. These experiments constituted a test of the hypothesis that protection of synapses in *Wld*^{S} mice depends on the "dose" of the chimeric gene. First, analysis using PDD diagrams provided insights into the pattern of synaptic degeneration at the axotomised NMJs of wild-type and *Wld*^{S} mice. The main states of axonal and synaptic degeneration defined for PDD analysis, namely : DF (Disconnected/fragmented) CP (Connected partial occupancy) O (Occupied), CF (Disconnected/fragmented), and V (Vacant), were all identified during the degeneration process in the different types of axotomised mice. Not all patterns occurred in all types of axotomy-induced mice. Those I observed indicated the different trajectories taken during synaptic degeneration following axotomy in these sets of mice. By following these trajectories we may conclude that axonal and synaptic degeneration occur by different mechanisms in homozygous and heterozygous *Wld*^{S} mice. Protection from synaptic degeneration by the *Wld*^{S} gene is therefore much more sensitive than axon degeneration to the *Wld*^{S} gene dose.

Surprisingly, my studies of *Wld*^{S} gene expression in the cerebellum provided evidence that synaptic *Wld*^{S} gene expression is reduced as *Wld*^{S} mice age and that this may explain why old *Wld*^{S} mice lose their synaptic protection, even in homozygotes. This outcome may explain the findings in my morphological studies

that axonal and synaptic degeneration patterns are similar in heterozygous *Wld*^{S} mice, old homozygous *Wld*^{S} mice and wild-type mice.

Thirdly, since the mechanism of the *Wld*^{S} gene protecting axons and synapses from degeneration still are not clear so far, I looked for other factors which might also have a protective effect on nerve terminal degeneration following axotomy. However, I was only able to confirm some of the findings of previous studies. For example, length of the distal nerve stump did not effect synaptic degeneration in axotomised *Wld*^{S} mice: thus, nerve terminal degeneration following tibial nerve section was no faster than that following sciatic nerve section. In addition, although BoTox was found to delay synaptic degeneration in young axotomised *Wld*^{S} mice, there was no effect in old axotomised *Wld*^{S} mice. Thus, of those aspects examined, by far the most potent effects on synaptic degeneration were *Wld*^{S} gene-dose and age.

More experiments should be done to extend these findings. First, PDD analysis could be applied to neonates and to some transgenic mouse models of neurodegenerative diseases, such as the SOD1 mouse model of ALS. Such analysis may offer a stringent test of Gillingwater & Ribchester's 'compartmental neurodegeneration' hypothesis. Second, single cell RT-PCR western blotting and quantitative immunostaining should be used to examine Wld^S protein expression in motor neurons of young homozygous, heterozygous and old homozygous *Wld*^{S}

mouse spinal cord. Third, chronic stimulation of axotomised distal nerve stumps should be tested in *Wld*^{S} mice, to find out whether the apparent lack of effect of blocking synaptic transmission with BoTox has its counterpart when transmitter release is instead increased after axotomy. For instances, although BoTox has only a slight effect on synaptic protection by *Wld*^{S}, whether increasing activity has minor or dramatic effect remain completely unknown. Together, such studies could provide to the insights we need to find better ways of protecting synapses in devastating diseases such as ALS, and perhaps other neurodegenerative diseases as well.

Reference

Abercrombie, M. & Johnson, M.L. (1946) Quantitative histology of Wallerian degeneration. I. Nuclear population in rabbit sciatic nerve. *Journal of Anatomy* **80**: 37-50

Adalbert R, Gillingwater TH, Haley JE, Bridge K, Beirowski B, Berek L, Wagner D, Grumme D, Thomson D, Celik A, Addicks K, Ribchester RR, and Coleman MP. (2005) A rat model of slow Wallerian degeneration (WldS) with improved preservation of neuromuscular synapses. *Eur J Neurosci* **21**: 271-277.

Adalbert, R., Nógrádi, A., Szabó, A., Coleman, M.P, (2006) The slow Wallerian degeneration gene in vivo protects motor axons but not their cell bodies after avulsion and neonatal axotomy. *Eur J Neurosci* **24**:2163-2168

Allt, G.. (1976) Pathology of the peripheral nerve. In *The Peripheral Nerve,* ed. Landon, D.N. Chapman & hall, London. 666-739

Amos, W.B. & White, J.G. (2003) How the Confocal Laser Scanning Microscope entered Biological Research, *Biology of the Cell* **95**: 335-342

Andreassen, O. A., Ferrante, R. J., Klivenyi, P., Klein, A.M. & Shinobu, L. A., et al. (2000) Partial deficiency of manganese superoxide dismutase exacerbates a transgenic mouse model of amyotrophic lateral sclerosis. *Ann. Neurol* **47**:447–55

Araki, T., Sasaki, Y. & Milbrandt, J. (2004) Increased nuclear NAD biosynthesis and SIRT1 activation prevent axonal degeneration. *Science* **305**: 1010-1013

Bagust, J., Lewis, D.M. & Westerman, R.A. (1973) Polyneuronal innervation of kitten skeletal muscles. *Journal of Physiology* **229**: 241-255

Ballin, R.H.M. & Thomas, P.K. (1969) Changes at the nodes of Ranvier during Wallerian degeneration: an electron microscope study. *Acta Neuropathologica (Berlin)* **14**: 237-249

Barry, J.A. & Ribchester, R.R. (1995) Persistent polyneuronal innervation in partially denervated rat muscle after reinnervation and recovery from prolonged nerve conduction block. *J Neurosci* **15**: 6327-39

Beckman, J.S., Carson, M., Smith, C.D. & Koppenol, W.H. (1993) ALS, SOD and

peroxynitrite. *Nature* **364**:584

Beirowski, B., Adalbert, R., Wagner, D., Grumme, D.S., Addicks, K., Ribchester, R.R., & Coleman, M.P., (2005) The progressive nature of Wallerian degeneration in wild-type and slow Wallerian degeneration (WldS) nerves. *BMC Neurosci* **6**: 6

Bennett, M.K. & Pettigrew, A.G. (1974) The formation of synapses in striated muscle during development. *Journal of Physiology* **241**: 515-545

Betz, W.J. & Angleson, J.K. (1998) The synaptic vesicle cycle. *Annual Review of Physiology* **60**: 347-363

Betz, W.J., Caldwell, J.H. & Ribchester, R.R. (1979) The size of motor units during post-natal development of rat lumbrical muscle. *Journal of Physiology* **297:** 463-478

Bhidayasiri, R., & Truong, D.D. (2005) Expanding use of botulinum toxin. *J Neurol Sci* **235**: 1-9

Birks, R., Katz, B. & Miledi, R. (1960) Physiological and structural changes at the amphibian myoneural junction, in the course of nerve degeneration. *Journal of Physiology* **150**: 145-168

Bittner, G.D. (1988) Long-term survival of severed distal axonal stumps in vertebrates and invertebrates. *American Zoologist* **28**: 1165-1179

Bixby, J.L. (1981) Ultrastructural observations on synapse elimination in neonatal rabbit skeletal muscle. *Journal of Neurocytology* **10**: 81-100

Blasi, J., Chapman, E.R., Link, E., Binz, T., Yamasaki, S., De Camilli, P, Südhof, T.C, Niemann, H. & Jahn, R., (1993) Botulinum neurotoxin A selectively cleaves the synaptic protein SNAP-25. *Nature* **365**: 160-163

Boillee, S., Yamanaka, K., Lobsiger, C.S., Copeland, N.G., Jenkins, N.A., Kassiotis, G., Kollias, G. & Cleveland, D.W. (2006) Onset and progression in inherited ALS determined by motor neurons and microglia. *Science* **312**: 1389–1392

Borodic, G.E., Ferrante, R., Pearce, L.B. & Smith, K. (1994) Histologic assessment of dose-related diffusion and muscle fiber response after therapeutic botulinum A toxin injections. *Mov Disord* **9**: 31-39

Bridge, K.E., Berg, N., Adalbert, R., Babetto, E., Dias, T., Spillantini, M.G.,

Ribchester, R.R. & Coleman, M.P. (2007) Late onset distal axonal swelling in YFP-H transgenic mice. *Neurobiol Aging* July 18

Brown, M.C., Booth, C.M., Lunn, E.R. & Perry, V.H. (1991) Delayed response to denervation in muscles of C57Bl/Ola mice. *Neuroscience* **43**: 279-283

Brown, M.C., Jansen, J.K.S. & Van Essen, D.C. (1976) Polyneuronal innervation of skeletal muscle in new-born rats and it's elimination during maturation. *Journal of Physiology* **261**: 387-422

Brown, M.C., Holland, R.L., & Ironton, R. (1980) Nodal and terminal sprouting from motor nerves in fast and slow muscles of the mouse. *J Physiol* **306**:493-510

Brown, M.C., Hopkins, W.G., & Keynes, R. J. (1982) Comparison of effects of denervation and botulinum toxin paralysis on muscle properties in mice. *J Physiol* **327**:29-37

Brown, M.C., Ironton, R. (1977) Motor neurone sprouting induced by prolonged tetrodotoxin block of nerve action potentials. *Nature* **265**: 459-461.

Brown, M.C., Booth, C.M., Lunn, E.R. & Perry, V.H. (1991) Delayed response to denervation in muscles of C57Bl/Ola mice. *Neuroscience* **43:** 279-283

Brown, M.C., Perry, V.H., Lunn, E.R., Gordon, S. & Heumann, R. (1991a) Macrophage dependence of peripheral sensory nerve regeneration: possible involvement of nerve growth factor. *Neuron* **6**: 359-370

Bruijn, L. I., Miller, T. M. & Cleveland, D. W. (2004) Unraveling the mechanisms involved in motor neuron degeneration in ALS. *Annu. Rev. Neurosci* **27**: 723–749.

Büngner, O.V. (1891) Uber die degenerations und regenerationsvorgange am nerven nach verletzungen. In: Ide, C. (1996) Peripheral nerve regeneration. *Neuroscience Research* **25:** 101-121

Buffelli, M., Burgess, R.W., Feng, G., Lobe, C.G., Lichtman, J.W., Sanes, J.R. (2003) Genetic evidence that relative synaptic efficacy biases the outcome of synaptic competition. *Nature* **424**: 430-434

Burne, J.F., Staple, J.K. & Raff, M.C. (1996) Glial cells are increased proportionally in transgenic optic nerves with increased numbers of axons. *Journal of Neuroscience* **16**: 2064-2073

Carroll, S.L. & Frohnert, P.W. (1998) Expression of JE (monocyte chemoattractant

protein-1) is induced by sciatic axotomy in wild type rodents but not in C57Bl/Wld^{s} mice. *Journal of Neuropathology and Experimental Neurology* **57**: 915-930

Caroni, P., Schneider, C., Kiefer, M.C. & Zapf, J. (1994) Role of muscle insulin-like growth factors in nerve sprouting: suppression of terminal sprouting in paralyzed muscle by IGF-binding protein 4. *J Cell Biol.* **125**: 893-902.

Chaudry, V., Glass, J.D. & Griffin, J.W. (1992) Wallerian degeneration in peripheral nerve disease. *Neurologic Clinics* **10**: 613-627

Chen, B.M. & Grinnell, A.D. (1995) Integrins and modulation of transmitter release from motor nerve terminals by stretch. *Science* **269**: 1578-1580

Coleman, M.P., Conforti, L., Buckmaster, E.A., Tarlton, A., Ewing, R.M., Brown, M.C., Lyon, M.F. & Perry, V.H. (1998) An 85-kb tandem triplication in the slow Wallerian degeneration (Wld^{s}) mouse. *Proceedings of the National Academy of Sciences of the USA* **95**: 9985-9990

Coleman, M.P. & Perry, V.H., (2002) Axon pathology in neurological disease: a neglected therapeutic target. *Trends Neurosci* **25**: 532-537

Conforti, L., Tarlton, A., Mack, T.G.A., Mi, W., Buckmaster, E.A., Wagner, D., Perry, V.H. & Coleman, M.P. (2000) A *Ufd2/D4Cole1e* chimeric protein and overexpression of *Rbp7* in the slow Wallerian degeneration (Wld^{s}) mouse. *Proceedings of the National Academy of Sciences of the USA* **97**: 11377-11382

Conforti, L., Fang, G., Beirowski, B., Wang, M.S., Sorci, L., Asress, S., Adalbert, R., Silva, A., Bridge, K., Huang, X.P, Magni, G., Glass, J.D. & Coleman, M.P. (2007) NAD(+) and axon degeneration revisited: Nmnat1 cannot substitute for Wld(S) to delay Wallerian degeneration. *Cell Death Differ* **14**: 116-127

Cook, R.D., Ghetti, B. & Wisniewski, H.M. (1974) The pattern of Wallerian degeneration in the optic nerve of newborn kittens: an ultrastructural study. *Brain Research* **75**: 261-275

Costanzo, E.M., Barry, J.A. & Ribchester, R.R. (1999) Co-regulation of synaptic efficacy at stable polyneuronally innervated neuromuscular junctions in reinnervated rat muscle. *Journal of Physiology* **521**: 365-374

Costanzo, E.M., Barry, J.A. & Ribchester, R.R. (2000) Competition at silent synapses in reinnervated skeletal muscle. *Nat Neurosci* **3**: 694-700

Court, F.A., Sherman, D L., Pratt, T., Garry, E.M., Ribchester, R.R., Cottrell, D. F., Fleetwood-Walker, S. M. & Brophy, P. J. (2004) Restricted growth of Schwann cells lacking Cajal bands slows conduction in myelinated nerves. *Nature* **431**: 191-195

Crawford, T.O., Hsieh, S-T., Schryer, B.L. & Glass, J.D. (1995) Prolonged axonal survival in transected nerves of C57Bl/Ola mice is independent of age. *Journal of Neurocytology* **24**: 333-340

Cregan, S.P., MacLaurin, J.G., Craig, C.G., Robertson, G.S., Nicholson, D.W., Park, D. S. & Slack, R. S. (1999) Bax-dependent caspase-3 activation is a key determinant in p53-induced apoptosis in neurons. *J Neurosci* **19**: 7860-7869

Dale, H.H., Feldberg, W. & Vogt, M. (1936) Release of acetylcholine at voluntary motor nerve endings. *Journal of Physiology* **86**: 353-380

Day, N.C., Wood, S.J., Ince, P.G., Volsen, S.G., Smith, W., Slater, C.R. & Shaw, P.J. (1997) Differential localization of voltage-dependent calcium channel α1 subunits at the human and rat neuromuscular junction. *Journal of Neuroscience* **17**: 6226-6235

De Paiva, A., Meunier, F.A., Molg, J., Aoki, K.R. & Dolly, J.O., (1999) Functional repair of motor endplates after botulinum neurotoxin type A poisoning: biphasic switch of synaptic activity between nerve sprouts and their parent terminals. *Proc Natl Acad Sci U S A* **96**: 3200-3205

Deckwerth, T.L. & Johnson, E.M. (1994) Neurites can remain viable after the destruction of the neuronal soma by programmed cell death. *Developmental Biology* **165**: 63-72

Dell Castillo, J. & Katz, B. (1954) Quantal components of the endplate potential. *Journal of Physiology* **124**: 560-573

Donat, J.R. & Wisniewski, H.M. (1973) The spatio-temporal pattern of Wallerian degeneration in mammalian peripheral nerves. *Brain Research* **53**: 41-53

Emanuelli, M., Carnevali, F., Saccucci, F., Peirella, F., Amici, A., Raffaelli, N. & Magni, G. (2001) Molecular cloning, chromosomal localization, tissue mRNA levels, bacterial expression, and enzymatic properties of human NMN adenylyltransferase. *Journal of Biological Chemistry* **276**: 406-412

Fang, C., Bernardes-Silva, M., Coleman, M.P. & Perry., V.H. (2005) The cellular distribution of the Wlds chimeric protein and its constituent proteins in the CNS, *Neuroscience* **135**, 1107-1118

Fatt, P. & Katz, B. (1951) An analysis of the end-plate potential recorded with an intracellular electrode. *Journal of Physiology* **115**: 320-370

Fatt, P. & Katz, B. (1952) Spontaneous subthreshold activity at motor nerve endings. *Journal of Physiology* **117**: 109-128

Feng, G., Mellor, R.H., Bernstein, M., Keller-Peck, C., Nguyen, Q.T., Wallace, M., Nerbonne, J.M., Lichtman, J.W., & Sanes, J.R. (2000) Imaging neuronal subsets in transgenic mice expressing multiple spectral variants of GFP. *Neuron* **28**: 41-51

Ferri, A., Sanes, J.R., Coleman, M.P., Cunningham, J.M. & Kato, A.C (2003) Inhibiting axon degeneration and synapse loss attenuates apoptosis and disease progression in a mouse model of motoneuron disease. *Curr. Biol* **13**: 669– 673

Fischer, L.R., Culver, D.G., Tennant, P., Davis, A.A., Wang, M., Castellano-Sanchez, A., Khan, J., Polak, M.A., Glass, J.D. (2004) Amyotrophic lateral sclerosis is a distal axonopathy: evidence in mice and man. *Exp Neurol* **185**: 232-40

Fischer, L.R., Deborah, G., Culver, D.G., Davis, A.A., Tennant, P., Wang, M., Coleman, M., Asress, S., Adalbert, R., Alexander, G. M. & Glass J.D. (2005) The *Wld*^{S} gene modestly prolongs survival in the SOD1^{G93A} fALS mouse. *Neurobiology of Disease* **19**: 293-300

Flucher, B.E. & Daniels, M.P. (1989) Distribution of Na^{+} channels and ankyrin in neuromuscular junctions is complementary to that of acetylcholine receptors and the 43kD protein. *Neuron* **3**: 163-175

Frey, D., Schneider, C., Xu, L., Borg, J., Spooren, W. & Caroni, P. (2000) Early and selective loss of neuromuscular synapse subtypes with low sprouting competence in motoneuron diseases. *Journal of Neuroscience* **20**: 2534–2542

Friede, R.L. & Martinez, A.J. (1970) Analysis of axon-sheath relations during early Wallerian degeneration. *Brain Research* **19**: 199-212

Fu, S.Y. & Gordon, T. (1997) The cellular and molecular basis of peripheral nerve regeneration. *Molecular Neurobiology* **14**: 67-116

George, J. M. (2001) The synucleins. *Genome Biol* **3**: review 3002.1-3002.6

Giess, R., Naumann, M., Werner, E., Riemann, R., Beck, M., Puls, I., Reiners, C. & Toyka, K.V. (2000) Injections of botulinum toxin A into the salivary glands improve sialorrhoea in amyotrophic lateral sclerosis. *J Neurol Neurosurg Psychiatry* **69**:

121-123

Giess, R., Werner, E., Beck, M., Reiners, C., Toyka, K.V., & Naumann, M. (2002) Impaired salivary gland function reveals autonomic dysfunction in amyotrophic lateral sclerosis. *J Neurol* **249**: 1246-1249

Gillingwater, T.H. & Ribchester, R.R. (2001) Compartmental neurodegeneration and synaptic plasticity in the Wld^s mutant mouse. *Journal of Physiology* **534**: 627-639

Gillingwater, T.H. Thomson, D., Mack, T.G., Soffin, E.M., Mattison, R.J., Coleman, M.P. & Ribchester, R.R. (2002) Age-dependent synapse withdrawal at axotomised neuromuscular junctions in Wld(s) mutant and Ube4b/Nmnat transgenic mice. *J Physiol* **543**: 739-755

Gillingwater, T.h. & Ribchester, R.R. (2003) The relationship of neuromuscular synase elimination to synaptic degeneration and pathology:Insights from *Wld^s* and other mutant mice *Journal of Neurocytology* **32**: 863–881

Gillingwater, T.H., Ingham, C.A., Coleman, M.P. & Ribchester, R.R. (2003), Ultrastructural correlates of synapse withdrawal at axotomized neuromuscular junctions in mutant and transgenic mice expressing the Wld gene, *J Anat* **203**: 265-276

Gillingwater, T.H., Inqham, C.A., Parry, K.E., Wright, A.K., Haley, J.E., Wishart, T.M., Arbuthnott, G.W. & Ribchester, R.R. (2006a) Delayed synaptic degeneration in the CNS of Wlds mice after cortical lesion. *Brain* **129**: 1546-56

Gillingwater, T.H., Wishart, T.M., Chen, P.E., Haley, J.E., Robertson, K., MacDonald, S.H., Middleton, S., Wawrowski, K., Shipston, M.J., Melmed, S., Wyllie, D.J., Skehel, P.A., Coleman, M.P. & Ribchester, R.R. (2006b) The neuroprotective *Wld^s* gene regulates expression of PTTG1 and erythroid differentiation regulator 1-like gene in mice and human cells. *Hum Mol Genet* **15**: 625-635

Glass, J.D., Brushart, T.M., George, E.B. & Griffin, J.W. (1993) Prolonged survival of transected nerve fibres in C57Bl/Ola Mice is an intrinsic characteristic of the axon. *Journal of Neurocytology* **22**: 311-321

Glass, J.D. & Griffin, J.W. (1994) Retrograde transport of radiolabeled cytoskeletal proteins in transected nerves. *Journal of Neuroscience* **14**: 3915-3921

Glickman, M.H. & Ciechanover, A. (2002) The ubiquitin-proteasome proteolytic pathway: destruction for the sake of construction. *Physiol Rev* **82**: 373-428

Gonzalez de Aguilar, J.L., Echaniz-Laguna, A., Fergani, A., René, F., Meininger, V., Loeffler, J. P., & Dupuis, L. (2007) Amyotrophic lateral sclerosis: all roads lead to Rome. *J Neurochem* **101**: 1153-60

Gramolini, A.O., Wu, J. & Jasmin, B.J. (2000) Regulation and functional significance of utrophin expression at the mammalian neuromuscular synapse. *Microscopy Research and Technique* **49**: 90-100

Gros-Louis, F., Gaspar, C. & Rouleau, G. A. (2006) Genetics of familial and sporadic amyotrophic lateral sclerosis. *Biochim. Biophys. Acta* **1762**: 956–972

Hall, S.M. (1993) Observations on the progress of Wallerian degeneration in transected peripheral nerves of C57Bl/Wld Mice in the presence of recruited macrophages. *Journal of Neurocytology* **22**: 480-490

Harlow, M.L., Ress, D., Stoschek, A., Marshall, R.M. & McMahan, U.J. (2001) The architecture of active zone material at the frog's neuromuscular junction. *Nature* **409**: 479-484

Hershko, A. & Ciechanover, A. (1998) The ubiquitin system. *Annual Review of Biochemistry* **67:** 425-479

Heumann, R., Korsching, S., Bandtlow, C. & Thoenen, H. (1987) Changes of nerve growth factor synthesis in non-neuronal cells in response to sciatic nerve transection. *Journal of Cell Biology* **104**: 1623-1631

Hirano, A., Nakano, I., Kurland, L.T., Mulder, D.W., Holley, P.W. & Saccomanno, G. (1984) Fine structural study of neurofibrillary changes in a family with amyotrophic lateral sclerosis. *J.Neuropathol. Exp. Neurol* **43**: 471–80

Honjin, R., Nakamura, T. & Imura, M. (1959) Electron microscopy of peripheral nerve fibres. iii) On the axoplasmic changes during Wallerian degeneration. *Okajimas Folia Anatomica Japonica* **33**: 131-156

Hoopfer, E.D., McLaughlin, T., Watts, R.J., Schuldiner, O., O'Leary, D.D. & Luo, L. (2006) Wld^{s} protection distinguishes axon degeneration following injury from naturally occurring developmental pruning. *Neuron* **50**: 883-895

Hubel, D.H., Wiesel, T.N. & LeVay, S. (1977) Plasticity of ocular dominance columns in the monkey striate cortex. *Philosophical Transactions of the Royal Society, London B* **278**: 377-409

Huttenlocher, P.R., Decourten, C., Garey, L.J. & Vanderloos, H. (1982)

Synaptogenesis in human visual-cortex - evidence for synapse elimination during normal development. *Neuroscience Letters* **33**: 247-252

Isacson, O., Bjorklund, L.M. & Schumacher, J.M. (2003) Toward full restoration of synaptic and terminal function of the dopaminergic system in Parkinson's disease by stem cells. *Ann Neurol* **53**

Iwai, A. (2000) Properties of NACP/alpha-synuclein and its role in Alzheimer's disease. *Biochim Biophys Acta* **26**: 95-109

Jahromi, B.S., Robitaille, R. & Charlton, M.P. (1992) Transmitter release increases intracellular calcium in perisynaptic Schwann cells *in situ*. *Neuron* **8**: 1069-1077

Jennings, C. (1994) Death of a synapse. *Nature* **372**: 498-499

Kasthuri, N., & Lichtman, J.W. (2003) The role of neuronal identity in synaptic competition. *Nature* **424**: 426-430

Katz, B. & Miledi, R. (1969) Tetrodotoxin-resistant electric activity in presynaptic terminals. *Journal of Physiology* **203**: 459-487

Keller-Peck, C.R., Walsh, M.K., Gan, W.B., Feng, G., Sanes, J.R. & Lichtman, J.W. (2001) Asynchronous synapse elimination in neonatal motor units: studies using GFP transgenic mice. *Neuron* **31**: 381-94

Kotzbauer, P.T., Trojanowsk, J.Q., Lee, V.M. (2001) Lewy body pathology in Alzheimer's disease. *J Mol Neurosci* **17**:225-32.

Korneliussen, H & Jansen, J.K.S. (1976) Morphological aspects of the elimination of polyneuronal innervation of skeletal muscle fibres in newborn rats. *Journal of Neurocytology* **5**: 591-604

Kriz. J., Nguyen. M. D. & Julien, J.P. (2002) Minocycline slows disease progression in a mouse model of amyotrophic lateral sclerosis. *Neurobiol. Dis* **10**:268–78

Kuida, K. (2000) Caspase-9. *Int J Biochem Cell Biol* **32**: 121-124

LeBlanc, A.C., Liu, H., Goodyer, C., Bergeron, C. & Hammond, J. (1999) Caspase-6 role in apoptosis of human neurons, amyloidogenesis and Alzheimer's disease. *J Biol Chem* **274**: 23426-23436

Levenson, D. & Rosenbluth, J. (1990) Electrophysiologic changes accompanying Wallerian degeneration on frog sciatic nerve fibres. *Brain Research* **523**: 230-236

Levy, D., Kubes, P. & Zochodne, D.W. (2001) Delayed peripheral nerve degeneration, regeneration and pain in mice lacking inducible nitric oxide synthase. *Journal of Neuropathology and Experimental Neurology* **60**: 411-421

Levy, J. R. & Holzbaur, E. L. (2006) Cytoplasmic dynein/dynactin function and dysfunction in motor neurons. *Int. J. Dev. Neurosci* **24**: 103–111

Lichtman, J.W. (1977) The reorganization of synaptic connexions in the rat submandibular ganglion during post-natal development. *Journal of Physiology* **273**: 155-177

Lichtman, J.W. (1994) Confocal microscopy, *Scientific American* **271**: 30-35

Lohof, A.M., Delhaye-Bouchaud, N. & Mariani, J. (1996) Synapse elimination in the central nervous system: functional significance and cellular mechanisms. *Reviews in Neuroscience* **7**: 85-101

Lotharius J., Brundin, P. (2002) Pathogenesis of Parkinson's disease: dopamine, vesicles and alpha-synuclein. *Nat Rev Neurosci* **3**: 932-42

Love, F.M. & Thompson, W.J. (1998) Schwann cells proliferate at rat neuromuscular junctions during development and regeneration. *Journal of Neuroscience* **18**: 9376-9385

Lubinska, L. (1977) Early course of Wallerian degeneration in myelinated fibres of the rat phrenic nerve. *Brain Research* **130**: 47-63

Luco, J.V., & Eyzaguirre, C. (1955) Fibrillation and hypersensitivity to ACh in denervated muscle: effect of length of degenerating nerve fibers. *J Neurophysiol* **18**: 65-73

Ludwin, S.K. & Bisby, M.A. (1992) Delayed Wallerian degeneration in the central nervous system of Ola mice: an ultrastructural study. *Journal of the Neurological Sciences* **109**: 140-147

Lunn, E.R., Perry, V.H., Brown, M.C., Rosen, H. & Gordon, S. (1989) Absence of Wallerian degeneration does hinder regeneration in peripheral nerve. *European Journal of Neuroscience* **1**: 27-33

Lyon, M.F., Ogunkolade, B.W., Brown, M.C., Atherton, D.J. & Perry, V.H. (1993) A gene affecting Wallerian nerve degeneration maps distally on mouse chromosome

4. *Proceedings of the National Academy of Sciences of the USA* **90**: 9717-9720

MacDonald, M., Beach, M.G., Porpiglia, E., Sheehan, A.E., Watts, R.J. & Freeman, M.R. (2006) The Drosophila cell corpse engulfment receptor Draper mediates glial clearance of severed axons. *Neuron* **50**: 869-81

Mack, T.G., Reiner, M., Beirowski, B., Mi, W., Emanuelli, M., Wagner, D., Thomson, D., Gillingwater, T., Court, F., Conforti, L., Fernando, F.S., Tarlton, A., Andressen, C., Addicks, K., Magni, G., Ribchester, R.R,, Perry, V.H. & Coleman, M.P. (2001) Wallerian degeneration of injured axons and synapses is delayed by an Ube4b/Nmnat chimeric gene. *Nat Neurosci* **4**: 1199-1206

Manolov, S. (1974) Initial changes in the neuromuscular synapses of denervated rat diaphragm. *Brain Research* **65**: 303-316

Maselli, R.A., Wollman, R. L., Leung, C., Distad, B., Palombi, S., Richman, D. P., Salazar-Grueso, E.F. & Roos, R.P (1993) Neuromuscular transmission in amyotrophic lateral sclerosis. *Muscle & Nerve* **16**: 1193–1203

Mastalgia, F.L., McDonald, W.I. & Yogendran, K. (1976) Nodal changes during the early stages of Wallerian degeneration of central nerve fibres. *Journal of the Neurological Sciences* **30**: 259-67

Mattison, R.J. (1999) Synapse withdrawal at the neuromuscular junction in a mouse with slow Wallerian degeneration (Wld^s). PhD Thesis, University of Edinburgh, UK.

Mattison, R.J., Thomson, D., Barry, J.A. & Ribchester, R.R. (1996) Sudden death of axotomized motor nerve terminals at neuromuscular junctions in Wld(s) mice. *Journal of Physiology* **495**: 152P-153P

Mattson, M.P., Partin, J. & Begley, J.G. (1998) Amyloid β-peptide induces apoptosis-related events in synapses and dendrites. *Brain Research* **807**: 167-176

Mattson, M.P., Pedersen, W.A., Duan, W., Culmsee, C., & Camandola, S. (1999) Cellular and molecular mechanisms underlying perturbed energy metabolism and neuronal degeneration in Alzheimer's and Parkinson's diseases. *Ann N Y Acad Sci* **893**:154-75

McArdle, J.J. (1975) Complex end-plate potentials at the regenerating neuromuscular junction of the rat. *Experimental Neurology* **49**: 629-638

McDonald, W.I. (1972) The time course of conduction failure during degeneration of

a central tract. *Experimental Brain Research* **14**: 550-556

Meier, T. & Wallace, B.G. (1998) Formation of the neuromuscular junction: molecules and mechanisms. *Bioessays* **20**: 819-829

Miledi, R. & Slater, C.R. (1968) Electrophysiology and electron-Microscopy of rat neuromuscular junctions after nerve degeneration. *Proceedings of the Royal Society, London, B* **169:** 289-306

Miledi, R. & Slater, C.R. (1970) On the degeneration of rat neuromuscular junctions after nerve section. *Journal of Physiology* **207:** 507-528

Minsky, M (1988) Memoir on Inventing the Confocal Scanning Microscopy, *Scanning* **10**,128-138

Mirsky, R. & Jessen, K.R. (1996) Schwann cell development, differentiation and myelination. *Current Opinion in Neurobiology* **6**: 89-96

Nicholls, J.G., Martin, A.R. & Wallace, B.G. (1992) *From Neuron to Brain* 3rd Ed. Sinauer Associates Massachusetts, USA.

Nieke, J. & Schachner, M. (1985) Expression of the neural cell adhesion molecules L1 and N-CAM and their common carbohydrate epitope L2/HNK-1 during development and after transection of the mouse sciatic nerve. *Differentiation* **30**: 141-151

Palade, G.E. & Palay, S.L. (1954) Electron microscope observations of interneuronal and neuromuscular synapses. *Anatomical Record* **118**: 335

Parson, S.H., Davie, N. & Ribchester, R.R. (1998) Synapse elimination in organ culture of Wld^s mouse skeletal muscle. *Journal of Physiology* **507**: 30P

Parson, S.H., Mackintosh, C.L. & Ribchester, R.R. (1997) Elimination of motor nerve terminals in neonatal mice expressing a gene for slow wallerian degeneration (C57Bl/Wlds). *European Journal of Neuroscience* **9**: 1586-1592

Patton, B.L., Cunningham, J.M., Thyboll, J., Kortesmaa, J., Westerblad, H., Edstrom, L., Tryggvason, K. & Sanes, J.R. (2001) Properly formed but improperly localized synaptic specialisations in the absence of laminin alpha 4. *Nature Neuroscience* **4**: 597-604

Perry, V.H., Brown, M.C. & Gordon, S. (1987) The macrophage response to central

and peripheral nerve injury. A possible role for macrophages in regeneration. *J Exp Med* **165**: 1218-1223

Perry, V.H., Brown, M.C. & Lunn, E.R. (1990a) Very slow retrograde and Wallerian degeneration in the CNS of C57Bl/Ola mice. *European Journal of Neuroscience* **3**: 102-105

Perry, V.H., Lunn, E.R., Brown, M.C., Cahusac, S. & Gordon, S. (1990b) Evidence that the rate of Wallerian degeneration is controlled by a single autosomal dominant gene. *European Journal of Neuroscience* **2**: 408-413

Perry, V.H., Brown, M.C., Lunn, E.R., Tree, P. & Gordon, S. (1990c) Evidence that very slow Wallerian degeneration in C57Bl/Ola mice is an intrinsic property of the peripheral nerve. *European Journal of Neuroscience* **2**: 802-808

Perry, V.H., Brown, M.C. & Tsao, J.W. (1992) The effectiveness of the gene which slows the rate of Wallerian degeneration in C57Bl/Ola mice declines with age. *European Journal of Neuroscience* **4**: 1000-1002

Peters, M.F., Sadoulet-Puccio, H.M., Grady, R.M., Kramarcy, N.R., Kunkel, L.M., Sanes, J.R., Sealock, R. & Froehner, S.C. (1998) Differential membrane localization and intermolecular associations of alpha-dystrobrevin isoforms in skeletal muscle. *Journal of Cell Biology* **142**: 1269-1278

Pevsner, J., Hsu, S.C., Braun, J.E., Calakos, N., Ting, A.E., Bennett, M.K. & Scheller, R.H. (1994) Specificity and regulation of a synaptic vesicle docking complex. *Neuron* **13**: 353-361

Pramatarova, A., Laganiere, J., Roussel J., Brisebois, K. & Rouleau, G. A. (2001) Neuron-specific expression of mutant superoxide dismutase 1 in transgenic mice does not lead to motor impairment.*J. Neurosci* **21**: 3369–3374

Pun, S., Santos, A.F., Saxena, S., Xu, L. & Caroni, P. (2006) Selective vulnerability and pruning of phasic motoneuron axons in motoneuron disease alleviated by CNTF. *Nature Neuroscience* **9**: 408 - 419

Raabe, T.D., Nguyen, T., Archer, C. & Bittner, G.D. (1996) Mechanisms of the maintenance and eventual degradation of neurofilament proteins in the distal segments of severed goldfish Mauthner axons. *Journal of Neuroscience* **16**: 1605-1613

Ramon Y Cajal, S. (1928) Degeneration and regeneration of the nervous system (trans. May, R.M.) Oxford University Press, London.

Redfern, P.A. (1970) Neuromuscular transmission in new-born rats. *Journal of Physiology* **209**: 701-709

Reynolds, M.L. & Woolf, C.J. (1992) Terminal Schwann cells elaborate extensive processes following denervation of the motor endplate. *Journal of Neurocytology* **21**: 50-66

Ribchester, R.R. & Taxt, T. (1984) Repression of inactive motor nerve terminals in partially denervated rat muscle after regeneration of active motor axons. *J Physiol* **347**: 497-511

Ribchester, R.R. (1988) Activity-dependent and -independent synaptic interactions during reinnervation of partially denervated rat muscle. *Journal of Physiology* **401**: 53-75

Ribchester, R.R., Pakiam, J.G., O'Carroll, C.M., Thomson, D., Mattison, R.J., Costanzo, E.M., Gillingwater, T.H. & Barry, J.A. (1999) Impaired neuromuscular transmission preceding synapse withdrawal in axotomized adult Wld^s mutant mouse skeletal muscle. *Journal of Physiology* **520**: 76P

Ribchester, R.R., Tsao, J.W., Barry, J.A., Asgari_Jirandeh, N., Perry, V.H. & Brown, M.C. (1995) Persistence of neuromuscular junctions after axotomy in mice with slow Wallerian degeneration (C57Bl/Wld^s). *European Journal of Neuroscience* **7**: 1641-1650

Ridge, R.M. & Betz, W.J. (1984) The effect of selective, chronic stimulation on motor unit size in developing rat muscle. *J Neurosci* **4**: 2614-2620

Robertson, J.D. (1956) The ultrastructure of a reptilian myoneural junction. *Journal of Biophysical and Biochemical Cytology* **2**: 381-394

Robitaille, R., Garcia, M.L., Kaczorowski, G.J. & Charlton, M.P. (1993) Functional colocalization of calcium and calcium-gated potassium channels in control of neurotransmitter release. *Neuron* **11**: 645-655

Robitaille, R. (1995) Purinergic receptors and their activation by endogenous purines at perisynaptic glial cells of the frog neuromuscular junction. *Journal of Neuroscience* **15**: 7121-7131

Robitaille, R., Jahromi, B.S. & Charlton, M.P. (1997) Muscarinic calcium responses resistant to muscarinic antagonists at perisynaptic Schwann cells of the frog neuromuscualr junction. *Journal of Physiology* **504**: 337-347

Rosen, D. R (1993) Mutations in Cu/Zn superoxide dismutase gene are associated with familial amyotrophic lateral sclerosis. *Nature* **362**: 59-62

Rosenthal, J.L. & Taraskevich, P.S. (1977) Reduction of multiaxonal innervation at the neuromuscular junction of the rat during development. *Journal of Physiology* **270**: 299-310

Rossetto, O., Seveso, M., Caccin, P., Schiavo, G., & Montecucco, C. (2001) Tetanus and botulinum neurotoxins: turning bad guys into good by research. *Toxicon* **39**: 27-41

Sagot, Y., Dubois-Dauphin, M., Tan, S.A., De Bilbao, F., Aebischer, P., Martinou, J.C. & Kato, AC. (1995) Bcl-2 overexpression prevents motoneuron cell body loss but not axonal degeneration in a mouse model of a neurodegenerative disease. *Journal of Neuroscience* **15**: 7727-7733

Salpeter, M.M. & Loring, R.H. (1985) Nicotinic acetylcholine receptors in vertebrate muscle: properties, distribution and neural control. *Progress in Neurobiology* **25**: 297-325

Sanes JR, Lichtman JW. (1999) Development of the vertebrate neuromuscular junction. *Annu Rev Neurosci* **22**:389-442

Schaefer, A.M., Sanes, J.R. & Lichtman, J.W. (2005) A compensatory subpopulation of motor neurons in a mouse model of amyotrophic lateral sclerosis. *J Comp Neurol* **490**: 209-219

Schiavo, G., Santucci, A., Dasgupta, B.R., Mehta, P.P., Jontes, J., Benfenati, F., Wilson, M.C. & Montecucco, C. (1993) Botulinum neurotoxins serotypes A and E cleave SNAP-25 at distinct COOH-terminal peptide bonds. *FEBS Lett* **335**: 99-103

Schlaepfer, W.W. & Hasler, M.B. (1979a) The persistence and possible externalisation of axonal debris during Wallerian degeneration. *Journal of Neuropathology and Experimental Neurology* **38**: 242-252

Schlaepfer, W.W. & Hasler, M.B. (1979b) Characterization of the calcium-induced disruption of neurofilaments in rat peripheral nerve. *Brain Research* **168**: 299-309

Sea, T., Ballinger, M.L. & Bittner, G.D. (1995) Cooling of peripheral myelinated axons retards Wallerian degeneration. *Experimental Neurology* **133**: 85-95

Sheller, R.A. & Bittner, G.D. (1992) Maintenance and synthesis of proteins for an

anucleate axon. *Brain Research* **580:** 68-80

Selkoe, D.J. (2003) Alzheimer's disease is a synaptic failure. *Science* **298**:789-91

Shaari, C.M., George, E., Wu, B.L., Biller, H.F., & Sanders, I. (1991) Quantifying the spread of botulinum toxin through muscle fascia. *Laryngoscope* **101**: 960-964

Sheller, R.A. & Bittner, G.D. (1992) Maintenance and synthesis of proteins for an anucleate axon. *Brain Research* **580**: 68-80

Sherrington, C.S. (1897) The central nervous system, Vol.III. In A textbook of physiology, 7th edition, M.Foster ed. (London: MacMillan)

Sherrington, C.S. (1906) The integrative action of the nervous system. Yale University Press, New Haven, USA.

Sisodia, S.S. (1999) Alzheimer's disease: perspectives for the new millennium. *J Clin Invest* **104**:1169-70

Son, Y. J. & Thompson. W. J. (1995) Schwann cell processes guide regeneration of peripheral axons. *Neuron* **14**: 125-132

Subang, M.C., Bisby, M.A. & Richardson, P.M. (1997) Delay of CNTF decrease following peripheral nerve injury in C57Bl/Wld mice. *Journal of Neuroscience Research* **49**: 563-568

Tan, E.K. (2006) Botulinum toxin treatment of sialorrhea: comparing different therapeutic preparations. *Eur J Neurol* **13**: 60-64

Tanner, S.L., Storm, E.E. & Bittner, G.D. (1995) Maintenance and degradation of proteins in intact and severed axons: implications for the mechanisms of long-term survival of anucleate crayfish axons. *Journal of Neuroscience* **15**: 540-548

Thesleff, S., Molgó, J. & Tågerud, S. (1990) Trophic interrelations at the neuromuscular junction as revealed by the use of botulinal neurotoxins. *J Physiol (Paris)* **84**:167-173

Thompson, W. & Jansen, J.K.S. (1977) The extent of sprouting of remaining motor units in partly denervated immature and adult rat soleus muscle. *Neuroscience* **2**: 523-535

Tsao, J.W., Brown, M.C., Carden, M.J., McLean, W.G. & Perry, V.H. (1994) Loss of the compound action potential: an electrophysiological, biochemical and

morphological study of early events in axonal degeneration in the C57Bl/Ola Mouse. *European Journal of Neuroscience* **6**: 516-524

Tsao, J.W., George, E.B. & Griffin, J.W. (1999) Temperature modulation reveals three distinct stages of Wallerian degeneration. *Journal of Neuroscience* **19**: 4718-4726

Uchitel, O.D., Protti, D.A., Sanchez, V., Cherskey, B.D., Sugimori, M. & Llinas, R. (1992) P-type voltage-dependent calcium channel mediates presynaptic calcium influx and transmitter release in mammalian synapses. *Proceedings of the National Academy of Science, USA* **89**: 3330-3333

Usherwood, P.N.R., Cochrane, D.G. & Rees, D. (1968) Changes in structural, physiological, and pharmacological properties of insect excitatory nerve-muscle synapses after motor nerve section. *Nature* **318**: 589-591

Van der Putten, H., Wiederhold, K.H., Probst, A., Barbieri, S., Mistl, C., Danner, S., Kauffmann, S., Hofele, K., Spooren, W.P., Ruegg, M.A., Lin, S., Caroni, P., Sommer, B., Tolnay, M. & Bilbe, G. (2000) Neuropathology in Mice Expressing Human α-Synuclein. *The Journal of Neuroscience* **20**: 6021-6029

Vial, J.D. (1958) The early changes in the axoplasm during Wallerian degeneration. *Journal of Biophysical and Biochemical Cytology* **4**: 551-555

W. B. Amos and J. G. White. (2003) How the Confocal Laser Scanning Microscope entered Biological Research, *Biology of the Cell* **95**: 335-342

Walsh, M.K. & Lichtman, J.W. (2003) In vivo time-lapse imaging of synaptic takeover associated with naturally occurring synapse elimination. *Neuron* **37**: 67-73

Wang, A.L., Yuan, M., & Neufeld, A.H. (2006) Degeneration of neuronal cell bodies following axonal injury in *Wld*^{S} mice. *J Neurosci Res* **84**: 1799-1807

Wang, G.K. (1985) The long-term excitability of myelinated nerve fibres in the transected frog sciatic nerve. *Journal of Physiology* **368**: 309-321

Wang J, Zhai Q, Chen Y, Lin E, Gu W, McBurney MW *et al.* A local mechanism mediates NAD-dependent protection of axon degeneration. (2005) *J Cell Biol* **179**: 349–355.

Wang, M.S., Fang, G., Culver, D.G., Davis, A.A., Rich, M.M., Glass, J.D. (2001) The WldS protein protects against axonal degeneration: a model of gene therapy for

peripheral neuropathy. *Ann Neurol* **50**: 773-779

Wang, M.S., Davis, A.A., Culver, D.G., Glass, J.D. (2002) WldS mice are resistant to paclitaxel (taxol) neuropathy, *Ann Neurol* **52**: 442-447

Wang, Z.Z., Mathias, A., Gautam, M. & Hall, Z.W. (1999) Metabolic stabilization of muscle nicotinic acetylcholine receptors by rapsyn. *Journal of Neuroscience* **19**: 1998-2007

Waxman, S.G. (1997) Axon-glia interactions: Building a smart nerve fibre. *Current Biology* **7**: 406-410

Weddel, G. & Glees, P. (1941) The early stages in the degeneration of cutaneous nerve fibres. *Journal of Anatomy* **76**: 65-93

Whittaker, V.P., Michaelson, I.A. & Kirkland, R.J.A. (1964) The separation of synaptic vesicles from nerve-ending particles ("synaptosomes"). *Biochemical Journal* **90**: 293-303

Winlow, W. & Usherwood, P.N.R. (1975) Ultrastructural studies of normal and degenerating mouse neuromuscular junctions. *Journal of Neurocytology* **4**: 377-394

Wishart, T.M., Parson, S.H., & Gillingwater, T. H. (2006) Synaptic vulnerability in neurodegenerative disease. *J Neuropathol Exp Neurol* **65** :733-739

Wood, S.J. & Slater, C.R. (1997) The contribution of postsynaptic folds to the safety factor for neuromuscular transmission in rat fast- and slow-twitch muscles. *Journal of Physiology* **500**: 165-176

Wood, S.J. & Slater, C.R. (1998) Beta-spectrin is colocalized with both voltage-gated sodium channles and ankyrin (G) at the adult rat neuromuscular junction. *Journal of Cell Biology* **140**: 675-684

Yrjanheikki, J., Tikka, T., Keinanen, R., Goldsteins, G., Chan, P.H. & Koistinaho, J. (1999) A tetracycline derivative, minocycline, reduces inflammation and protects against focal cerebral ischemia with a wide therapeutic window. *Proc. Natl. Acad. Sci, USA* **96**: 13496–500

Zhou, D.X., Lambert, S., Malen, P.L., Carpenter, S., Boland, L.M. & Bennett, V. (1998) Ankyrin (G) is required for clustering of voltage-gated Na channels at axon initial segments and for normal action potential firing. *Journal of Cell Biology* **143**: 1295-1304

Zhu, S., Stavrovskaya, I.G., Drozda, M., Kim, B.Y. & Ona, V. (2002) Minocycline inhibits cytochrome c release and delays progression of amyotrophic lateral sclerosis in mice. *Nature* **417**:74–78

Appendix I

Neurofilament Synaptic Vesicle and AchR Immunocytochemistry Protocol

1. Fix in 4% Paraformaldehyde 30-45 mins

   4g Paraformaldehyde

   100ml 1 x Phosphate Buffered Saline

   Heat to 60-70°C Whilst stirring continuously

   Add 4-5 drops of 0.1 M NaOH

   Wait until solution clears

   Chill to 4°C in fridge

2. Wash 3 times for 10 mins in fresh 1x PBS

   All steps now undertaken on a platform rotator at room temperature and in a sealed dark box to keep light out.

3. Incubate in a 0.1 M glycine solution for 1 hour

4. Incubate in a fresh 5μg/ml TRITC-α-BTX solution for 30 mins

5. Wash 3 times for 10 mins (or 6 x 5mins) in blocking soln;

   In 1x PBS

   4% BSA

   0.5% Triton X-100

   0.1M Lysine

6. Incubation in 1 antibody solution overnight:

   4 ml Blocking solution

20µl NF antibody

20µl SV2 antibody

7. Incubate for 1 hour in fresh primary solution

8. Wash 3 times for 10 mins in blocker

9. Incubate in 2 antibody solution for 4 hours

   4 ml 1x PBS

   20µl FITC sheep-anti-mouse antibody

10. Wash 3 times for 30 mins in 1x PBS

11. Mount preparation in Vectashied (Vector Laboratories Inc.) on a slide and coverslip.

12. Store in dark box at 4 C

Fluorescence Staining for *Wld*^{S} protein

To make high Mg2+ACSF

(ACSF composition)

To 500ml distilled water add:	3.65g	NaCl
	1.05g	$NaHCO_3$
	2.25g	Glucose
	0.09g	KCl
	0.10g	NaH_2PO_4
	0.5ml	1M solution $CaCl_2$
	2.0ml	1 M solution $MgCl_2$

1) Fix in 4% paraformaldehyde for 20 mins

2) Wash in PBS x 2 (10mins)

3) Incubate in blocking solution overnight in cold room on rocker.

Blocker: 4g bovine serum albumin+0.5µl Triton-X+ 100ml PBS, dissolved on hotplace

4) Remove blocking solution and apply Primary antibodies (Wld^{18} ab) overnight at 4 C:

5) Wash in PBS x 3 (10 mins) at room temperature

6) Apply secondary antibodies overnight at 4 C.

TRITC or FITC: 50µl TRITC or FITC anti-rabbit ab + 950µl PBS

7) Wash in PBS x 3 (10mins) at room temperature

8) Apply Topro-3 (1µl topro-3 stock + 1ml PBS) for 10 mins

9) Quick wash in PBS and mount in Mowiol.

Procedure for Wld^{s} Protein Expression Analysis

1. Load Image in order of laser power (20, 30, 40, 50, 60 etc)
2. If necessary extract red channel
3. Make Large ROI (Save as Big Selection.roi)
4. Duplicate
5. Discard original image
6. Load next Image
7. Repeat 2-6 until all images loaded
8. Make Stack
9. Make 30 x 30 pixel ROI (Save as Selection3030.roi)
10. From lowest to highest laser power in stack:
11. Select spot
12. Measure
13. Next slice
14. From Results:

15. Copy all

16. Paste into Excel

17. Select integrated density Column

18. Paste special : Values and Transpose

19. Paste to new line

20. Back to images

21. Clear Results

22. Load Selection3030.roi (if necessary)

23. Measure Background region in each slice

24. Copy Results to Excel

25. Select Integrated density

26. Paste Special Value Transpose

27. Subtract Background from Spot at each laser power

28. Plot graph of laser power vs. corrected brightness of spot (i.e. background subtracted spot) for each spot

29. Calculate mean (average) and Standard deviation of spot brightness for all spots at each laser power

30. Plot graph of laser power versus mean (average) and standard deviation of spot brightness

31. Also keep mean value from each image

32. Calculate mean spot brightness from several images and standard deviation (= standard error of the mean).

Non-sprouting Buffer

20mM sodium Acetate

100mM Arginine

1% Mannitol

100mM Sodium Sulphate

0.1% BSA (Albumin, Bovine)

pH 6.9

For 100mls

Component	MW	Wt	Conc^{n}
Na Ac	82.03	164.3mg	20mM
Arg.	210.7	421.4mg	100mM
Mann.	-	1.0g	1%
Na SO_4	142.0	284.0mg	100mM
BSA	-	100.0mg	0.1%

Dissolve above componets in distilled water.

Once dissolved adjust pH to 6.9 then pass through a 0.22µm millipore filter to sterilize solution.

Split into aliquots and store in freezer.

Botulinum Toxin A- BoTox

Botulinum Toxin A from Clostridium botulinum

Supplier- Sigma Cat# B8776

LD_{50} for subcutaneous in mice is 4ng/kg

i.e. 0.12ng/30g mouse

50µl containing	15ng
10µl	3ng
Dilute to 200µl***	3ng
20µl	0.3ng
10µl	0.15ng
5µl	0.075ng

***Dilute using non-sprouting buffer solution

Pipette into 30µl aliquots.

Store @ -20°C in freezer.

i.e. 6 expts @ 0.075ng/animal.

Appendix II

Abstracts of the Neuroscience Conferences

FENS Forum 2004

For lectures, symposia and workshops, time indicates the beginning of the session.
For posters, authors are expected to be present at their posters at the time indicated.

Close window

First author: Fan, Li (poster)

Poster 42 - Mon 12/07, 16:00 - Hall I
Session 109 - Synaptogenesis II
Abstract A109.6, published in *FENS Forum Abstracts, vol. 2, 2004.*
Ref.: *FENS Abstr., vol.2, A109.6, 2004*

Author(s) **Fan L., Gillingwater T. H., Thomson D., Thomson A. & Ribchester R. R.**

Addresse(s) *Divison of Neuroscience, University of Edinburgh, Edinburgh, EH8 9JZ, UK*

Title Neuroprotective phenotype at neuromuscular junctions in homozygous and heterozygous WldS mutant mice.

Text In WldS mutant mice axonal (Wallerian) degeneration is delayed 10-fold after axotomy in homozygotes, resulting from expression of the chimeric gene Wld (1). Synapses are less well protected and retract from endplates after axotomy. With age, protection of neuromuscular synapses by the Wld gene is lost completely. Here we examined the extent of synaptic protection in heterozygous WldS mice. To generate heterozygotes, we cross-bred BalbC mice with homozygous Thy1YFP/Wlds mice, that also express fluorescent protein in motoneurones. We compared synaptic and axonal preservation 3-4 days after axotomy with homozygous Wlds and wild-type thy1YFP mice. Sciatic nerve lesions were performed under N2O/halothane anaesthesia. 1-4 days later, mice were killed and both tibial nerves removed. Lumbrical muscles were also removed and postsynaptic acetylcholine receptors were labelled with TRITC-a-BTX. In wild-type mice, most axons had degenerated within 1-2 days. In heterozygous Wlds mice, axonal preservation in the lesioned tibial nerve was similar to that observed in homozygotes. However, virtually all (>95%) axotomised intramuscular axon branches and motor nerve terminals at neuromuscular junctions in heterozygous WldS mice had degenerated, as in wild-type mice. This was distinct from both young (1-2 month old) homozygous WldS muscles, where 90-100% of nerve terminals persisted at 3 days post axotomy, and older WldS mice (>7 months) where synapses were lost but preterminal axons remained. The data support a compartmental model of neurodegeneration(2) and suggest that moderate levels of Wld protein expression are not sufficient to protect synapses from the effects of axotomy. Regulation of other factors will be required to fully protect synapses from degeneration or elimination.

1. Mack, T. G. A. et al. (2001). Nat Neurosci 4:1199-1206
2. Gillingwater et al (2002) J. Physiol. 543.3.

Theme Development
Synaptogenesis and activity-dependent development / Synapse formation: PNS

Program Number: 670.16 **Day / Time:** Tuesday, Nov. 15, 11:00 AM - 12:00 PM

Rapid degeneration of motor nerve terminals in heterozygous WldS mice

L.Fan; T.H.Gillingwater; J.E.Haley; D.Thomson; A.Thomson; R.R.Ribchester SPON: British Neurosci. Assoc.

Centre for Neuroscience Research, Univ. of Edinburgh, Edinburgh, United Kingdom

WldS mutant mice express a chimeric gene that delays Wallerian degeneration by about a factor of ten. Synapses are less well protected and with age, protection of neuromuscular junctions is lost completely (Gillingwater et al., 2002, J Physiol. 543, 739-755). Here we focused on neuromuscular synaptic protection in heterozygous WldS mice. We mated Thy1YFP16/WldS homozygous mice with BalbC mice. Sciatic nerve lesions were performed in F1 heterozygotes under N2O/halothane anaesthesia. Mice were killed and lumbrical muscles with attached nerves were removed 6-240h later. ACh receptors were labelled with TRITC-α-BTX. Axonal preservation in these WldS/+ mice(ca. 100%) was indistinguishable from WldS homozygotes for at least 72 hours. But virtually all motor nerve terminals became fragmented and disconnected from their parent axons in WldS/+ mice within 24 hours, as in wild-type mice. At 17 hrs, $80.68 \pm 3.66\%$ (S.E.M., n=3 mice) of terminals in WldS/+ mice had degenerated in this fashion, compared with $88.11 \pm 4.72\%$ (n=3) at 14.5 hours in +/+ mice. The rapid synaptic degeneration in heterozygotes contrasted with more gradual and asynchronous synaptic retraction in young adult WldS/WldS mice. At 5 days, $80.76 \pm 2.12\%$ (n=4 muscles) of motor nerve terminals in WldS/WldS mice were still connected to their parent axon terminals although $58.82 \pm 3.67\%$ of these only partially occupied motor endplates. Older WldS/WldS mice (> 7 months of age) showed rapid synaptic degeneration, as in young WldS/+ mice. Immunostaining showed similar numbers of neurones strongly expressing WldS protein, but the intensity of staining in WldS/WldS was about twice that in WldS/+ mice. The expression levels did not decline with age. The data confirm that synaptic protection is sensitive to WldS gene dose but high levels of WldS protein expression are insufficient to preserve neuromuscular synapses in mature mice. Attempts to transfer WldS-induced neuroprotection to neurological mutants should take account of these factors.

Support Contributed By: MRC,Wellcome Trust,BNA

Citation: L.Fan, T.H.Gillingwater, J.E.Haley, D.Thomson, A.Thomson, R.R.Ribchester. Rapid degeneration of motor nerve terminals in heterozygous WldS mice. Program No. 670.16. *2005 Abstract Viewer/Itinerary Planner.* Washington, DC: Society for Neuroscience